A DIRECT CURRENT (DC) RESISTIVITY SURVEY OF THE EASTERN PART OF AHMADU BELLO UNIVERSITY MAIN CAMPUS, SAMARU-ZARIA

BY

IBRAHIM NOUHOU
B.Sc. (Hons.) PHYSICS

A THESIS SUBMITTED TO THE POST GRADUATE SCHOOL AHMADU BELLO UNIVERSITY, IN PARTIAL FULFILLMENT OF THE REQUIREMENTS FOR THE AWARD OF THE DEGREE OF MASTER OF SCIENCE IN APPLIED GEOPHYSICS.

DEPARTMENT OF PHYSICS,
AHMADU BELLO UNIVERSITY,
ZARIA.

AUGUST, 2003

CERTIFICATION

This M.Sc. thesis entitled a "Direct Current Resistivity Survey of the Eastern part of A.B. U. Main Campus— Samaru" by Ibrahim NOUHOU meets the regulation governing the award of the Degree of Master of Science in Applied Geophysics of the Physics Department, A.B.U. Zaira; and is approved for its contribution to scientific knowledge and literacy presentation.

_____ Date:
……..
Prof C. 0. Ajayi
Chairman Supervisory Committee

_____
Dr. P.O. Sule Date :
…….
Member Supervisory Committee

_____
Dr. M. N. Umego Date:
…….
Head, Department of Physics

_____
Date:
…….
Dean, Post Graduate School

DECLARATION

I hereby declare that this thesis is a record of my own research work and has not been previously presented for a degree at any other University. Information derived from published and unpublished works of others have been acknowledged in the text.

_____ _____

Ibrahim Nouhou Date

DEDICATION

This thesis is dedicated to my humble uncle M. Abdou A. Adamou and my parents.

ACKNOWLEDGEMENT

All praises be to Allah (SWT), the most Compassionate and most Merciful for sparing my life and giving me the opportunity to write this educative project, and witness the end of this academic strife.

I must first and foremost express my profound gratitude to the head of this department (Dr. M.N. Umego) as he kept a close look on this work, particularly on critical and decisive phases, despite his complex commitments.

Kindness to Prof C. 0. Ajayi and Dr. P. 0. Sule who, in spite of their numerous engagements, diligently contributed to the successful accomplishment of this academic masterpiece.

I also wish to express my sincere gratitude to the entire staff of this department for their support throughout the windy paths of this program.

I must recognise the presence of Miss Fatima Zahra Youssouf, Department of Water Resources and Environmental Science of this institution. The Ministry of National Education and Ministry of Education, Research and Technology of Niger Republic laid the foundation of my education. I hereby write to express my sincere appreciation to them for their educative policies.

I am extremely indebted to my parents, Uncle Abdou A. Adamou, Mr. Ibrahim Salissou (Magaji), Mr. Abdou Daouda, Mr. Maman Touani, and Elh. Mohammed Abubacar Nakowa for their financial support as well as their moral upbringing.

I wish to acknowledge Baba'n and Mama'n Zaflra for their compassion and care. My early school friends are duly remembered. These are Idrissa Sanda (Moah), Salouhou Hamidine, and Yahouza Zakari. Worthy of mention are my University colleagues Maman

Garba, Moussa Elh. Alassane, Ali Mounoumi, Ouzeirou Moudjitaba, Usman Nuhu Adamu, Moussa Abdou, Mansour Moussa, Umar Ado Farouq, Ibrahim Dandano, Bello Nakone, Seidou Hankouraou, Ahmed Zabeiru and Pascal Ayi. The list is not exhaustive.

I seize this opportunity to say ‘thank you’ to my fellow compatriots in Niger Republic. I also use this occasion as a medium for expressing my sincere gratitude to all Nigerians for the lovely stay and experiences I have gained in this country. May Nigeria continue to prosper. Amen.

ABSTRACT

A direct current (D.C.) resistivity survey, employing the vertical electrical sounding (VES) at 39 stations evenly distributed, was carried out at the Eastern part of Ahmadu Bello University-Zaria, comprising Areas E, F, G, Faculty of Agriculture, A.B.U. Gymnasium, and Area BZ. The survey was carried out in order to understand the basement topography, tectonic history along the two river channels in the study area (River Samaru and River DanFodio), as well as possible sites or zones for locating boreholes.

Results from the interpretation of the data collected suggest 3-4 geoelectric layers.

The first layer whose resistivity values vary between 44-135OQm is associated with top soils (consisting of fresh and weathered laterite, clay and sandy clay, and Fadama loam); which has a thickness ranging from 1 and 8m.

The derived geologic sections suggest that the second or third layer consists of either fractured basement or weathered basement, which constitutes the main aquifer of interest in the study area. The thickness of the weathered basement varies between *5* and 53m, with resistivity values ranging between 66 and 25OQm.

The results of this work also show that the two rivers Samaru and DanFodio are structurally controlled because they originated prior to fractures. These two rivers constitute a great deal of the groundwater potentials of the study area.

The fresh basement constitutes the third or fourth layer with resistivity values ranging between 1025 and 924 1am. It is shallowest at VES24 (East of Area F) with a depth of 7m and deepest at VES05 (53m), inside the Forestry Research Institute.

Result from the radial depth sounding plots revealed 2-3 fault patterns along the two water courses; suggesting that the latter may have originated prior to faulting or fracturing rather than a mere erosion feature.

The most prominent targets for boreholes are all along the Samaru River with the exception of VES24, all of Area E, F, and G, as well as Faculty of Agriculture compound, East of NAERLS, and the A.B.U gymnasium.

TABLE OF CONTENTS

TITLE PAGE

Title Page.....i

Certification.....ii

Declaration.....iii

Dedication.....iv

Acknowledgement.....v

Abstract.....vii

Table of Contents.....ix

Abbreviations xii

List of Tables.....xiii

List of Figures.....xiv

CHAPTER ONE

INTRODUCTION

1.0 The Study Area.....1

1.1 Physiography of the Study Area.....1

1.2 Geology, Hydrogeology, and Structures.....3

1.2.1 The Basement Complex 3

1.2.2 The Superficial Deposits.....5

1.2.3 Structural Geology.....7

1.2.4 Hydrogeology of the Study Area 7

1.2.5 Vegetation and Land Use.....8

1.3 Previous Studies in the study Area. 8

1.4 Objectives of the Present Study.....11

3.1 Interpretation of Electrical Data.....29

3.2 Results.....29

3.1.1 Geoelectric Sections.....30

3.1.2 The Geologic Sections.....38

CHAPTER FOUR

MAPS PRODUCED FROM THE INTERPRETED DATA

4.0 Maps produced from the interpreted data.....50

4.1 Isoresistivity Map of the Weathered Basement.....50

4.2 Weathered Basement Thickness Map of the Study Area.....52

4.3 Depth to Basement Map of the Study Area.....52

4.4 Isoresistivity Map of the Fresh Basement.....55

4.5 Result from the Radial Depth Sounding.....57

4.5.1 Summary of the Radial Depth Sounding: Results of the Five Stations.....57

4.5.2 Deductions from the Interpreted Data.....58

4.6 Groundwater Potentials of the Study Area.....58

CHAPTER FIVE

CONCLUSION AND RECOMMENDATION

5.0 Work Done so Far.....62

5.1 Conclusion.....62

5.2 Recommendations.....63

REFERENCES.....65

APPENDIX I: Interpretation of the Normal Depth Sounding Plots of the 39 VES Stations.....65

APPENDIX II: Geoelectric Stratification of the Study Area……..……..107

APPENDIX III: Radial Depth Sounding Plots…..……..……110

ABBREVIATIONS

AB/2: Half electrode spread length.

CST: Constant Separation Traversing. D. A. C.: Division of Agricultural Colleges.

L A. R.: Institute for Agricultural Research

N. A. E. B. L. S.: National Agricultural Extension Research and Liaison Services.

MN/2: Half the spacing between voltage electrodes in a Schlumberger array; otherwise Known as *1*.

YES: Vertical Electrical Sounding.

LIST OF TABLES

Table 2.1 Resistivity values of Rock types in Basement Complex Areas compiled by (Ajayi et al., 1989) ……..16

Table 2.2 Azimuth and Locations of the 39 VES stations…… 22

Table 2.3 Azimuth and location of the Radially Sounding Stations……. 23

Table 3.1 Resistivity values used in deriving the Geologic Sections in this work…40

Table 4. 1 Radial depth Soundings and Directions of Anisotropy ……57

LIST OF FIGURES

Fig 1.1 Map of the Study Area; (A. B. U. East: Comprising of Areas E, F, G, BZ, and Agric. Faculty) …….. .2

Fig. 1. 2 Simplified Geological Map of Nigeria …… 4

Fig 2. 1 General Four-Electrode Configuration for Resistivity Measurement Consisting of a pair of Current Electrodes (A,B) and a pair of Potential Electrodes (C,D) ……...14

Fig. 2. 2 Geologic Well-log obtained by Pressag Ltd at Jania'a Village (Courtesy of Kaduna State Water Board) ……16

Fig.2.3 The Schlumberger General Spread ……18

Fig 2.4 Abem Terrameter SAS 300: Controls and Indicators ……... 20

Fig 2.5 The Schlumberger Symmetric Spread …….. 21

Fig.2.6 VES Points and Profile Layout Extracted from Fig. 1.1 …….. 25

Fig. 2.7 YES Field curve at VESO2 (Konar Biye, Area G) …….. 27

Fig. 3. 1 Geoelectric section for profile P_1 ……. 31

Fig. 3. 2 Geoelectric section for profile P_2……..33

Fig. 3.3 Geoelectric section for profile P_3……35

Fig. 3.4 Geoelectric section for profile P_4……37

Fig. 3.5 Geoelectric section for profile Ps…….. 39

Fig. 3.6 Geologic Section for Profile P_1……. 41

Fig. 3.7 Geologic Section for Profile P_2……. 43

Fig. 3.8 Geologic Section for Profile P_3……..…45

Fig. 3.9 Geologic Section for Profile P_4……..…47

Fig. 3.10 Geologic Section for Profile P_5……..49

Fig. 4. 1 Isoresistivity Map of the Weathered Basement of Eastern Part of ABUZaria…….. 51

Fig. 4.2 Weathered Basement Map of the Eastern Part of ABU Zaria …….. 53

Fig 4.3 Depth to Basement Map of the Eastern Part of ABU Zaria……. 54

Fig 4.4 Basement resistivity map of the eastern Part of ABU Zaria…….. 56

Fig 4.5 Groundwater Potentials of the Study Area……... 61

CHAPTER ONE
INTRODUCT ION

1.0 The Study Area

Ahnudu BeIIo University (ABU) Zaria occupies the extreme northwest of the Kubanni River Basin-Zaria The Kubanni River itself occupies the central part of the southeast sector of the Zaria sheet (N^0 102.5W) of the 1: 50,000 sheet series of the Nigeria ordinance survey imps. The Kubamii basin is approximately bounded by latitudes I $1^0$4'25"N aid $11^0$10'46"N and longitudes *$7^0$36'55"E* ~yt~j $7^0$44'12"F

The study area (Fig.1 1) is &5 km long and 15 km wide; with the longest side along the Sokoto Road. Roughly it has an oval shape. Bo~mded to the southwest by Biye River, to the north by Sokoto Road mxl to the east by Danfodio River. The Samaru River flowing in the northwest; southeast direction bisects the study area into areas E and F to the west, aid Area BZ and the Faculty of Agriculture to the east.

The study area has an effective land surflmce area of *4* km^2. Most of the study area *is* occupied by residential quarters (BZ, E, F, aid (1) and the remaining part consists of the Faculty of Agriculture and the Gyninasiunt

1.1 Physiography of the Study Area

A. B. U., being part of the Kubonni river Basin in the Northern part of Nigeria, has a tropical savannah climate with very distinct dry and wet seasons (Olufenii, 1985) The mean animal rainfall fix Zauia over ~ period of 4~) years is about 1092 mm (Hore, 1970). The wet season usually starts in April and ends about September marking the beginning of the dry season.

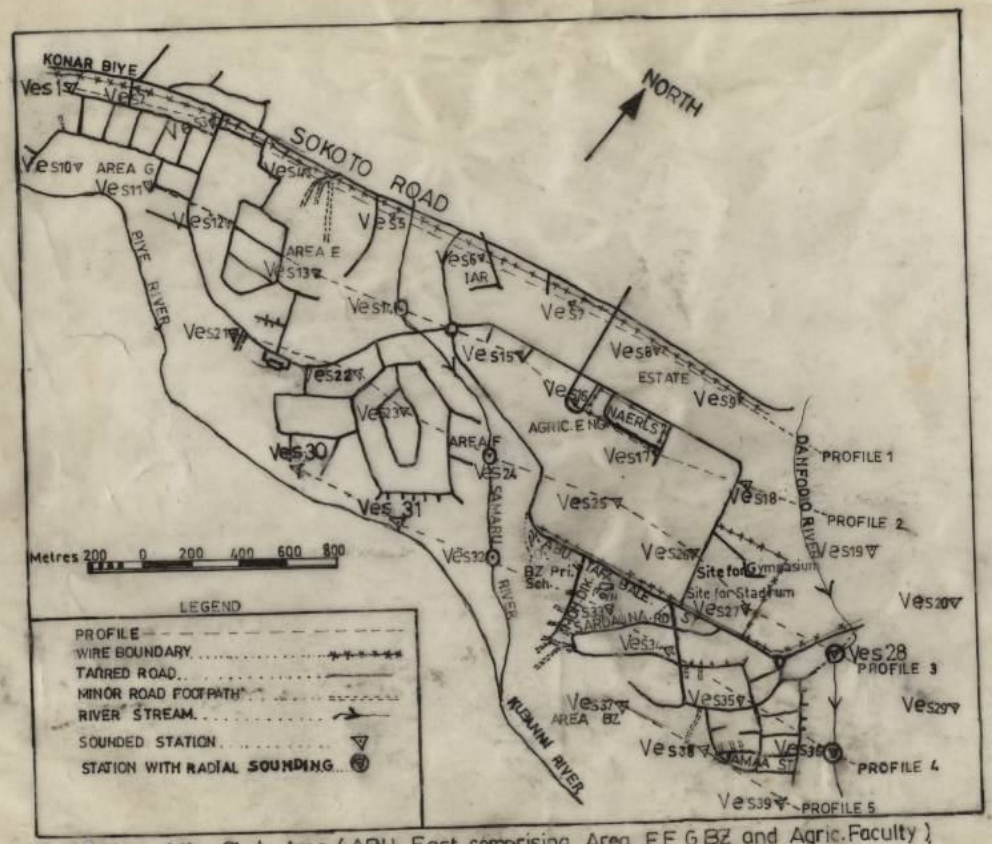


Fig. 1: Map of the Study Area; (ABU East comprising Area E F G BZ and Agric. Faculty)
Courtesy of URP Dept. A.B.U. Zaria.

The dry season occurs between October to March with mean daily maximum temperature of 35^0C in April and drops to the minimum of 33^0C in October. As part of Zaria environs, the study area is a dissected portion of the Zaria-Kano plain, which developed on the crystalline metamorphic rocks of the Nigerian Basement Complex (Torkaski, 1972). Extensive exfoliation and chemical weathering have produced residual granitic inselbergs such as the one supporting the overhead water tank at Area BZ. There are no bills within the study area

During the reshaping of the crystalline basement complex by the combined effect of weathering and river erosion, an extensive older laterite cover of possible paleocene age developed (Du Preez, 1956). This laterite is now preserved as low scarp-bounded plateau remnants, mainly interfluves. Such laterite plateaux can be seen to the south of Area G bordering River B~e, and south of Area BZ. Furthermore, water erosion has exposed the crystalline basement along the streams Biye, and Samaru.

The dissection of this older peneplain laterite and the formation of the younger laterite and older alluvium are the results of the Pleistocene erosion cycles (Du Preez and Barber, 1965). During the phase of the geormrphological development, a sandy cover was deposited, part of which was laid directly above the basement and its mobilised cover (Tokarski, 1972).

1.2 Geology, Hydrogeology, and Structures

1.2.1 The Basement Complex

The study area is underlain by PreCambrian rocks typical of the Nigerian Basement Complex covering in excess of *50%* of the land surface of the Federation (Fig. 1.2), older granites outcrop in the stream valleys (River Biye, River Danfodio

1.2 Geology, Hydrogeology, and Structures

1.2. The Basement Complex

The study area is underlain by PreCambrian rocks typical of the Nigerian Basement Complex covering in excess of *50%* of the land surface of the Federation (Fig. 1. 2), older granites outcrop in the stream valleys (River Biye, , and Samaru). An instance of this outcrop is the presence of gneiss inselbergs supporting the overhead water tank in Area BZ.

The older granite are non-porphyritic and variably foliated. Foliation, where present, is defined by general regional alignments of tabular microcline porphyroblast up to *5* cm long (Trustwell and Cope, 1963). Crosscutting sheets and irregular masses of pegmatite, applite and vein quartz are widespread.

The gneiss complex, which is another basement rock present in the study area, is medium to coarse gained and moderately, to weakly foliated. They are principally made up of quaig oligoclase, biotite and occasionally porphyroblastic microcline (McCurry, 1970).

The summary of the different basement rocks found in the basin and which are covered by Quatemary to recent deposits can be summarized as

Follows:

1. Coarse porphyritic-biotite granite;
2. medium-coarse grained biotite granite gneiss;

and Samaru). An instance of this outcrop is the presence of gneiss inselbergs supporting the overhead water tank in Area BZ.

The older granite are non-porphyritic and variably foliated. Foliation, where present, is defined by general regional alignments of tabular microcline porphyroblast upto *5* cm long (Trustweli and Cope, 1963). Crosscutting sheets and irregular masses of pegmatite, applite and vein quartz are widespread.

The gneiss complex, which is another basement rock present in the study area, is medium to coarse gained and moderately, to weakly foliated. They are principally made up of quartz, oligoclase, biotite and occasionally porphyroblastic microcline (McCurry, 1970).

The summary of the different basement rocks found in the basin and which are covered by Quatemary to recent deposits can be summarized as follows:

1. Coarse porphyritic-biotite granite;
2. medium-coarse gained biotite granite gneiss;
3. applite granite with pegmatite and quartz veins cutting across most of the bodies and,
4. Weathered basement, which is part of the basement complex that had been weathered and disintegrated beyond recognition. The above listed rocks occupy *13.5%* of the Kubanni basin total area and constitute part of the main aquifer (Eigbefo, 1978).

1.2.2 The Superficial Deposits

The superficial deposits that cover most of the basement rocks in the study area act as recharge to the aquifer. These deposits are the older laterites. The older laterite remnants are recognised partly by their reddish brown cellular aspects, and by their relative freedom from impurity (Wright and McCurry, 1970).

The younger laterite sheets are topographically lower and are mainly exposed stream channels. They also differ from the older laterites in being generally brown, less cellular and less free of impurity as well as being rarely more than 6 m thick.

The older alluvium and younger laterite are observed in most places in the basin Alluvial deposits postdating the older laterite and broadly contemporaneous with younger laterite overlie most of the area (Wright and McCurry, 1970).

Accumulations of fine grey-brown sands, clays, red sand and gavel reach thickness of 15 mm some places (Olowu, 1967).

The following indicates a complex depositional history:

1. scattered exposures of laterites and sometimes gravels which may either be underlain or overlain by alluvium,
2. local discontinuities marked by layers of quartz fragments and
3. ancient drainage channels filled by stream deposits, and now exposed in present day erosion gullies.

The younger alluvium is the product of the most recent cycle of erosion. It consists of grey-brown sands, sills, and clays over 10 in thick in some places (Olowu, 1967). There is a river cut in the deposits along the Samaru River directly opposite BZ primary schooL

The superficial deposits rest almost everywhere on the weathered basement. The thickness of this weathered zone is not certain but there is evidence that it can attain 16 m or more especially where the older laterite is still preserved (McCurry, 1970).

1.2.3 Structural Geology

The structural geology of an area is of great importance especially when the search for groundwater is among the ultimate aims. This is most true in areas of crystalline rocks such

as the ones covering our study area. The amount of recharge and discharge is controlled and determined by the structures such as faults, fractures, joints, fissures, etc. These joints sometimes store water themselves especially where such features are of appreciable depth (Akpoborie, 1972).

The basement structure of A. B. U. East is relatively simple because of the uniform nature of the regional foliation trends (McCurry, 1970). Akpoborie (1972)
has observed that the older granite inselbergs are intensively fractured forming channels for the collection and flow of rainwater in the basement aquifer.

1.2.4 Hydropology o.f the study area

The hydrogeology of the study area will be considered in two aspects namely surface water and groundwater. This study area comprises two rivers: River Danfodio and River Samaru: all of these two rivers are intermittent. These two rivers are tributaries of Kubanni River.

The volume of water in all of the above-mentioned rivers depends on the season. During the rainy season, there is always a great increase in flow volume in the main river (Kubanni), while in the two rivers there is hardly water in the streams during the dry season.

Rainfall is one of the dominant factors that determine the occurrence of groundwater in the study area. During the rainy season, the study area enjoys a fairly high amount of rainThll The higher the precipitation over an area, the greater will be the recharge. It has been observed that wells dug away from the river normally

contain water at shallow depth.. However, the water table falls progressively throughout the dry season The amount of water in the well is determined by the location of the well from the river (Olowu, 1967). Generally, the closer a well is to the river channel, the smaller the falL This fall is mainly controlled by the subsurface percolation of water into larger river valleys.

1.2.5 Vegetation and Land Use

The Ahniadu Bello University Zaria has vegetation typical of the savannah region and is characterised by bushes generally less than 3 mhigh but interrupted by large isolated trees. Normally, thick vegetation helps in trapping rainwater and prevents surface runoff; which also results in high erosion and gullies. The vegetation in the study area is subdivided into two categories namely: mango trees in residential areas and bushes dotted with isolated large trees typical of the savannah. However windbreaks can be identified along Tafawa Balewa Road, Faculty of Agriculture, and extreme northwest of area G along the Sokoto Road.

As the vegetation outside the built up areas is very scanty, its effect is to keep the water table as high a level as possible over a long period of time (Olufemi, *1985).* The land, apart from hosting the Faculty of Agriculture, IAR, NAERLS and residential Areas E, F, G, BZ serves as farmland where staple and cash crops are grown.

1.3 Previous Studies In the Area

In the last forty years the Kubanni basin has witnessed a series ‘of geotechnical investigations. Some of the studies are single while others are integrated. All have been carried out with the sole aim of determining the

geological characteristics of the Kubanni basin. It is worth mentioning that not all of these works incorporated our study area, however, the importance of these (past studies) is by

giving the proper understanding of the study area. The first literature on the area is of geophysical nature, mainly resistivity

(Du Preez, 1956). He discovered the presence of step dipping water-bearing joints in some granitic outcrops in the basin. However, the location of these joints as at the time of the investigation was obscure. Vertical Electrical Sounding (yES) was used three years later, Ososami, (1968) in order to assess groundwater potentials of parts of the Kubanni Valley. The specific area of interest then was the A. B. U. Main Campus (Samaru) and environs. He found that the aquifer in his study area is of variable thickness between I to 30 m, even though he could not distinguish the boundary between the weathered basement and fresh basement. Neither was he able to identify the types and extent of the components of the aquifer in his study area nor of the entire basin.

Messrs Pressag Nigeria Limited carried out a resistivity survey in Jania'a Kubanni village in the early SOs as reported by Olufemi, (1985). The aim of that work was the sitting of a borehole in the village. The out come of their work suggested the presence of faults within the bedrock and these were believed to have been responsible for the down throw of certain parts of the bedrock in the study area.

It was not sure whether or not this phenomenon occurred in other parts of the basin. Two years later, Hassan (1987) using geoelectric investigation over the western half of Knbanni basin, concluded that the bedrock in his study area was undulating with depth generally increasing towards the southern part of the study

area. He also suggested the existence of a great depression in the southern part of the study area. The deepest part of the basin could not be defined because of the wide separation of his profiles.

The earliest geologic work was that of Trusweli and Cope (1963). They reported the existence of substantial late and post orogenic trans-current faulting in areas adjacent to Kubanni basin Also, Wright and McCurry (1970) studied the basement geology of Zaria sheet 102 S-W within which the Kubanni basin lies. They have found out that the Basement Complex, which covers the entire Zaria area, is made up mostly of older granites and biotite granite-gneiss. They also reported the presence of a sub-vertical crush belt about 1.6 m wide, crossing the Kubanni River about two and half metres from Samaru.

Previous works of geologic and hydrogeological importance are considered below. These include the work of Tokarski (1972) who had worked in the area west of the Main Campus. The study revealed the heterogeneous terrace arrangement and ground water occurrences m that part of the basin. He concluded that the components of the Quaternary deposit in the area we re Aeolian cover and upper savannah loam.

Olowu, (1967) studied the surface water and its effect on the groundwater in the Zaria area. He found that all the streams were seasonal (includin& Rivers Biye, DanFodio and Samaru). He also found that all the hand-dug wells away from the rivers have their water table falling throughout the dry season

Akpoborie (1972) discovered, from his study of the hydrogeological structures, which control underground water in Samaru, (that structures developed in rocks such as joints and fractures), control the flow of groundwater into the basin Also Eigbefo (1978) from this hydrogeological investigation of the basin established that the depth to water table at various points varied from 3 to 30 in He was also able to conclude
that the thickness of the weathered basement aquifer within the basin ranges from about ito 60 in

1.4 Objectives of the Present Work.

The specific objectives of the study are:

i. To produce a geo-electric section at each sounding point, in order to determine the subsurface layering and the depth to basement at each point.

ii. To determine from the geoelectric sections in (1) the components of the aquifer and the respective thickness of each component beneath each sounding point.

iii. To produce a depth – to – basement map in order to obtain a good picture of basement topography (geometry) and overburden thickness within the basin

iv. To assess its groundwater potentials and determine suitable places to site borehole.

v. To determine whether the drainage pattern in the study is structurally controlled.

vi To carry out detailed resistivity mapping of A. B. U. (East).

CHAPTER TWO
METHODOLOGY

2.0 General Remarks

The science of geophysics applies the principles of physics to the study of the internal structure of the eartk This involves the taking of measurements at, in or near the Earth's surface that are influenced by the internal distribution of physical properties. Of course resistivity of subsurface materials is a case in point.

There are several methods of electrical surveying. Some methods like magnetotelluric (MI), self potential (SP), teiluric method make use of naturally occurring fields, whereas electrical resistivity, induced polarisation (IP), electromagnetic (EM) methods make use of artificially generated voltage into the ground.

Electrical resistivity methods utilise direct currents or low frequency (AC) currents to investigate the electrical properties of the subsurface. When carrying out electrical (DC) survey, artificially generated electric currents are introduced into the ground and the resulting potential differences are measured at the surface. Deviations
from the normally expected potential differences of the subsurface provide
intbrmation on the form and electrical properties of the subsurface geology (Kearey and Brooks, 1988).

2.1 Theory of the DC Resistivity Method: Elementary Theory Potential us a Homogeneous medium

The simplest approach to the study of resistivity of earth materials is to consider a continuous current flowing in an isotopic homoguious medium

Let δA be an element of surface and J the current density in Amp/m^2, the current passing through δA is JδA, the current density and the electric field E are related to Ohm' law by;

$$J = \sigma E \quad \ldots\ldots (2.1)$$

where E is in volts/metre and σ is the conductivity of the medium in siemens/metre. The electric field is derived from the gradient of the applied voltage, which is a scalar potential V in volts.

$$E = -\nabla V \quad \ldots\ldots (2.2)$$

Therefore,

$$J = -\sigma \nabla V \quad \ldots\ldots (2.3)$$

Assuming that there are neither current sources nor sinks within an enclosed volume bounded by a surface A, we can write:

$$\int_A J \cdot dA = 0 \quad \ldots\ldots (2.4)$$

Gauss's theorem states that the volume integral of the divergence of current throughout a given region is equal to the total charge enclosed, so that we have:

$$\int_V \nabla \cdot J dV = 0$$

Taking dV as an infinitesimal volume enclosing a given point, we get for this point:

$$\nabla . J = -\nabla . \nabla (\sigma V) = 0, \textit{ therefore,}$$

$$\nabla \sigma . \nabla V + \sigma \nabla^2 V = 0 \quad \ldots\ldots (2.5)$$

If σ is constant throughout, the first term vanishes and we have Laplace's equation, that is, the potential is harmonic

$$\nabla^2 V = 0 \quad \ldots\ldots (2.6)$$

The two boundary conditions that must be satisfied at any contact between two regions (medium1 and medium2) of different conductivity are:

- The potential must be continuous across the boundary. The continuity of V implies that $\delta V/\delta x$, x being parallel to the boundary is also continuous.
- The normal component of the current density is also continuous:

$$(\delta V/\delta x)^1=(\delta V/\delta x)^2$$

Thus we have:

$$V^{(1)} = V^{(2)}; (\delta V/\delta x)^{(1)} = (\delta V/\delta x)^{(2)}; J_n^{(1)} \equiv J_n^{(2)} \quad \text{..... (2.7a)}$$

$$E_t^{(1)} = E_t^{(2)}; \sigma_1 E_n^{(1)} = \sigma_2 E_n^{(2)} \quad \text{..... (2.7b)}$$

There are several field configurations used in resistivity methods. However, the one of interest is that of point electrodes at the surface.

2.1.1 The General Four Electrode Method.

Figure 2.1 below shows an arrangement consisting of a pair of current electrodes and a pair of potential electrodes. The current electrodes A and B act as source and sink respectively. At the detection electrode C, the potential due to the source A is $+ \rho I/(2\pi r_{AC})$, while the potential due to the sink B is $- \rho I/(2\pi r_{CB})$.

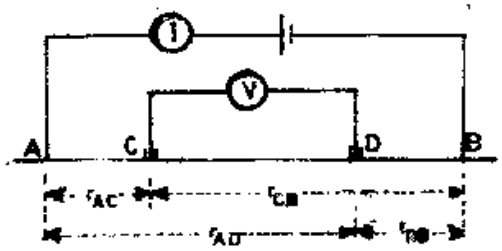


Fig. 2.1 General four-electrode configuration for resistivity measurement consisting of a pair of current electrodes (A, B) and a pair of potential electrodes (C, D)

The combined potential at C is:

$$U_C=\rho I/2\pi(1/r_{AC} - 1/r_{CD}) \quad \text{.....(2.8)}$$

Similarly the resulting potential at D is:

$$U_D=\rho I/2\pi(1/r_{AD} - 1/ r_{DB}) \quad \ldots\ldots(2.9)$$

The potential difference measured by a voltmeter connected between C and D is:

$$\Delta U = U_C - U_D = \rho I/2\pi[(1/r_{AC} - 1/ r_{CB}) - (1/r_{AD} - 1/ r_{DB})] \quad \ldots\ldots(2.10)$$

All quantities in this equation can be measured on the ground surface except the resistivity, which is given by:

$$\rho = 2\pi\Delta U/I[1/ \{(1/r_{AC} - 1/ r_{CB}) - (1/r_{AD} - 1/ r_{DB})\}] \quad \ldots\ldots(2.11)$$

2.1.2 Parameters Affecting DC Resistivity Survey in the Basement Complex

The Nigerian Basement Complex is part of the Pan-African Craton which covers over two thirds of Nigeria's land surface. The topsoil is underlain by laterite. The lateritic cover is underlain by the weathered zone overlying the Crystalline Basement Complex. The latter is fractured and jointed in some places and cut across by dikes. The water table lies between the weathered zone and the crystalline basement complex (Hazell, 1992).

A clearer picture of the basement complex is shown in the following well log obtained by Messrs Preussag Limited (Drilling Engineers). The well log was obtained at Jama'a village (Fig. 2. 2). This shows that the topsoil is lateritic consisting of clayey silty material which may be up to 9 m thick. The second layer consists of fine sand. These two layers overlie the weathered basement rocks. Below the weathered basement is the fresh basement.

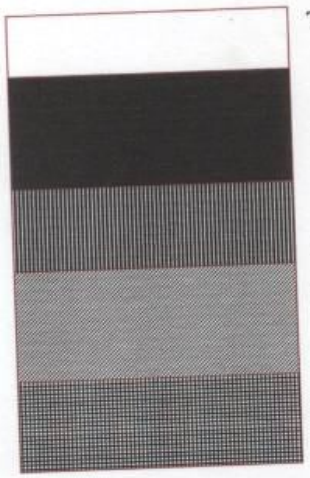


Fig. 2. 2 Geological Well-Log obtained by Preussag Ltd in Jama'a Village (Courtesy of Kaduna State Water Board).

The most predominant physical property sought for is the resistivity of these rocks. Table 2.1 shows the resistivity values of rock types in the Nigerian Basement Complex (Ajayi and Hassan, 1989)

Table 2.1. Resistivity Values of Rock Types in the Nigerian Basement Complex (Ajayi and Hassan, 1989)

Rock Type	Resistivity (Ωm)
Fadama loam	30-90
Sandy clay and sandy silt	100-200
Sand and gravel laterite	150 -1000
Weathered basement	20-200
Fractured basement	500-1000
Fresh basement	> 1000

2.2 Data collection

For an effective data acquisition to be carried out, a number of steps have to be followed. From the above stems the choice of electrode configuration, precautions, taken, instrumentation, and field procedure.

2.2.1 Choice of the Electrode Configuration

The Schlumberger array was chosen because of the following advantages it enjoys over Wenner array.

The Schlumberger required moving only two electrodes at a time compared to the four electrodes moved in Wenner array. Thus the field procedure is relatively simple requiring less labour and saves time.

Because the potential electrodes are kept constant, the near surface resistivity variation is constant. However for large values of the half spread length (L) it is necessary to increase the half electrodes spacing (*l) in* order to get a measurable potential.

The configuration has a greater depth of penetration compared to the Wenner. The Schlumberger array is legitimate as choice because over most part of Zaria area the depth of weathered basement rarely exceeds 30 m (Shemang, 1990).

2.2.2 The Schlumberger Array

This is an array in which the current electrodes are spaced much further apart than the potential electrodes. It corresponds to the two current electrodes at surface (Telford *et al.*, 1976).

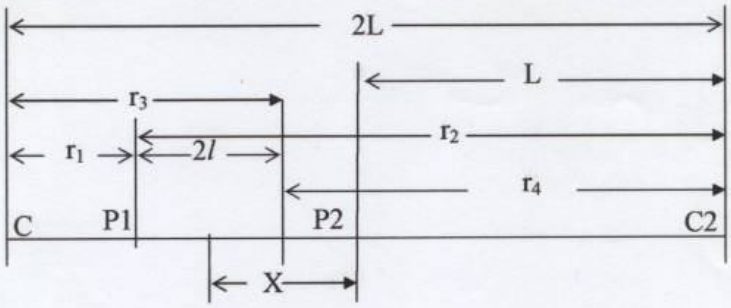


Fig. 2. 3 The Schlumberger general spread.

For the Schlumberger general (non-symmetric) spread shown in Fig *2.3*:

$r_1 = C_1P_1 = (L - x) - l$, $r_2 = C_2P_1 = (L + x) + l$,

$r_3 = C_1P_2 = (L - x) + l$, and $r_4 = C_2P_2 = (L + x) - l$

The smallest current potential electrode distance is always considerably greater than the distance between the two potential electrodes (factor of 10 or more), equation (2.11) becomes:

$$\rho_a = \frac{2\pi}{I} \frac{\Delta U}{\left[\frac{1}{(L-x)-l} - \frac{1}{(L+x)+l}\right] - \left[\frac{1}{(L-x)+l} - \frac{1}{(L+x)-l}\right]} \quad \text{..... (2.12)}$$

$$\rho_a = \frac{\Pi}{2l} \frac{[L^2 - x^2]\Delta U}{[L^2 + x^2]I} \quad \text{..... (2.13)}$$

For the case, the symmetrical Schlumberger spread that $x = 0$, and the equation above becomes:

$$\rho_a = \frac{\pi l^2}{2l}\left(\frac{\Delta U}{I}\right) \quad \text{..... (2.14)}$$

Putting $x = 0$ in equation (2.12) give the expression for the case when the electric field is approximately measured. This is the practical case:

$$\rho_a = \pi[\,L^2/2l - l/2]\Delta U/\,I = K\Delta U/I \quad \text{.............................. (2.15)}$$

Where K is the geometric factor $K = \pi[L^2/2l - l/2]$,

and:

$$\frac{\Delta U}{I} = R(\Omega),$$

is directly read from the terrametre.

2.2.3 Precautions taken

Before starting the measurements, a continuity test for all the cables was carried out. After each day's work, a continuity test for all the cables are repeated in order to make sure that the cables were in correct order and ready for the field work on the following day.

To obtain a satisfactory performance of the terrametre, the battery was connected to the mains in order to maintain the 12 V nominal voltage.

Two spare crocodile clips were taken to the field. Apparent resistivities were calculated and then plotted, while in the field according to Milsom (1988). Due to poor data quality the sounding at the following stations; VES4, VES8, VES9, VES12, VES14, and VES30 were repeated.

2.2.4 Instrumentation

For this survey, ABEM terrametre SAS300 was used. The ABEM Terrametre controls and indicators are shown in fig 2.4. Its microprocessor consists of three basic sub-units for the performance of the following: monitoring, control, and computation. The power supply consists of an electrically isolated transmitter

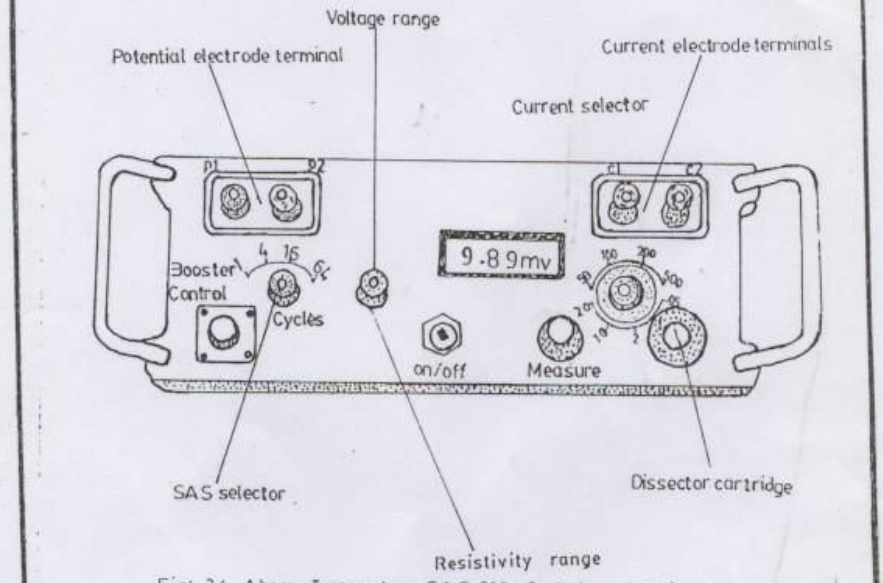


Fig: 2.4 Abem Terrameter SAS 300 Controls and Indicators

20

providing regulated signal currents. There is a receiver for the discrimination and measurement of the voltages correlated with the transmitted current signal.

This instrument can be used for electrical resistivity surveys as well as self-potential surveys. The terrametre SAS300 measures signal voltages created by the transmitter signal current with rejection of both DC voltage and noise when operating in the electrical resistivity mode, (Atlas Copco. ABEM, 1981).

2.2.5 Field Procedure

The fieldwork consisted basically of two parts namely normal depth sounding and radial depth sounding. Fig 2.5 below shows the typical Schlumberger array used in the fieldwork. A and B represent the current electrodes, while M and N represent the potential electrodes.

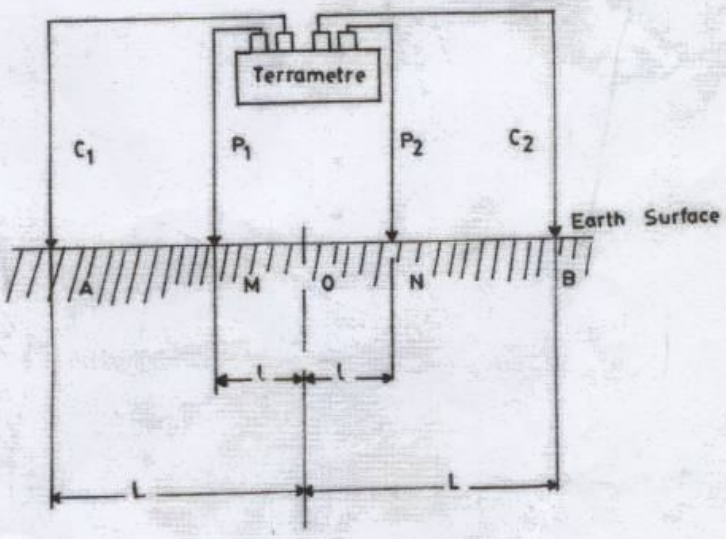


Fig. 2. 5 The Schlumberger Symmetric Spread used in the Field Work.

AB/2 = L, while MN/2 = *l*

The field procedure was effected by expanding the current electrodes A and B while keeping the potential electrodes spacing constant unless at crossover points,

21

Table 2.2 Azimuth and Locations of the 39 VES Stations.

LOCATION	AREA "G".					AREA "F"						
STATION	VES 1	VES2	VES3	VES 10	VES 11	VES 14	VES 22	VES23	VES 24	VES 30	VES 31	VES32
AZIMUTH	E-W	E-W	E-W	E-W	E-W	NE-SW	E-W	E-W	NE-SW	E-W	NE-SW	E-W

AREA "E"					IAR	IAR	ESTATE DEPT.	EAST OF ESTATE	CROP PROT. DEPT.	NAERLS		EAST OF NAERLS
VES4	VES5	VES12	VES13	VES21	VES6	VES7	VES 8	VES 9	VES15	VES16	VES17	VES 18
E-W	E-W	N-S	E-W	E-W	E-W	E-W	E-W	E-W	E-W	E-W	E-W	E-W

NAERLS PROJECT FIELD		GYMNA-SIUM	AREA BZ								BEHIND DANFODIO	PHARM DEPT.	WATER RES. DEPT.
VES25	VES26	VES27	VES 28	VES33	VES34	VES 35	VES 36	VES 37	VES 38	VES39	VES 19	VES 20	VES 29
E-W	N-S	N-S	NNE - SSW	N-S	N-S	N-S	E-W	E-W	SE-NW	E-W	E-W	NE-SW	N-S

2. 2. 6 Radial Depth Soundings

Five radial depth soundings were carried out at suitable locations in the river channels. The station number, azimuth, and locations are shown in table 2. 3.

Table. 2. 3. Azimuth and location of the radially sounded stations

Stations	Locations	Azimuth		
		Direction ρ_1	Direction ρ_2	Direction ρ_3
VES14	River Samaru	N-S	SW-NE	NW-SE
VES24	River Samaru	N – E	NW - SE	E - W
VES32	River Samaru	NW-SE	NE-SW	E-W
VES28	River DanFodio	SE-NW	ENE-WSW	NNE-SSW
VES36	River DanFodio	NW-SE	NE-SW	E-W

2.2.7 Problems Encountered

The work was slow (prior to mastering of the terrametre. Moreover, the data quality leaves much to be desired. It was in respect of this problem that the six stations mentioned in section (2. 2. 3 above) were repeated. Rugged topography as well as buildings made it compulsory to choose azimuth to convenience. Where river flowed, the azimuth was taken perpendicular to the watercourse.

2.3 Data Processing

Much of the geophysical surveying is concerned with the measurement and analysis of waveforms and sectors that express the variation of some measurable quantity as a function of distance or time or both of them. The variation of resistivity of earth materials with distance that is both depth and extent is a case in point.

where at least two readings were recorded for the same value of distance AB/2, but two different values of l.

The following values of (L) were used: 1.00, 1.50, 2.50, 3.75, 5.00, 7.50, 10.00, 15.00, 25.00, 37.50, 50.00, 75.00, 100.00 and 150.00 m. Three values of l were used namely 0.5, 1.5 and 5.0 m. The spacing MN/2 = 0.5 m was used for the first seven values of AB/2 with crossover at 7.5 and 10 m, and a new value of MN/2 = 1.5 m was used for L = 15.00, 25.00, 37.50 and 50.00 m; with crossover at L = 37.50 and 50.00 m. For the Schlumberger symmetric spread, the geometric factor $K = \pi(L^2/2l - l/2)$ was utilised in the conversion of the resistance to resistivity values at each sounding point.

The survey consists of thirty-nine VES stations located on five profiles viz: P_1, P_2, P_3, P_4 and P_5; each of them parallel to Sokoto Road (azimuth E-W). The profiles; P_1, P_2, P_3, P_4 and P_5 consist of the following number of VES stations respectively: 10, 10, 9, 7 and 3. However, the azimuth and location of each VES station were chosen according to the field convenience and shown in table 2.2.

Figure 2.6 shows the map portraying profiles and their respective VES stations.

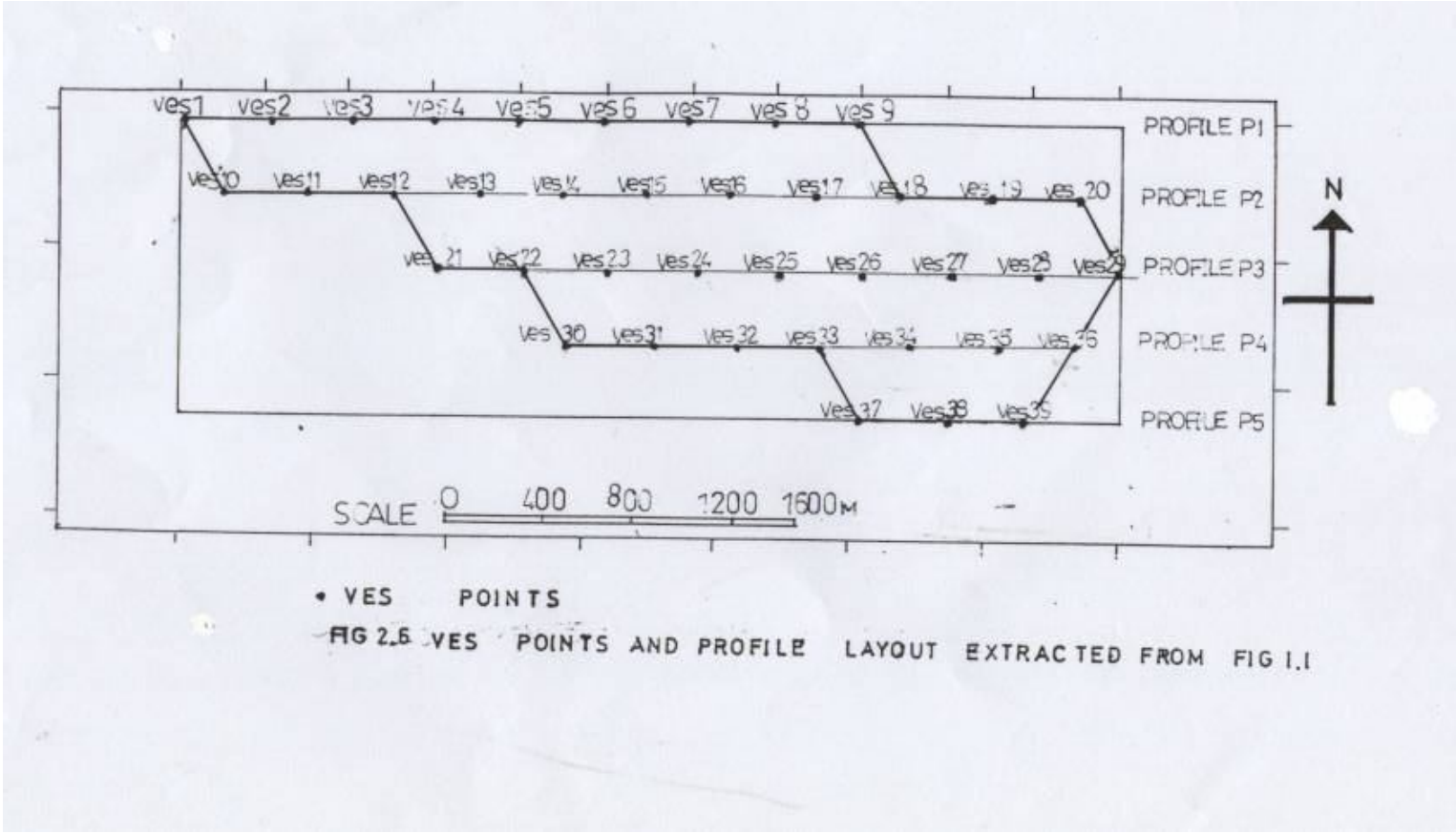


FIG 2.6 VES POINTS AND PROFILE LAYOUT EXTRACTED FROM FIG 1.1

Both of the normal depth soundings and the radial depth soundings were processed using equation (2.15 b) in section (2. 2. 2). The geometric factor for each electrode spread was multiplied by the corresponding terrametre reading in ohms to obtain the apparent resistivity value in ohm-metre. However, radial and normal soundings differ markedly in the way they are plotted. The former is a linear curve while the latter is a log-log curve.

2.3.1 Normal Depth Sounding

The computed apparent resistivity (ρ_a) values obtained for the various spacing at any given station (location) were plotted against their corresponding AB/2 values. Figure (2.7) shows the interpretation of the field curve at VES01. This curve is of H-type (Telford et al., 1976). The first layer has a resistivity of 158Ωm. Field evidence showed that the first layer is sandy clay. The second layer of resistivity 98Ωm most likely represents the weathered basement, whereas, the third layer with resistivity 3875Ωm most likely represents the fresh basement (Ajayi and Hassan, 1989).

Appendix I shows the entire field curves used in this work. On the other hand, appendix II shows the results of the various VES interpretations of the field curves depicting the VES station numbers, number of layers, resistivity values, layer thicknesses, and interface depths, for all the thirty-nine VES stations.

2.3.2 Radial Depth Sounding

A total of five radial depth soundings were carried out, namely at the following stations: VES14, VES24, VES28, VES32 and VES36. The apparent resistivity values are plotted on a linear graph paper. The origin was taken as the station location. Then the apparent resistivity values were marked on either sides of

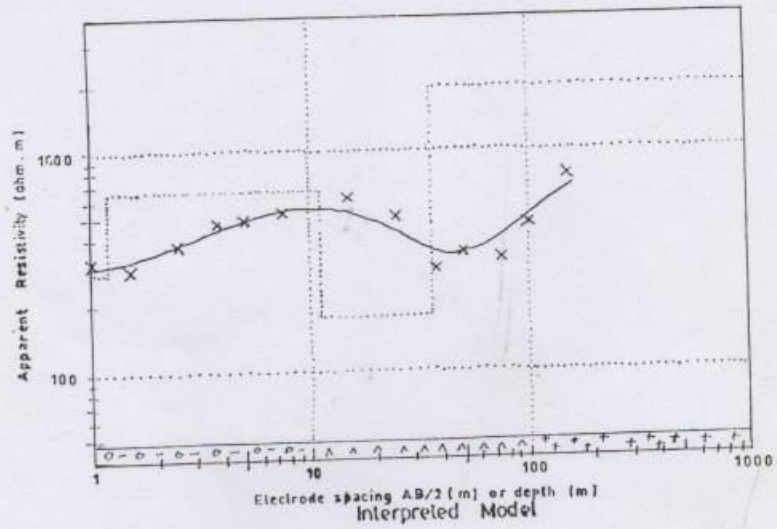
Vertical Electrical Sounding VES 01

(Schlumberger Array)

KONA BIYE

11 June 2000

Orientation 001A



Interpreted Model

Layer	Resistivity (ohm. m)	Thickness (m)	Depth (m)
1	280	1.2	1.2
2	650	10.0	11.2
3	175	24.8	36.0
4	1095		

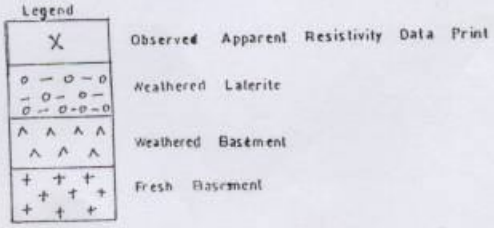


Fig: 2 7 Interpretation of Field Curve for VES 01

the particular station as we proceeded away from it. Then a curve joining the six points of equal spacing (AB/2) was drawn, giving the radial plot, for that station. All the radial plots are shown in appendix III.

A preliminary interpretation of the normal depth sounding field curves were made to provide the following parameters: resistivity values, thickness as well as the depth to each layer, (Milsom, 1988). These parameters were fed into the computer for further processing of the interpretation. The preliminary interpretations were carried out in order to minimise the number of iterations the computer would have to carry out before the final interpretation was completed. The interpretation was carried out using the interpretation software Sondel. The basic procedure followed in the interpretation is as follows:

i. a trial model was first assumed

ii. then a theoretical field curve was computed using the trial (initial) model;

iii. the computed curve was compared with the observed (field) curve and their errors (differences) were calculated;

iv. the model was modified as necessary and steps (ii) and (iii) repeated to improve the agreement between the computed and the observed data until the "best" possible fit was obtained.

The above procedure was used for the data collected at each of the thirty-nine VES stations sounded.

CHAPTER THREE
DATA INTERPRETATION AND RESULTS

3.0 Data Interpretation

The analysis of field curves and sections observed from the geophysical data represent the most essential aspect of geophysical data processing and interpretation. The geoelectric and geologic interpretation of the entire data obtained in the field work is discussed below.

3.1 Interpretation of the Electrical Data

Electrical surveys are among the most difficult of all the geophysical methods to interpret quantitatively because of the complex theoretical basis of the technique. In resistivity interpretation, mathematical analysis is most highly developed for VES, less for constant spacing traverse (CST) over two dimensional structures and least for CST over three dimensional bodies (Kearey and Brooks, 1988). The resistivity method utilizes a potential field and consequently is subject to ambiguity problems as the gravity and magnetic methods. Moreover, the potential field involved requires a solution using Laplace's equation and insertion of the boundary conditions for the particular structure under consideration, or by integrating directly. This further complicates the problem. In practice, however, the geophysicist must be blessed with sound experience and a perfect knowledge of the geology of the area under trial.

3.2 Results

The result from the field curves VES show that most of them are H-type curves, out of which twenty-eight of them are bell-shaped. It is assumed that the

geological formation are continuous between the VES points in producing the geoelectric and geologic sections and the production of various geophysical maps, namely: surface layer thickness, surface layer resistivity, weathered layer resistivity, basement resistivity, and depth to basement.

3.2.1 The Geoelectric Sections

The essence of any resistivity work is the production of a set of geoelectric and geologic sections as well as contour maps. The thirty-nine stations were partitioned into five profiles: P_1, P_2, P_3, P_4 and P_5 . All the five profiles have an east-west azimuth.

Profile P_1: This profile consists of the first nine VES stations namely, from VES01 to VES09. The minimum number of layers is three and the maximum is five. This profile is 3.2 km long with azimuth east west along the
A. B. U. fence bordering Sokoto Road.

The first layer resistivity ranges from 44 Ωm at VES08 to 553 Ωm at VES05 and is the thinnest of all of them as shown in Fig. 3.1. The second layer is irregularly shaped in the sense that three of them are arranged vertically rather than horizontally. The resistivity values range from 12 Ωm at VES07 to 650 Ωm at VES01. The third layer has a resistivity ranging from 111 Ωm at VES09 to 3569 Ωm at VES03, with the latter being a representative of the fresh basement. The fresh basement resistivity values range from 1063 Ωm to 3641Ωm and represents the fourth layer for the following VES stations: VES1, VES4, VES5, VES7, VES8, and VES9. At VES02, the fresh basement is the fifth layer; whereas, at VES03, the fresh basement is at the third layer.

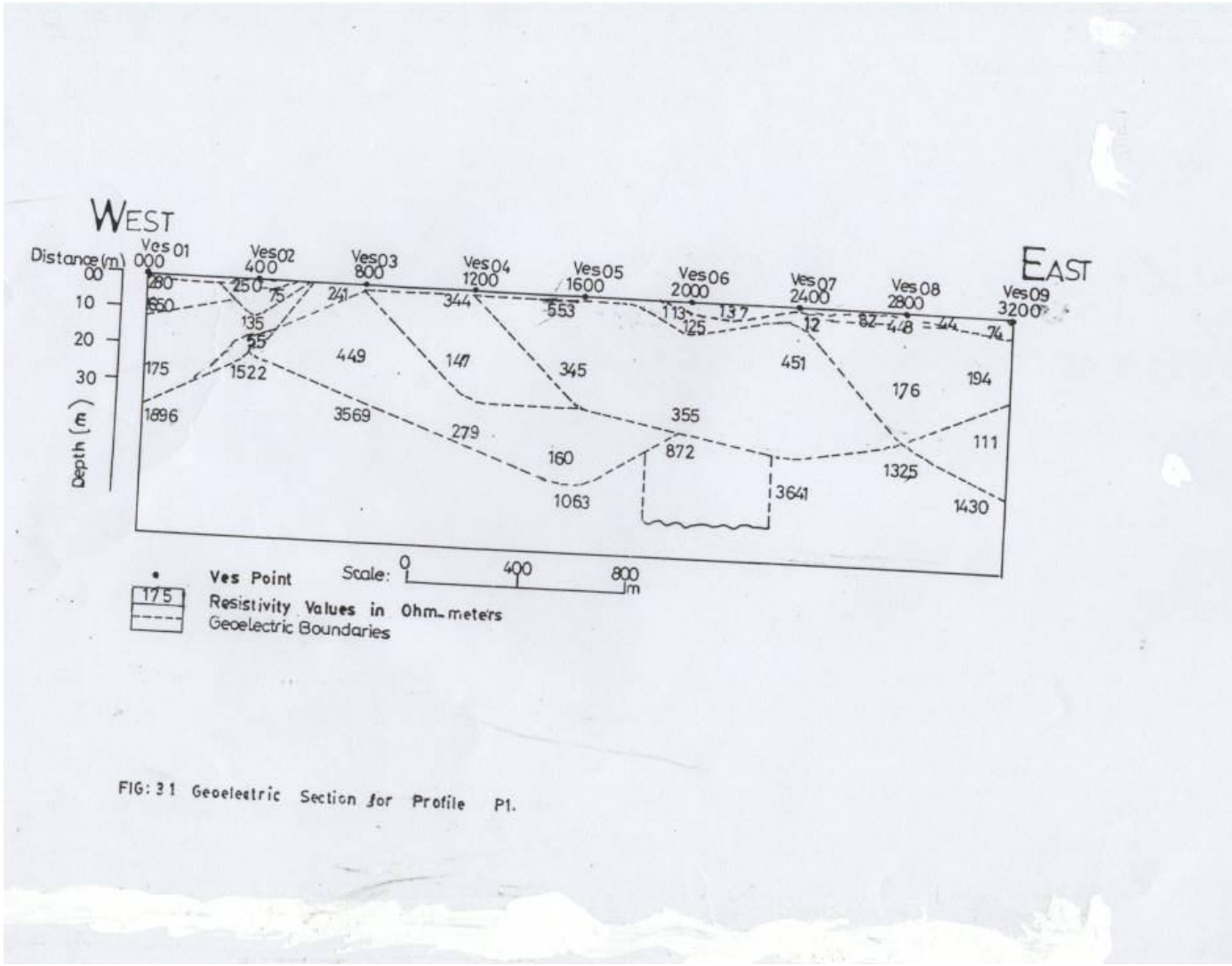


FIG: 3 1 Geoelectric Section for Profile P1.

The depth to basement varies between 21.0 m at VES02 and 53.55 m at VES05. However, at station VES06, the depth to the basement is beyond the sensitivity of our maximum electrode spread. The first layer thickness varies from 0.2 m (VES02) at the surface of the earth to 6.00 m at VES09.

Profile P_2: This profile consists of eleven stations namely: VES10 to VES20. The number of geoelectric layers underlying each VES station along this profile is four except at station VES17 having three geoelectric layers as shown in Fig. 3.2. The first layer thickness varies between 0.35 m at station VES16 and 5.71 m at station VES15. On the other hand, the first layer' highest resistivity value was recorded at station VES13 of resistivity value 1350Ωm and the lowest resistivity value was recorded at station VES15 with a resistivity value of 58Ωm. the second layer thickness varies from 0.86 m at station VES19 to 9.00 m at station VES18. The second layer resistivity values vary from 2005.00Ωm at VES13 to 32.54Ωm at VES14. The third layer resistivity values range between 250.00Ωm at VES13 to 17.00Ωm at VES20, with exception of the resistivity value of 3165.17Ωm at VES17. The former range of resistivity values is part of the overburden while the latter resistivity value of 3165.17Ωm most likely represents the resistivity of the fresh basement not only because of the relatively high resistivity value but also because of infinite thickness. The fourth layer resistivity values range between 1009.80Ωm at VES19 to 3080.00Ωm at VES20 except at station VES10 and VES14 of respective resistivity values 557.40Ωm. The former most likely represents the fresh because of its higher resistivity values and infinite depth while the latter may strongly represent part of the overburden.

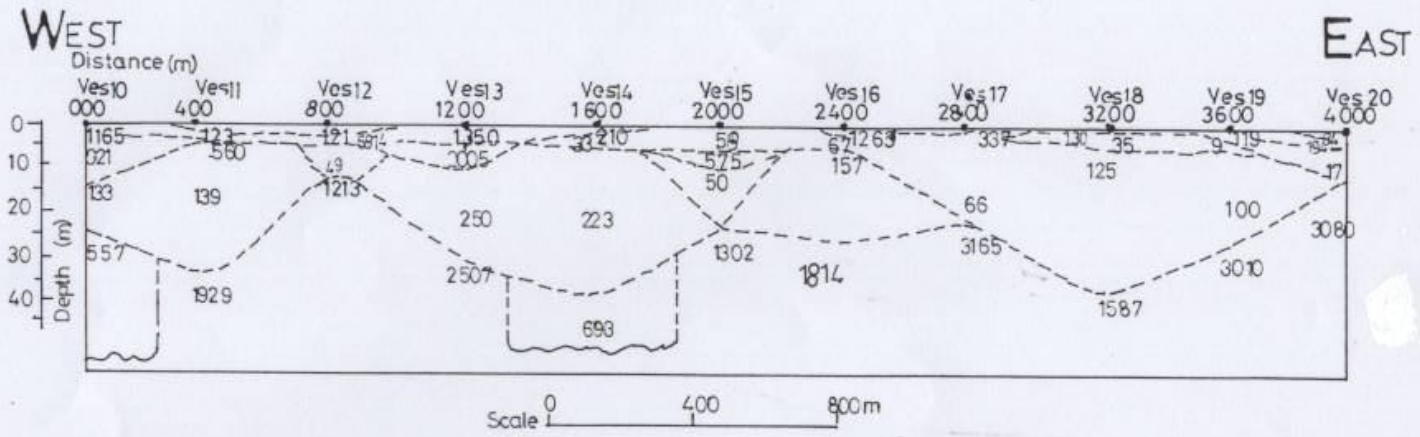


Fig: 3-2 Geoelectric Section for Profile P_2

Finally, the overburden is deepest at either station VES10 or VES14, however, finite estimate shows that it is deepest at station VES18; 42.00 m.

Other thicknesses of geographical interest as per the aim and objectives of this work are 38.52 m, 38.52 m, 34.10 m, 41.96 m, 24.03 m, 27.57 m, 23.64 m, 42.00 m and 29.67 m at stations VES10, VES11, VES13, VES14, VES15, VES16, VES17, VES18 and VES19 respectively.

Profile P_3: This profile has an east-west azimuth as shown in Fig. 3.3 and consists of nine stations viz: VES21, VES22, VES23, VES24, VES25, VES26, VES27, VES28 and VES29.

Profile P_3 has three categories of layers as far as their number per station is concerned. Stations VES24, VES25, VES26, VES27 and VES28 have three geoelectric layers, station VES23 and VES29, four layers each while stations VES21 and VES22 have five layers each.

The first layer resistivity value range between 698.00 Ωm at station VES21 to 76.00Ωm at VES24 with respective thicknesses 0.88 m and 0.80 m. however, the highest resistivity was recorded at station VES25, 1.00 m thick while the lowest resistivity value was recorded at VES23 only 0.23 m thick. The second thickness varies from 14.98 m at station VES26 to 2.65 m at VES25. The resistivity values for these layers vary between 222.00 Ωm at VES25 to 33.00 Ωm at station VES29. A cluster of very thing geoelectric layer can be identified at along the profile portion encompassed between stations VES21 to VES23. However, one trend is sure: the over burden lithological stratification seems to strictly obey the normal weathering process. Nonetheless, three divergences to this observation can be readily identified at stations VES21, VES22, VES27 and VES29 as the existence of vertical extents

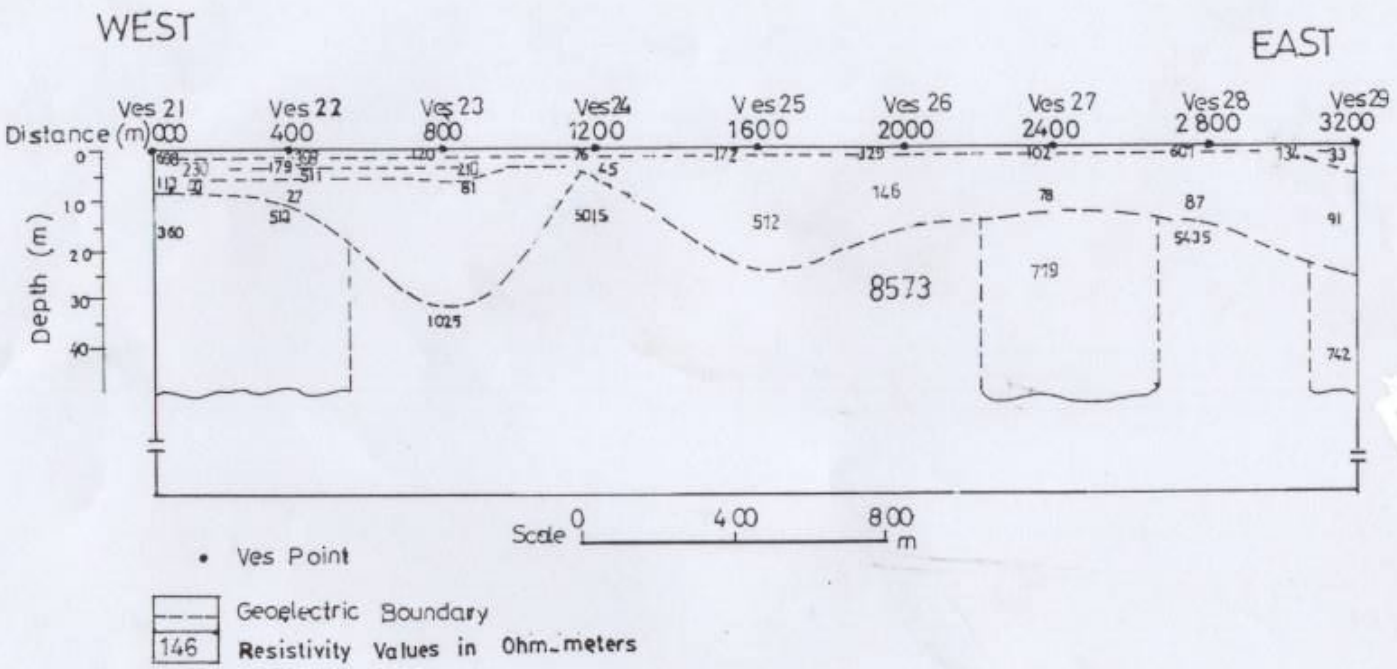


Fig: 3.3 Geoelectric Section for Profile P_3

beyond the sensitivity of our electrodes' spread. The third geoelectric layer at station VES24, VES25, VES26, VES27 and VES28, the forth geoelectric at stations VES23 and VES29, the fifth geoelectric layer at stations VES21 and VES22 most likely represent the fresh basement not only because of their relatively high resistivity values(> 1000Ωm) but also because of their infinite thicknesses.

Last but not least, the overburden is likely deep at VES21, VES27 and VES29 for the reasons pertaining thickness and intermediate resistivity values. Other interesting features of the overburden as per thickness concerns are also exhibited at stations VES21 and VES22.

Profile P_4: This profile consists of seven stations namely: VES30, VES31, VES32, VES33, VES34, VES35 and VES36 as shown in Fig.3.4. It consists of three horizontal layers showing the normal succession of weathering process from the surface of the earth to the fresh basement. The first layer has thickness fluctuating between 0.53 and 2.10 m. Its resistivity varies between 86 Ωm west of area F at VES30 and 201Ωm at the extreme end of the traverse at VES36.

The second layer is thickest (23.43m); below VES34 at the centre of area BZ with resistivity fluctuating between 43 and 150 Ωm. The third layer is of infinite thickness with a minimum resistivity of 1048 Ωm west of area F.

Profile P_5: This is the shortest profile as it consists of three stations only namely: VES37, VES38, and VES39 as shown in Fig. 3.5. The number of layers is three at VES37 and VES38 and four at VES39. The first layer has thickness of less than 1m throughout the profile, and resistivity of 92 Ωm at VES37, 138 Ωm at VES38, and 363 Ωm at VES39.

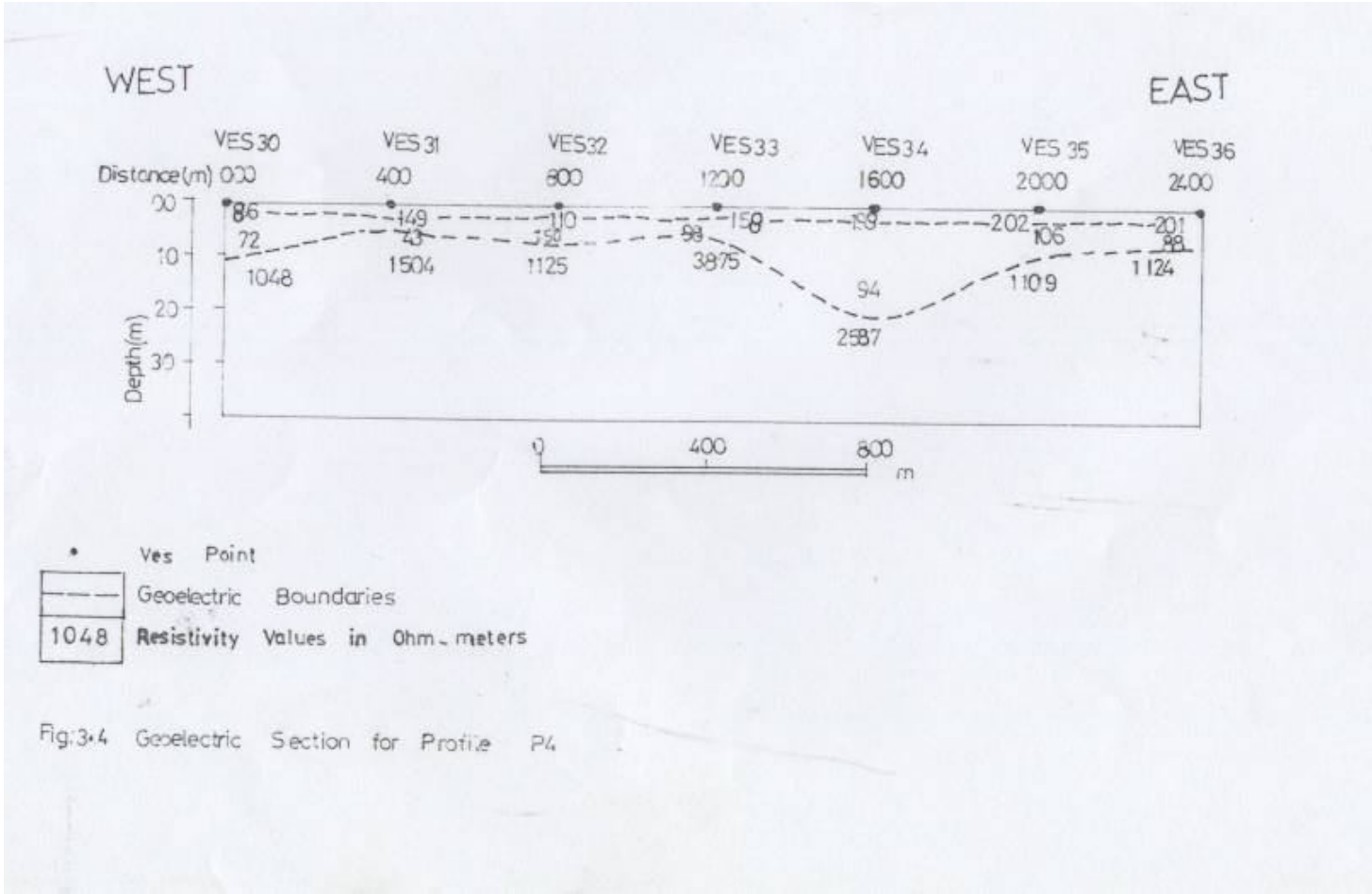


Fig. 3.4 Geoelectric Section for Profile P4

The second layer thickness at VES39 is 27 m and a resistivity of 97Ωm, it is about 4 m and a resistivity of 68 Ωm at VES37 and 38 Ωm at VES38. The third layer at station VES39 has a thickness of 3 m and a resistivity of 145Ωm.

3.2.2 The Geologic Sections

It is assumed that the geologic formations are continuous between VES points in producing the geoelectric sections as well as in the production of the various geophysical maps. The geologic interpretation of the geoelectric sections would be pointless without an effective use of some geological controls (Worthington, 1977). The geologic sections of the profiles discussed in section 3.2.1 above are subsequently drawn based on the following geologic controls.

(a). The nature of each superficial materials encountered in the field were noted while at sounding station, (Milsom, 1988). The type, colour, and texture of these rocks around were equally noted.

(b). Use was made of borehole logs from basement areas compiled by Shemang (1990), Aminudeen (1990), Ajayi and Hassan (1988) as shown in table 2.1

Subsequently, table 3.1 below was used in deriving the geologic sections as well as the various geophysical maps. It takes several thousand years before the geologic history of an area can change (Hockney, 1986). In view of this, it was assumed that the variation of resistivity of the earth materials at present will be negligible from the past works. Therefore, the error would be insignificant. By collating this information, the first step in obtaining the geologic sections was to convert each layer of the geoelectric sections, showing the different geoelectric

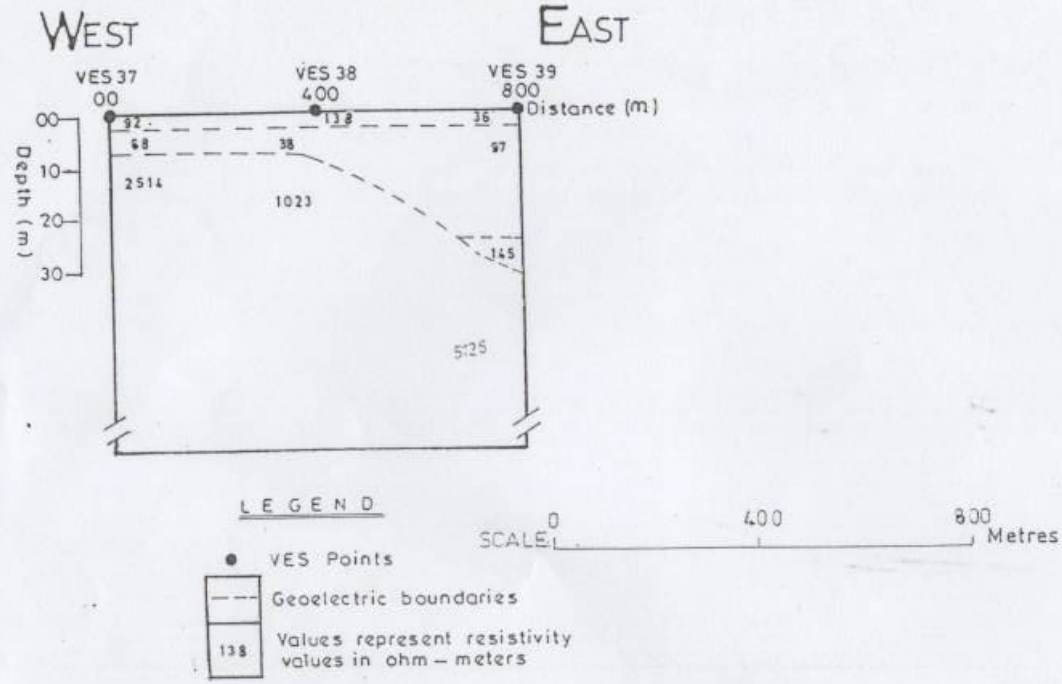


FIG. 3.5 : GEOELECTRIC SECTION FOR PROFILE P_5

Table: 3. 1 Resistivity Values used in deriving the Geologic Sections in this Work.

Rock Type	Resistivity (Ωm)
Fadama loam	30-140
Wet clay	20-30
Wet sandy clay	20-30
Sandy clay and sandy silt	91-200
Weathered laterite	201-850
Fresh laterite	851-3500
Weathered basement	10-499
Fractured basement	500-1000
Fresh basement	> 1000

Geologic Section for Profile P_1: The geologic section for the normal depth sounding obtained along Sokoto Road is shown in Fig 3.6. This section consists essentially of three geologic layers viz: the top soil consisting of a group of layers, the weathered basement and the fresh basement. However, third geologic layer at station VES06, of resistivity value 872Ωm most likely represents the fractured basement because its resistivity values range between 500Ωm to 1000Ωm normally associated with fractured basement (Ajayi and Hassan, 1989).

As earlier started the first layer represents the top soil. It resistivity values varying between 12.00Ωm at VES06 to 650.00Ωm at VES01. The rock types making up the top soil are wet sand, fadama loam, wet clay and weathered laterite as testified by field evidence. The wet sand occurred only at VES02 with a thickness of 0.2 m and resistivity value of 250.00Ωm. Fadama loam of resistivity value ranging from

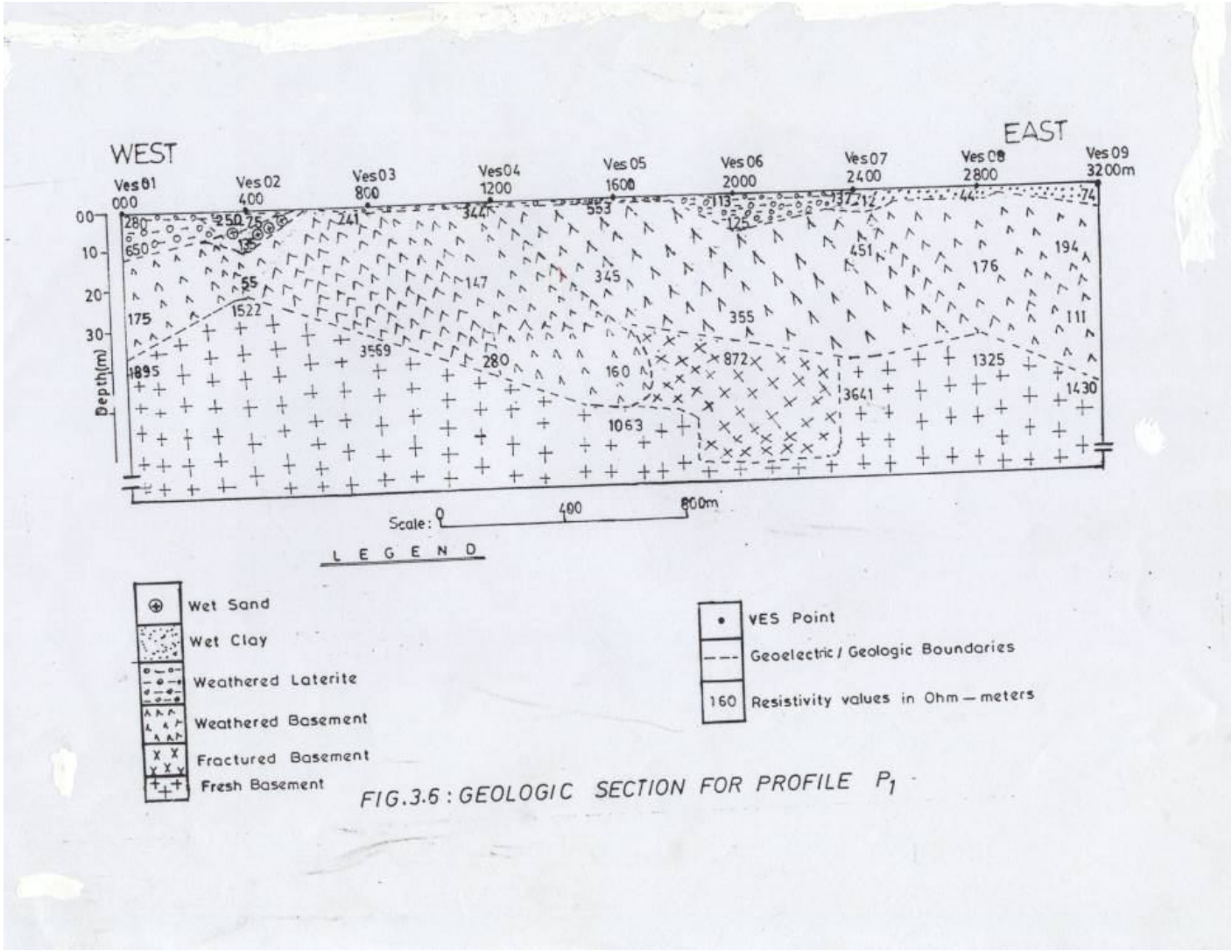


FIG.3.6 : GEOLOGIC SECTION FOR PROFILE P_1

44Ωm at VES08 to 137.00Ωm at station VES07 constitutes the top soil right from VES06 to VES09 wet clay of resistivity value 22.00Ωm at VES07 most likely underlies the fadama loam because its resistivity values are comprise within the range from 20Ωm to 30Ωm, normally associated with wet clay (Ajayi and Hassan, 1989). Weathered laterite of resistivity values ranges from 241Ωm at VES03 to 650Ωm at VES01 of respective thicknesses 1.69 m and 11.20 m where also encountered. The weather basement constituted a very thin layer between VES03 to VES05.

The second geoelectric layer most likely represents the weathered basement because its resistivity values are within the range from 55Ωm to 451Ωm (Ajayi and Hassan, 1989). The weathered basement is thickest at VES05, 52.55 m and thinnest at VES02 having a thickness of 20.80 m.

The third layer at VES06 most likely represents the fractured basement because its resistivity values is within the range 500Ωm to 1000Ωm, normally associated with fractured basement (Ajayi and Hassan, 1989). Mention of the fact that the thickness of this layer is beyond the sensitivity of our electrodes' spread.

Elsewhere the fresh basement is most likely represented by the third layer because its resistivity values are within the range 1000Ωm and above, normally associated with fresh basement (Ajayi and Hassan, 1989).

Geologic Section for Profile P_2: This profile consists of four geologic layers: the weathered basement, the fractured basement and the fresh basement or for resistivity values are concerned as shown in Fig. 3.7. The topsoil shown by field evidence consisted of fadama loam, weathered laterite and fresh laterite. Fadama loam was observed to exist at VES15, in between stations VES11 and VES12 and also from

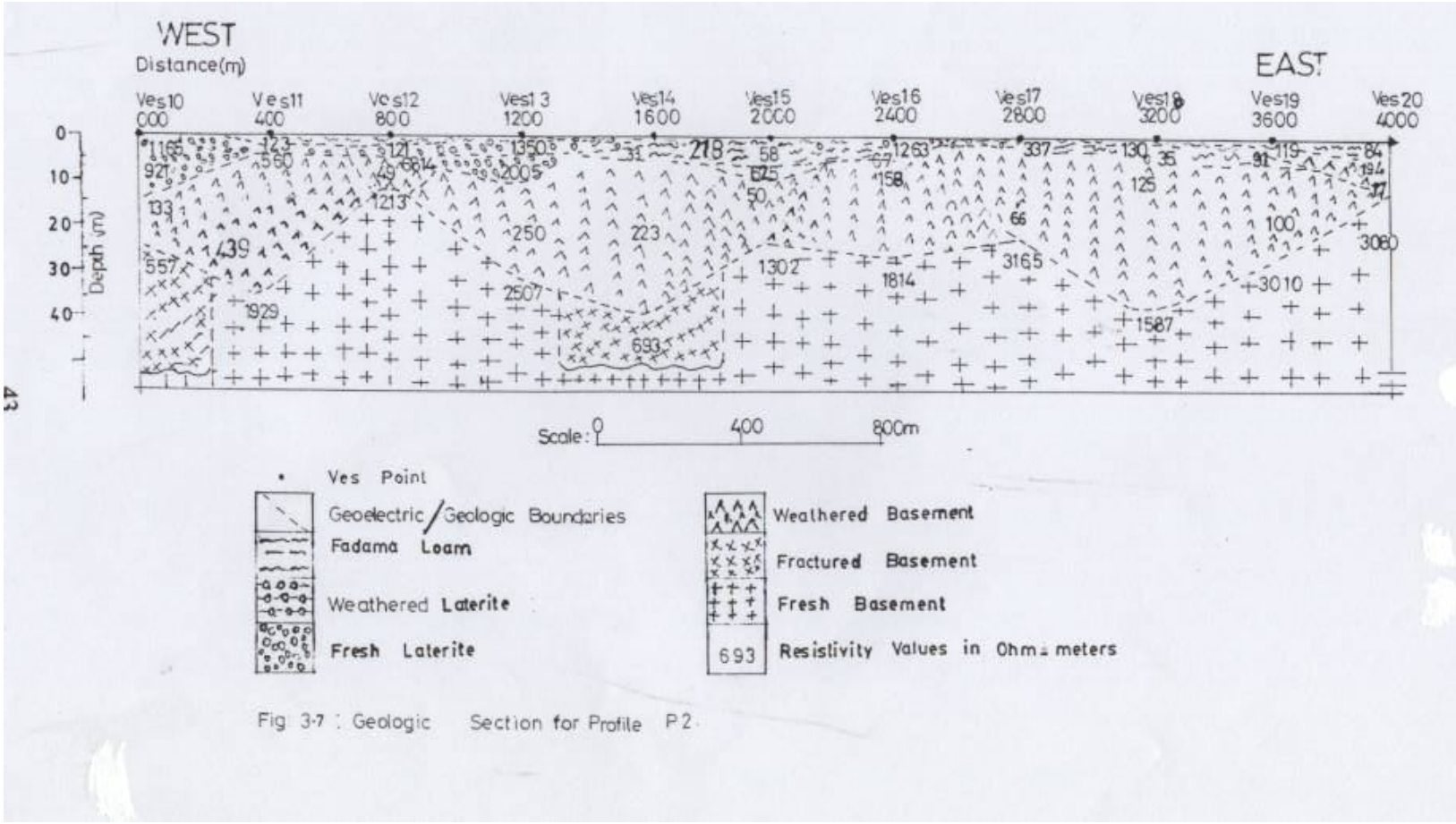


Fig 3-7 : Geologic Section for Profile P2

VES18 to VES20. The lowest resistivity value of this rock type was 58.00Ωm at station VES15 while the highest resistivity value was 130.00Ωm at station VES18. This rock type is thickest at VES18; 4.0 m and thinnest at VES20; 0.61 m only.

Laterite rock as observed to take alternate position of the Fadama loam at the surface of the profile. Therefore, fresh laterite was known to exist between VES10 and VES11 and in between VES12 and VES14 and at VES16. Its resistivity values peaked at VES12 (6814Ωm) where the lowest of the three resistivity values was 1165Ωm sampled at VES10. This rock types is thickest (14.61 m) at VES10 and thinnest at VES16 (0.35 m).

A thin film of weathered layer cover was observed in between VES11 and VES12, somewhere in between VES13 and VES15, exactly sampled at VES14. Underlying the top soil is most likely the weathered basement from one end of the profile to the other. This statement is almost true because its resistivity values range from 33 Ωm at VES14 to 250Ωm at VES13 Normally associated with weathered basement (Ajayi and Hassan, 1989). This geologic layer is thinnest at VES11 and VES12 (6.25 m) and thickest at VES18 (41.12 m). The third geological layer at VES10 and VES14 most likely represents the fractured their resistivity values are within the range from 500Ωm to 1000 Ωm, normally associated with fractured basement (Ajayi and Hassan, 1989). Its depth is beyond the sensitivity of our electrodes' spread.

The information got from the weathered basement and the fractured basement present a very interesting feature as far as the ground water potential are concerned not only because of the relatively low resistivity values but also because of its substantial thickness. Geological speaking, the third layer represents the fresh basement. However, its infinite thickness as well as its resistivity values within the range from 1000Ωm and above most likely suggests the presence of the fresh basement (Ajayi and Hassan, 1989). This fresh basement is shallowest at VES11 and VES12 (6.25 m overburden thickness) and thickest at VES18 where the overburden thickness is 42.0 m

Geologic Section for Profile P_3: This profile consists of four types of geological layers viz: the top soil, the weathered basement, the fractured basement and the fresh

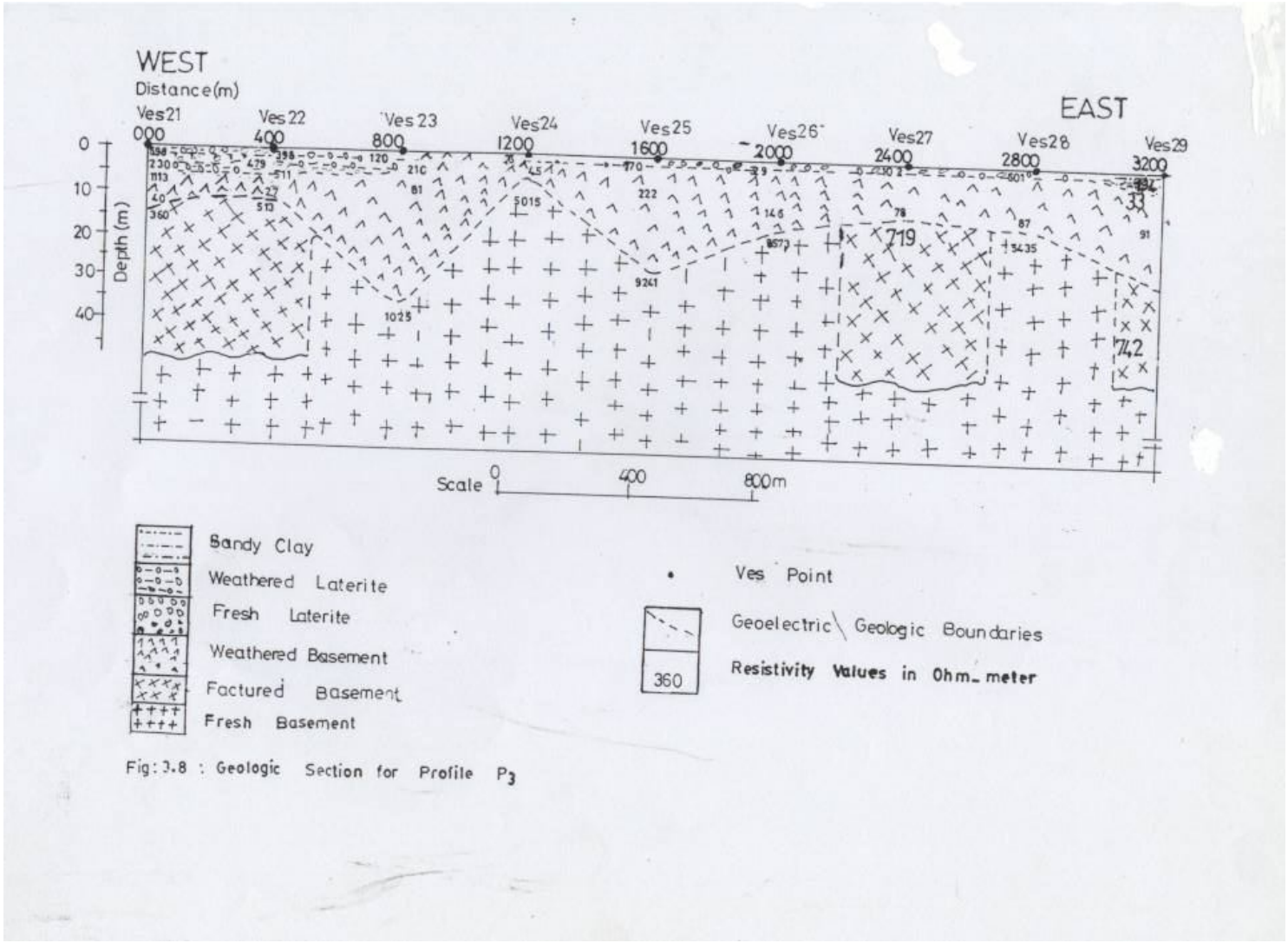


Fig: 3.8 : Geologic Section for Profile P_3

basement in terms of their resistivity as shown in Fig. 3.8. The top soil itself consists of four rock types namely: sandy clay, weathered laterite, fresh laterite and fadama loam from VES24 to mid way between VES28 and VES29. The top soil consist of a thin film of sandy clay, 0.8 m thick at VES23 1.0 m at VES25, 0.75 m thick at VES27 and 0.35 m at VES29: 18 film of weathered laterite 0.75 m thick at VES26 and 0.73 m thick at VES28. Sandy clay with a thickness 2.79 m at VES29 underlies the fadama loam. In between VES21 and VES22, weathered laterite of resistivity values ranging from 230Ωm to 698Ωm constitutes the top soil; with thickness varying between 2.35 m to 5.50 m. However, weathered basement is seen to extrude at VES24 inside Biye river (Area F) with respective resistivity range and thickness of 45Ωm to 76Ωm and
4.62 m.

The second geologic layer is most probably the weathered basement because its resistivity values range from 10Ωm to 499Ωm normally associated with weathered basement (Ajayi and Hassan, 1989). The thickness of this layer varies between 4.09 m at VES24 to 33.08 m at VES23.

The third layer at VES21, VES22, VES27 and VES29 with depth beyond the sensitivity of the highest electrodes' spread most likely represents the fractured basement because its resistivity values are within the range from 500Ωm to 1000Ωm, normally associated with the fractured basement (Ajayi and Hassan, 1989). The third geologic layer at VES23, VES24, VES25, VES26 and VES28, and the forth geologic layer at VES21, VES22, VES27 and VES29 most likely represent the fresh basement because its resistivity values are within the range 1000 Ωm and beyond, normally associated with the fresh basement rocks (Ajayi and Hassan, 1989).

Geologic Section for Profile P_4: The geologic section for this profile is shown in Fig 3.9, which consists of three geologies layers. The first layer, most likely, consists of two rock types and its thickness (3m) shows that it is the topsoil. During the fieldwork, clay was observed to exist in the ground surface right from inside Area F (VES30), to Area BZ at the junction between Sardauna Road and Bowuna Road (VES34). The second rock type most likely represents the weathered basement

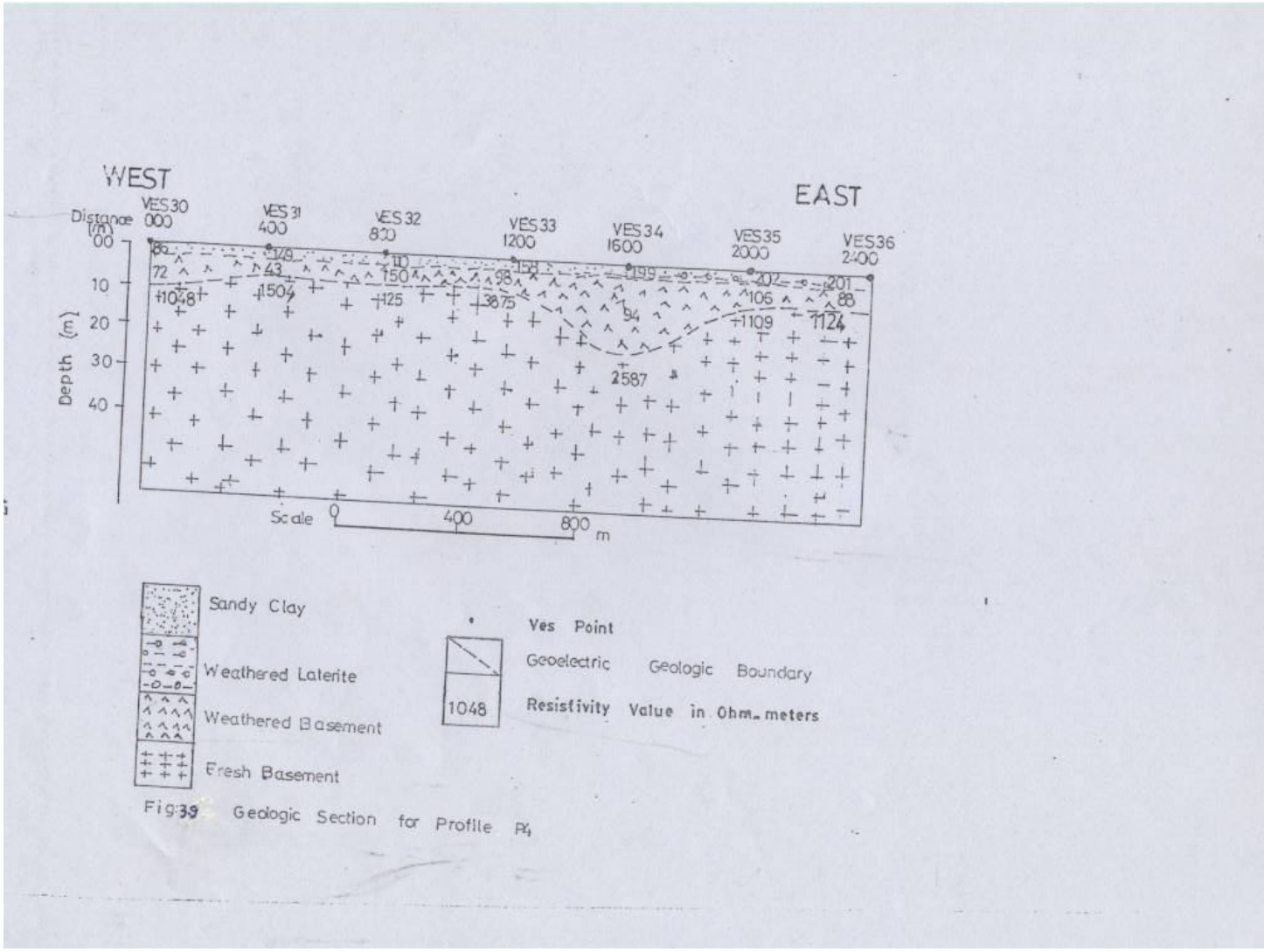


Fig 39 Geologic Section for Profile P4

because its resistivity values range between 10Ωm and 499Ωm, normally associated with weathered basement (Ajayi and Hassan, 1989). It extends to the top layer from Samaru Creek near VES36 to VES20 and VES29. It is narrowest at VES33, 15m S-E of flat BZ 16, and thickest at VES34, junction between Sardauna Road and Bowuna Road. The third layer is likely to be fresh basement because the resistivity values fall within the range 1000Ωm and above; this is normally associated with fresh basement. (Ajayi and Hassan, 1989). The fresh basement is shallowest at VES31 where it is only 2.68m deep and deepest at VES34 where it is 22.5 m.

Geologic Section for Profile P_5: The geologic section for this profile is shown in Fig. 3.10. It's the shortest profile as it consists of three VES stations: VES37, VES38 and VES39. This profile has three geologic layers. The first geologic layer represents clay as shown by field evident of thickness ranging from 0.63 m to 0.80 m and the resistivity values varying between 36Ωm at VES39 to 138Ωm as at VES38. The second geologic layer most likely represents the weathered basement because the resistivity values are within the range from 10Ωm to 499Ωm, normally associated with weathered basement (Ajayi and Hassan, 1989). The second geologic layer has thickness ranging from 4.00 m at VES37 to 30.10 m at VES39. The third geologic layer most likely represents the fresh basement because the resistivity values are within the range from 1000Ωm and above, normally associated with fresh basement (Ajayi and Hasaan, 1989).

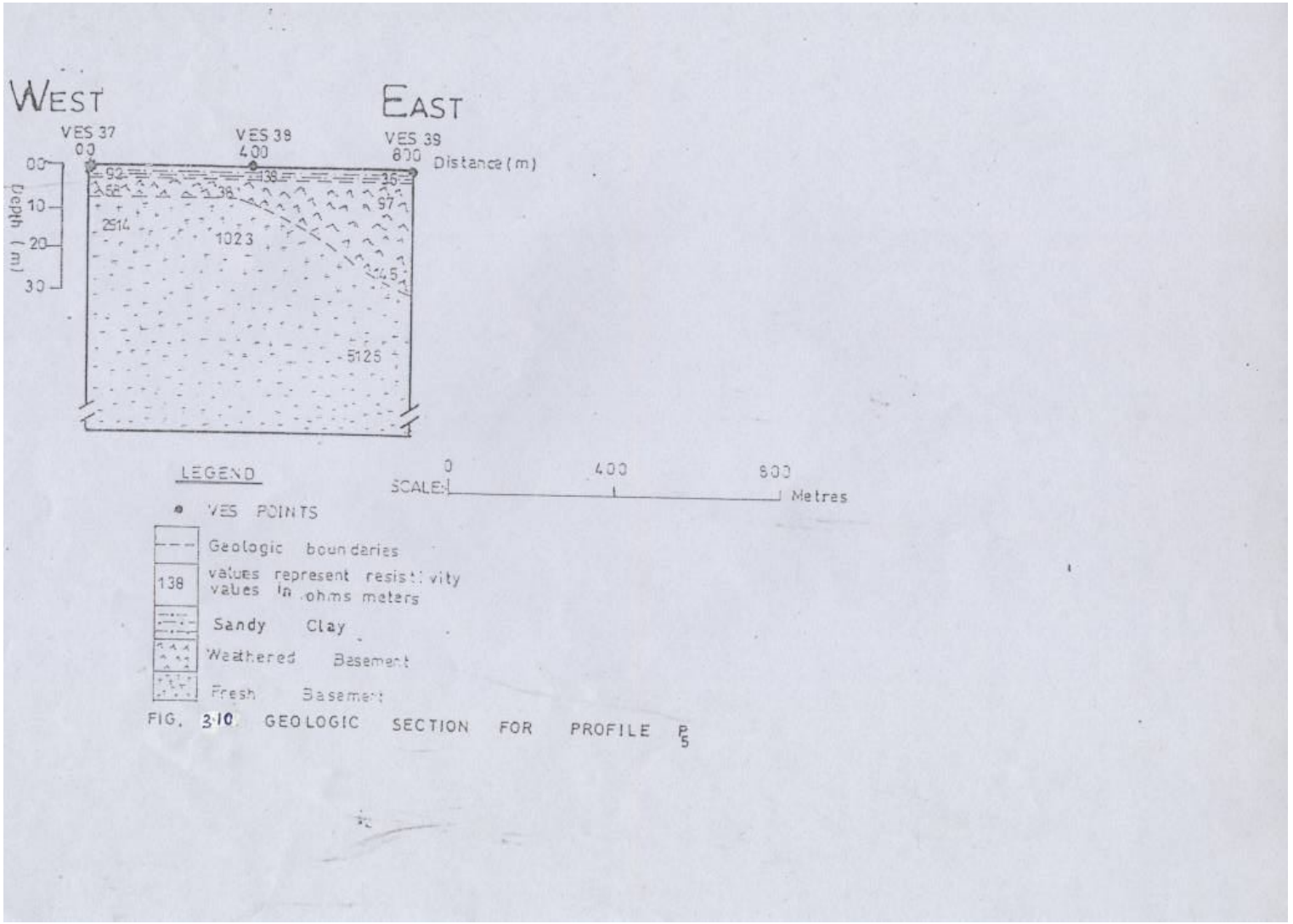


FIG. 3.10 GEOLOGIC SECTION FOR PROFILE P_5

CHAPTER FOUR
MAPS PRODUCED FROM INTERPRETED DATA

4.0 Maps Produced From Interpreted Data

Using the total VES data, four different contour maps were produced. These are the depth to basement (overburden thickness) the study area, the weathered layer thickness map of the study area, isoresistivity map of the weathered basement a of the study area, and isoresistivity map of the fresh basement study area. Details of each of these maps areas are discussed below.

4.1 Isoresistivity Map of the Weathered Basement

The isoresistivity map is shown in Fig. 4. 1. The lowest resistivity value is 43 Ωm sampled at VES31, Department of Pharmaceutical Sciences while the highest resistivity value of the layer was obtained at DAC is 250 Ωm East of Area E inside Samaru River. The lowest resistivity in the former case strongly suggests that the formation is saturated with water, while in the latter case the geologic formation is more or less fractured. Areas of high resistivity values are Area G, around VES10 and VES03; IAR at VES06; at station VES29 and inside the site for Stadium at VES27. The zone comprising of Area F, (IAR), and West of Estate Department has higher resistivity values. Thus, suggesting that the formation stated above may contain less water. Elsewhere, the weathered basement is more or less saturated with water due to its lower resistivity values.

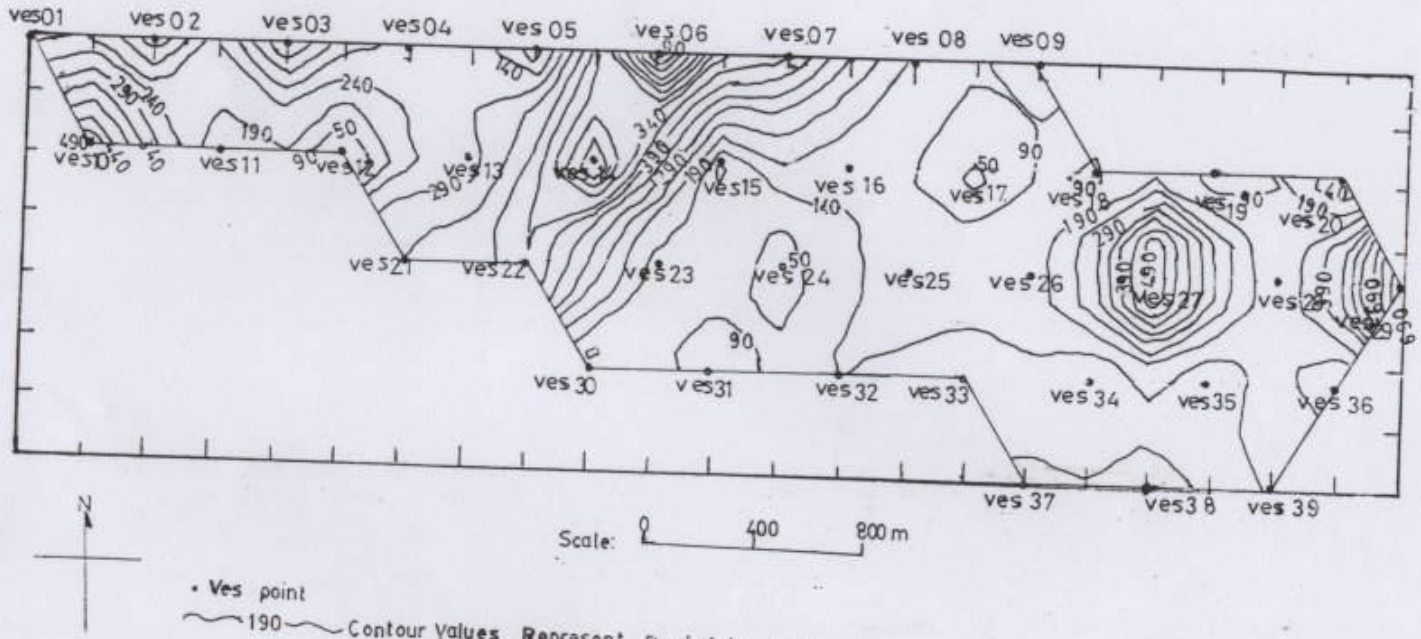


Fig.4.1 Weathered Layer Resistivity Map of the Study Area.

4.2 Weathered Basement Thickness Map

The map is shown in Fig 4.2. The weathered basement beneath each VES stations as well as across the study area was assumed to consist of either of the fractured basement and weathered layer. This implies the overburden devoid of the top soil this is because the top soil consists of lateritic rocks, clay, and sandy clay and fadama loam; are not components of the aquifer. This aquifer thickness map shows that the aquifer thickness increases in the northward trend from the south direction. The weathered layer was thicker around VES06 with a thickness of about 38 m and thinnest around VES39. Substantial aquifer thickness could be observed from east of VES02 to around VES29 across the study area. The thickness basement varied from about 30 m around VES03 to 14 m around VES29

4.3 Depth to Basement Map of the Study Area

The depth to basement is shown in Fig. 4.3.the depth to basement consists of the sum of the top soil thickness, weathered basement thickness and the fractured basement thickness. Where the thickness of the fractured basement was beyond the sensitivity of our electrodes' spread, that portion of the weather basement was considered as fresh basement. The examples of VES06, VES10, VES14, VES21, VES22, VES27 and VES29 were cases in point. The fresh basement was shallowest around VES36, VES37 and VES38 where the thickness of the overburden is about 4 m. the overburden got thicker and thicker northward from the south. That trend was similar to the one of the weathered basement thickness as discussed in section 4.2. the fresh basement was deepest around VES05, VES07 and VES09 where the average thickness was about 40 m. the study area was substantially thick, of

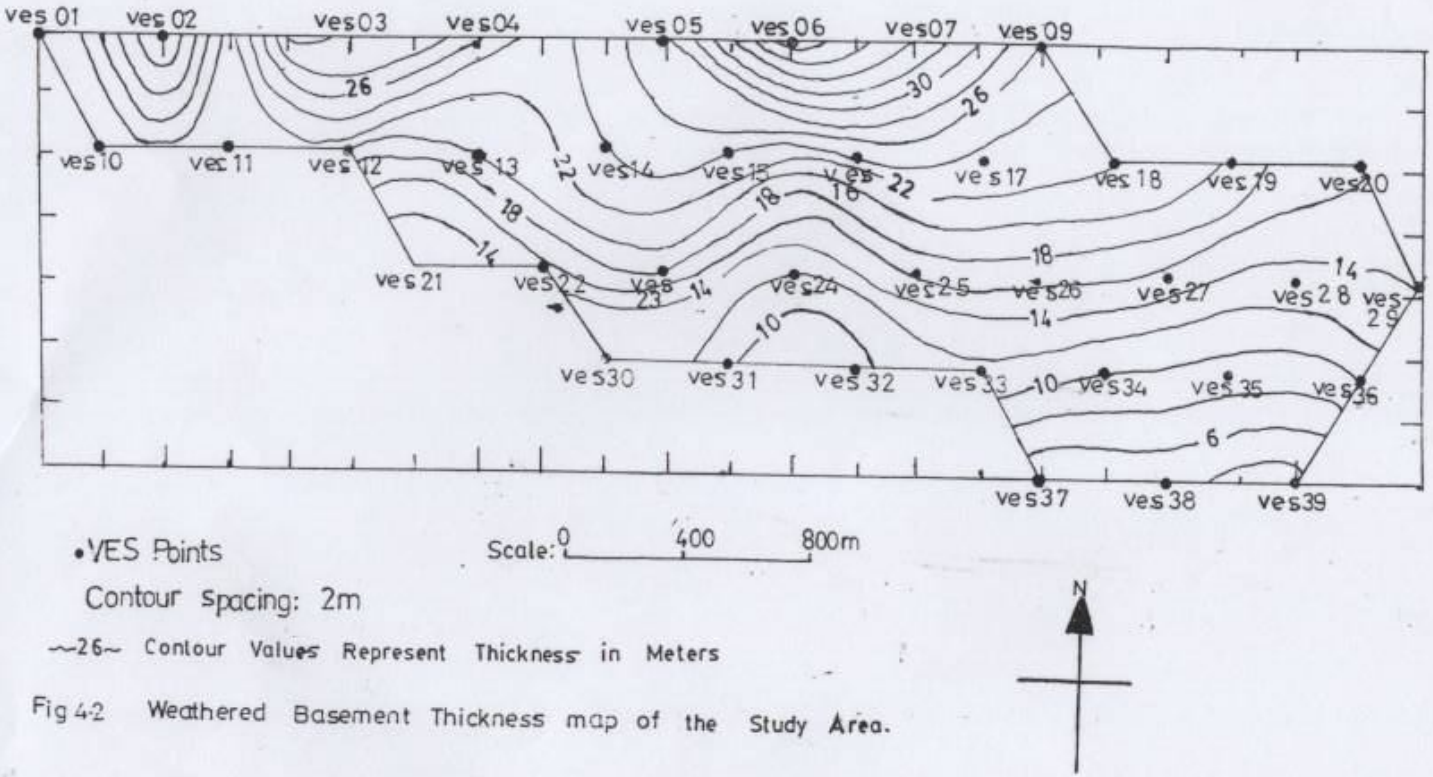


Fig 4.2 Weathered Basement Thickness map of the Study Area.

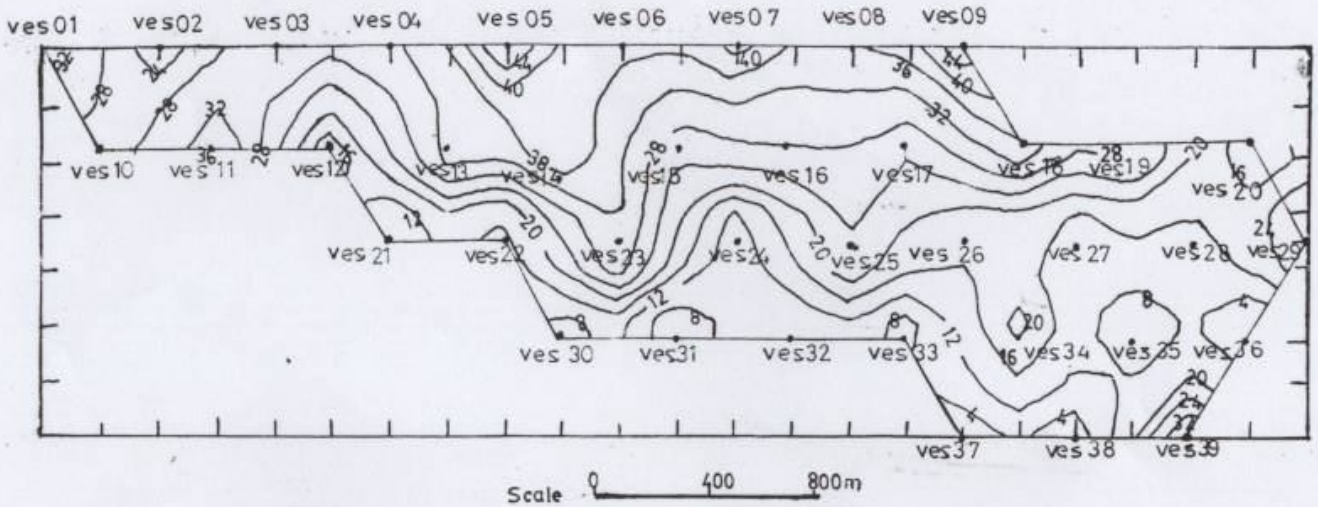


Fig4.3 Depth to Basement map of the Study Area

thickness ranging from 20 m to 30 m except around VES12, VES2, VES22, VES24, VES26, VES27 VES28 VES29 VES30, VES31, VES32, VES33, VES35, VES36, VES37 and VES38.

4.4 Isoresistivity Map of the Fresh Basement

This isoresistivity map of the fresh basement is shown in Fig. 4.4. As mentioned above, two distinct features of the fresh basement were considered viz: fresh basement and fractured basement. The former referred to the resistivity values within the range from 1000Ωm to infinity, normally associated with fresh basement rocks (Ajayi and Hassan, 1989). The latter referred to the fractured basement with depth greater than the sensitivity of the maximum electrodes' spread and resistivity values ranging from 500Ωm to 1000Ωm, normally associated with fractured basement rocks (Ajayi and Hassan, 1989).

The highest resistivity value recorded was 9241Ωm at VES25 inside NAERLS project field, while the lowest resistivity value recorded was 1023m at VES28, extreme southern side of Area BZ.

On the other hand, maximum resistivity value of 872Ωm was obtained for the fractured basement and the minimum value of 360Ωm was obtained at IAR and at the extreme south of Area E respectively.

Deductions from the basement resistivity map suggested that the area can be divided into two regions; the eastern part characterized with high basement resistivity greater 1800 Ωm. There is a resistivity high around VES25 and VES26. This region is referred to as the fresh basement region. The region is associated with relatively low basement resistivity (800 - 1400Ωm) and sparsely distributed contour lines, which increases northward. This area is referred to as the fractured basement region.

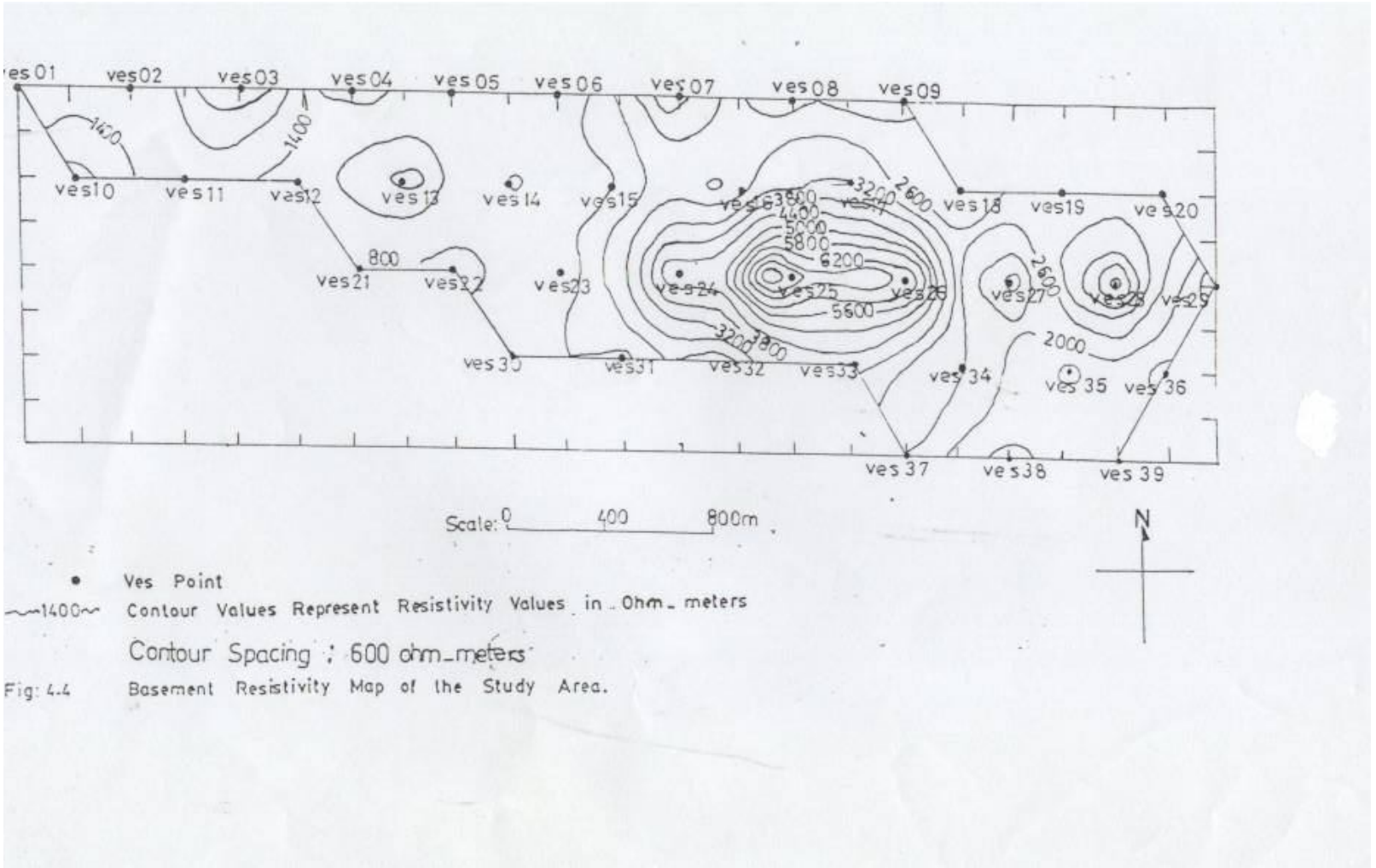


Fig: 4.4 Basement Resistivity Map of the Study Area.

4.5 Results from the Radial Depth Sounding

Three radial depth soundings were carried out along Samaru river as follow: inside the Forestry Research Institute (VES14), east of Area F (VES24), and west of Area BZ Primary School (VES32). Two other radial depth soundings were carried out along River Danfodio at VES36 and VES28. This was carried out with the primary aim of determining the fracture patterns within the study area. The radial depth sounding plots are shown in appendix III.

Table: 4.1 Radial Depth Soundings and Directions of Anisotropy

Station No	Shallow Depth 0-5m	Intermediate Depth 5-15m	Great Depth 15-50m	Anisotropy at Depth 50-150m	Estimated Depth to Basement
VES28	NW – SE	NE – SW	NW – SE	NE – SW	15m
VES14	E – W	NNW – SSE	WWN – EES	E – W	50m
VES36	isotropic	NE – SW	SE – NW	SE – NW	7m
VES32	N – S	NW – SE	NW – SE	E – W	8m
VES24	N – S	N – S	E – W	NE – SW	46m

4.5.1 Summary of the Radial Depth Soundings: Results for the five Stations

A summary radial depth sounding is shown in table 4.1. The result suggests that for the five stations, the table is subdivided into four depths of characteristic anisotropy as follows: shallow depth (0-5m), intermediate at (5-15m), great depth (15-50m), and at depth (50-150m). The results of the radial depth sounding suggest that river is structurally controlled. The radial depth plots show six directions of anisotropy viz: the NE - SW, N – S, WWN – EES, SE –NW, NNW – SSE, and E – W. These are the major fractured pattern associated with the Nigerian basement complex (McCurry, 1970). These patterns probably reflect the evolutionary history of the study area.

4.5.2 Deduction from the Interpreted Data

A combination of the weathered layer resistivity map in Fig. 4.1, weathered basement thickness map in Fig. 4.2, fresh basement resistivity in Fig. 4.3, depth to fresh basement in Fig. 4.4, show that the study area has great ground water potentials. This is especially the case of the region between VES03, VES04 and VES12; and the area comprising VES05, VES06 and VES07. When the above mentioned deductions are matched with the results of the radial depth soundings in appendix III, the ground water potentials of study area gets even wider. This stems from the fact that the two river channels: River Samaru and River Danfodio are deeply fractured. Therefore, they constitute an integral part of the aquifer system of the study area.

4. 6 Groundwater Potentials of the Study Area

The aim of DC resistivity method with application to groundwater exploration is as an improvement over traditional hand dug wells and as a guide to geologic mapping. Moreover, one of the primary objectives of the D.C. resistivity survey in basement terrain is to site structures or geologic formations accommodating voluminous amount of groundwater. The usual target for this type of survey is either weathered basement or fractured basement.

The geologic section for profile P_1 (fig 3.6) suggests that the weathered basement is thickest at VES05, just 80m west of Samaru River, about 52 m thick. Further to the east at VES06, The aquifer gets even deeper because the thickness of the fractured basement is beyond the sensitivity of maximum electrodes' spread. At the extreme east of the profile at VES09, the weathered basement is 41.85 m thick. The best side for borehole along this profile is around VES06,

As for the geologic section for profile P_2, three regions of interest are identified as far as ground water potentials are concerned viz: VES10 and environs, the region around VES13, VES14 and VES18. The first two regions (VES10 and in between VES13 and VES14) have a common feature. The weathered basement at either of these places was underlain by fractured basement of depth beyond the sensitivity of the maximum electrodes' spread. The weather basement is 11.68 m thick at VES10 and 38.67 m thick at VES14. AT VES18, the weathered basement is 29.0 m thick. The best sites for boreholes are the VES10 (west of Area G) and VES14 (inside Samaru River).

The ground water potentials as for the geologic section for profile P_3 are located in four regions viz: the region between VES21 to VES23, VES25, VES27 and VES29. The weathered basement is very thin in between VES21 and VES22 with thickness ranging from 3.66 m to 5.31 m. But at VES23, VES25, VES27 and VES29 the weathered basement is substantially thick with respective thicknesses 33.80 m, 26.50 m, 11.33 m and 23.30 m. the fractured basement thickness at VES21, VES27 and VES29 extends beyond the sensitivity of the maximum electrodes' spread used in this work. Therefore, the best sites for boreholes along this profile are the region in between VES21 to VES23, VES27 and VES29.

Along the geologic section for profile P_4, the weathered basement was thickest (20.4 m thick) inside Area BZ. This profile shows lest potentials for ground water.

Other relevant information about aquifer system can be obtained from the weathered thickness map in Fig. 4.2. This figure shows that the weathered map gets thicker from the south proceeding northwards. Around VES37, the weathered basement is about 4 m thick while at VES06 (IAR), the weathered is 40 m thick. The

following zones seem to contained ground water potentials. A synthesis of the geologic sections shows that (Fig. 3.6 to Fig. 3.9) and the weathered thickness map (Fig. 4.2) lead to the production of Fig. 4.5; map illustrating the ground water potentials of the study area. At VES11 and VES12 (west of Area E and east of Area G), the weathered basement is very thin (6.25 m thick), moreover, the fresh basement resistivity values are relatively high, about 2000Ωm suggesting that the fresh basement is relatively preserved (Mallam et al., 1998). The area comprising of south-east of Area F at VES24, VES32 (along Samaru River) and VES31, southern part of NAERLS project field in compassing VES25 and VES26, Area BZ Primary school (VES33), southern part of Area BZ (VES37 and VES38) and around VES20 and VES28 while all the rest of the study area most likely abounds with ground water potentials. However, environs like VES15, VES16, VES35 and VES36 have been mentioned to contained ground water potentials because of their relatively low fresh basement resistivity values, suggesting that the latter may be fractured (Mallam et al., 1998).



Fig 4·5 GROUNDWATER POTENTIALS OF THE STUDY AREA

CHAPTER FIVE

CONCLUSION AND RECOMMENDATIONS

5.0 Work Done So Far

A DC resistivity survey of the Eastern part of ABU Zaria Main Campus, Samaru was carried out employing the Schlumberger configuration.

The field work involved normal depth sounding at thirty nine (39) VES stations as well as radial depth sounding at five (5) of these thirty nine (39) VES stations viz: VES14, VES24 and VES32 along Samaru River, VES28 and VES36 along Danfodio River. The normal depth soundings lead to the production of five (5) geoelectric sections and four (4) geological sections. The following four geophysical maps were also produced: isoresistivity map of the weathered basement, weathered basement thickness map, depth to basement map and basement resistivity map of the study area. The five radial depth soundings enabled us to determine the possible fracture patterns along the two river channels in the study area by drawing five radial depth plots indicating variations of resistivity anisotropy.

The five geoelectric sections, four geologic sections, four geophysical maps and five radial depth sounding plots enabled us to produce a map assessing the groundwater potentials of the study area.

5.1 Conclusion

The following conclusions were drawn:

i) The information got from the geologic sections shows that the topsoil consists of either fresh laterite, weathered laterite, clay, sandy clay, fadama loam and weathered basement.

ii) The second geologic layer was made of weathered basement. That weathered layer extended from one end of the profile to the other.

iii) The third geologic layer at VES06, VES10, VES14, VES21, VES22, VES27 and VES29 represented the fractured basement with thickness beyond the sensitivity of the maximum electrodes' spread used in this field work.

iv) Elsewhere the third geologic layer represented the fresh basement. Considering all of the above, the basement lithology could be summarised into three stratified geologic layers: the top soil consisting of weathered laterite, fresh laterite, clay, sandy clay, fadama loam or weathered laterite. The shallowest depth basement (4.09 m) deep as shown in appendix II was located at VES24 (east of Area F) while the basement was fresh deepest at VES05 (53.15 m). These two points were located inside Samaru River.

So the most suitable targets for boreholes are: VES05, VES06, VES09, VES10, VES14, VES18, VES21, VES22, VES27 and VES29. Moreover as the two river channels (River Danfodio and River Samaru) are deeply fractured mention most be made of the following regions as boreholes targets: All along Danfodio River as well as all along Samaru River within the study area.

Further more, the radial depth soundings show that both Danfodio River and Samaru River originated prior to faulting and fracturing rather than a mere erosion feature: thus enhancing the ground water potentials of the study area.

5.2 Recommendations

Other geophysical methods such as gravimetrics and the seismic refraction method can be utilised to supplement the resistivity method used in this work. This is

because the gravity and seismic methods enable us to establish appropriate depths, topographies and character of the basement which could assist in correlation with the results obtained by the resistivity depth sounding.

However, the information obtained from the normal as well as the radial depth soundings alone suffice to assess the groundwater potentials of the study area. Therefore, boreholes should be sited along River Samaru. All of this study area abounds with groundwater except Area BZ, Area E and the site for stadium.

REFERENCES

Ajayi, C. O and Hassan, M. (1989); *The Delineation of Aquifer Overlying the Basement Complex in the Western Part of the Kubanni Basin of Zaria-Nigeria*. Journal of Mining and Geology, Vol. 26, No. 1, pp. 117 -125.

Akpoborie, I. A. (1972); The *Hydrogeological Control of Structures along Samaru*. M.Sc. Thesis (Unpublished). Geology, Department, *A. B. U.* Zaria.

Aminudeen, A. I. (1990), *Geoelectrical Investigation for Groundwater in four Villages in Roni L. G. A., Kano State, Nigeria*. Unpublished M.Sc. Thesis, Department of Physics, A. B. U. Zaria.

Atlas Copco, ABEM (1981); *Geophysical Instruments Ltd. ABEM Terrametre SAS 300* Instrument Manual.

Du Preez, J. W and Barber, W. (1965); *Original, Classification and Distribution of Nigeria laterite*. GSN Report No 810.

Eigbefo, C. (1978); *Hydrogeology of Kubanni Drainage Basin*. Unpublished M.Sc Thesis , Geology Dept. A.B.U. Zaria.

Hassan, M (1987); *Geoelectric Investigation of the Western Half of the Kubanni River Basin-Zaria*. Unpublished M.Sc. Thesis A. B. U. Zaria.

Hazell, J. R. T., Cratchley, C.R, and Jones C. R. C., (1992); *Hydrogeology of Crystalline Aquifer in Africa*. Geological Society Special Publication No. 66, pp. 155-182.

Hockney, R. D. (1986); *The Geology of the Lokoja-Auchi Area, Sheet 62*. G. S. N. Bulletin No. 39.

Hore, P.N (1970) *Weather And Climate , Zaria And Its Region*, Edited by Mortimore MJ, Department of Geography, Paper No. 4, and ABU Zaria.

Kearey, P. and Brooks, M. (1988); *An Introduction to Geophysical Prospecting*. Blackwell Scientific Publication. Oxford OX2 OEL, England, pp. 203-206.

Mallam, I., Ajaiyi, C.O. and Sule, P.O (1998); *Direct Current Resistivity Prospecting for Ground Water in Alu –Igbagum ,Yagba Lga*. Zuma; JPAS Vol. 1 , no .1

McCurry, P. (1970); *The Geology of the Zaria Sheet 102 S-W Zaria and its Region*. Dept. Of Geology A. B. U. Zaria Occasional Papers.

Milsom, J. (1988); *Field Geophysics*. John Wiley & Sons Ltd, Baffins Lane, England, pp. 96-99

Olowu, J. (1967); *Preliminary Investigations of the Groundwater Conditions in Zaria, Sheet No. 102 S-W*. G. S. N. Report No. 1462.

Olufemi, R.*O. (1985), Hydrogeology of Jama'a Kubanni Area, Sheet No. 102 Zaria.* Unpulished B.Sc Thesis, *A.B.U. Zaria.*

Ososami, I.A. *(1968); "Assessment of the Ground Water in the Kubanni Valley.* Unpublished M.Sc. Thesis, A.BU. Zaria

Shemang, E. M., Ajayi C. O. and Osazuwa I. B., (1992); *the Basement Rocks and Tectonism in Kubanni River Basin, Zaria-Nigeria: Deductions from D. C. Resistivity Data.* Journal of Mining and Geology, Vol. 28.

Shemang, E. M., (1990); *Electrical Depth Sounding at Selected Well Sites within the Kubanni River, Zaria.* Unpublished M.Sc. Thesis, A. B. U. Zaria.

Telford, W. M., Geldert, L. P. Sherif, R.E, and Keys D.A, (1976). *Applied Geophysics.* Cambridge University Press, Cambridge England, pp. 632-6, 656-7

Torkaski, A. (1972); *Heterogeneous Terrace Arrangement West of A. B. U.* Occasional Paper No. 2. Department of Geology, A. B. U., Zaria.

Trustwell, J. F. and Cope, R. N. (1963); *The Geology between Zaria and Kaduna.* Savannah, Vol. 1. No. 2, pp. 241-3.

Wright, J.B, And McCury, P. (1970); *The Geology of Parts of Niger and northern Nigeria provinces.* GSN Bulletin No. 29, 52 p.

Worthington, P. F. (1977); *Geophysical Investigation for Groundwater Resources in the Kalahari Basin.* Geophysics Vol. 42, pp. 838-849.

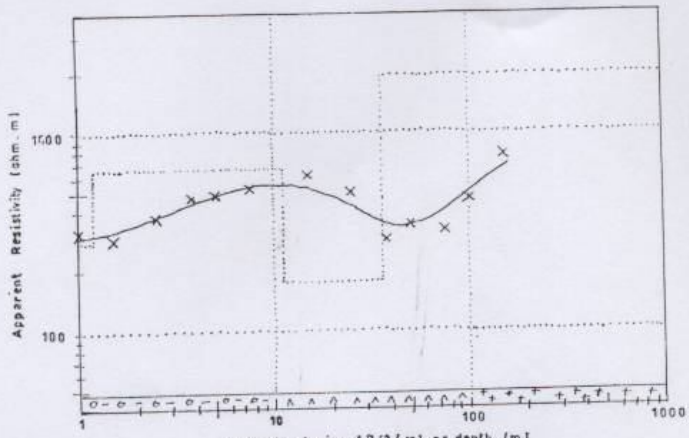
Verlical Electrical Sounding VES 01

(Schlumberger Array)

KONA BIYE

11 June 2000

Orientation 001A



Interpreted Model

Layer	Resistivity (ohm.m)	Thickness (m)	Depth (m)
1	280	1.2	1.2
2	650	10.0	11.2
3	175	24.8	36.0
4	1095		

Legend



Observed Apparent Resistivity Data Print

Weathered Laterite

Weathered Basement

Fresh Basement

Interpretation of Field Curve for VES 01

VES 02

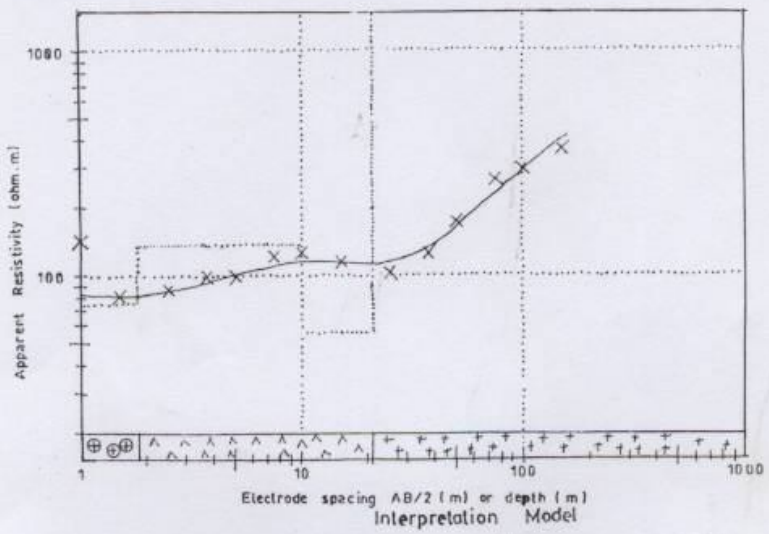
Vertical Electrical Sounding

(Schlumberger Array)

AREA G GATE

Orientation 090µ

11 June 2000



Interpretation Model

Layer	Resistivity (ohm m)	Thickness (m)	Depth (m)
1	150	0.2	0.2
2	75	1.6	1.8
3	135	8.0	9.8
4	55	11.2	21.0
5	1523		

Legend

X Observed Apparent Resistivity Data Point

Wet Sand

Weathered Basement

Fresh Basement

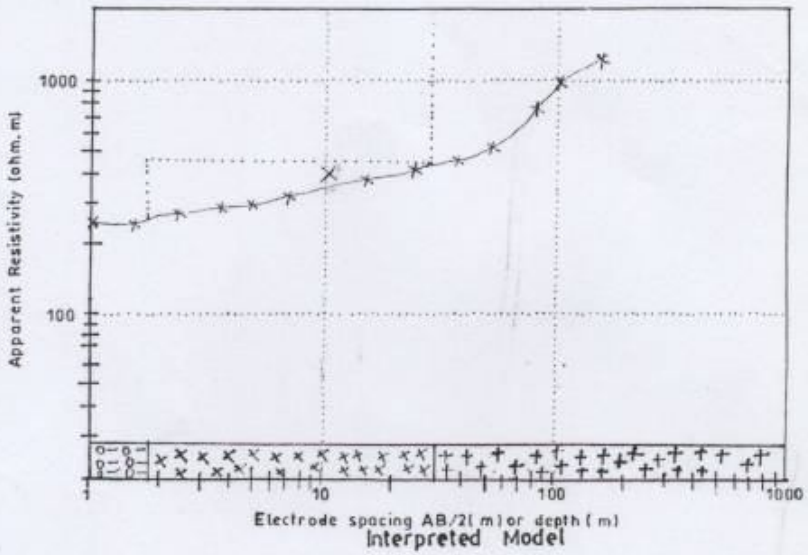
Interpretation of Field Curve for VES 02

Vertical Electrical Sounding VES03

(Schlumberger Array)

EASTERN BZ

Orientation 001/μ 27 May 2000



Interpreted Model

Layer	Resistivity (ohm m)	Thickness (m)	Depth (m)
1	240.5	1.69	1.69
2	449.5	30.18	31.87
3	3568.8		

Legend

X Observed Apparent Resistivity Data Point

Weathered Laterite

Fractured Basement

Fresh Basement

Interpretation of Field Curve for Ves 03

Vertical Electrical Sounding

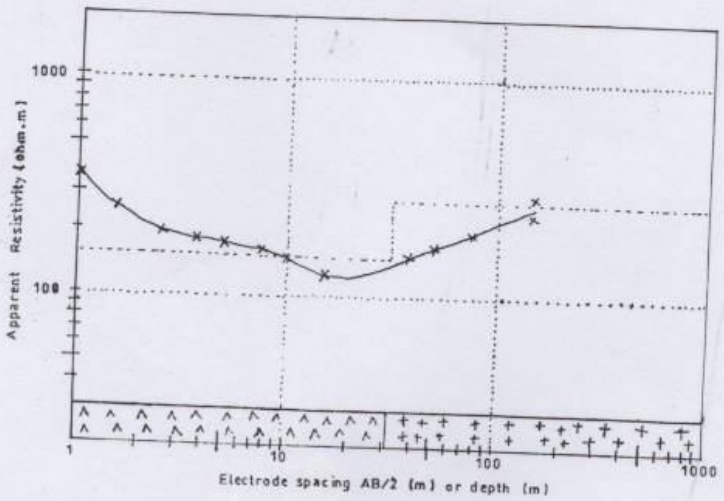
VES04

(Schlumberger Array)

West Forestry Research Institute

Orientation 090 M

10 June 2000



Layer	Resistivity (ohm m)	Thickness (m)	Depth (m)
1	3438	1.04	
2	147.1	29.70	1.04
3	279.6		30.74



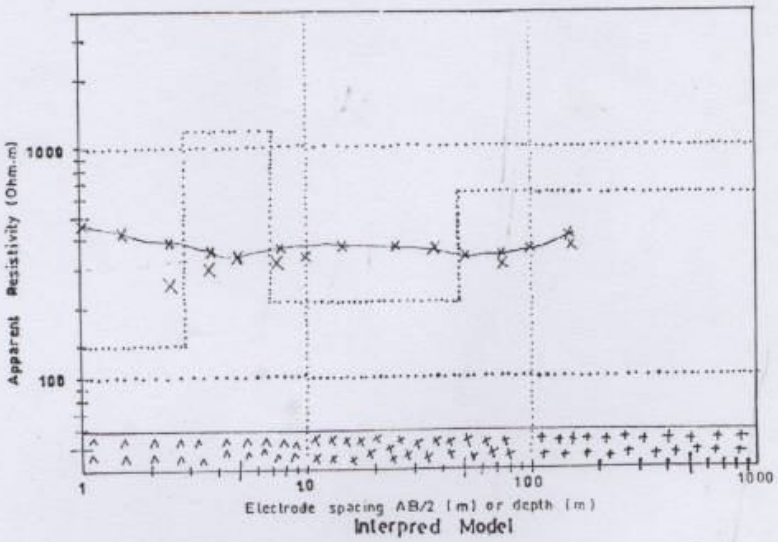
Interpretation of Field Curve for VES 04

Vertical Electrical Sounding VES05

(Schlumberger Array)

EAST OF BARREN ROAD TO FORESTRY RESEARCH INSTITUTE

Orientation 090μ 19 May 2000



Interpred Model

Layer	Resistivity (ohm m)	Thickness (m)	Depth (m)
1	552.7	0.6	0.6
2	344.6	29.81	30.41
3	160.0	22.74	53.15
4	1063.4		

Legend

X Observed Apparent Resistivity Data Point

Weathered Basement

Fractured Basement

Fresh Basement

Interpretation of Field Curve for VES05

Vertical Electrical Sounding

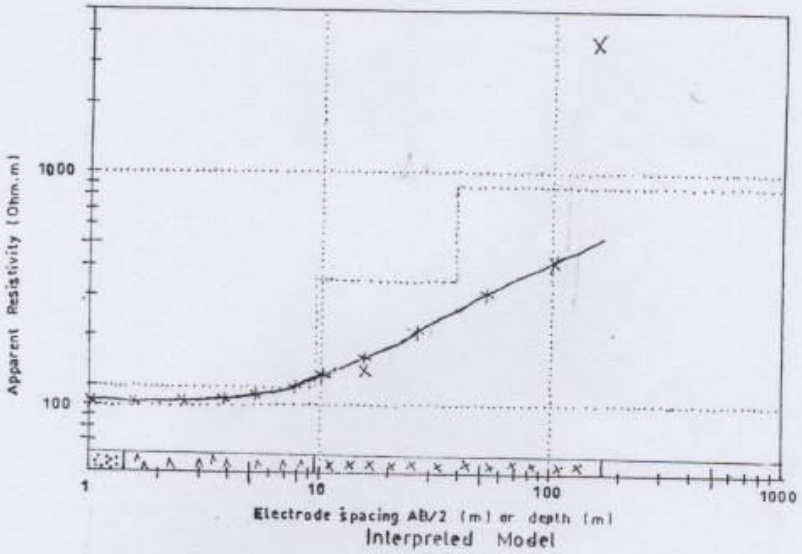
VES06

(Schlumberger Array)

WEST SIDE OF IAR GATE

Orientation 090M

19 May 2000



Interpreted Model

Layer	Resistivity (ohm. m)	Thickness (m)	Depth (m)
1	113.0	1.50	1.50
2	124.6	7.83	9.33
3	354.8	27.62	36.95
4	872.0		

Legend

X Observed Apparent Resistivity Data Point

Wet Clay

Weathered Basement

Fractured Basement

Interpretation of Field Curve for VES06

72

Vertical Electrical Sounding

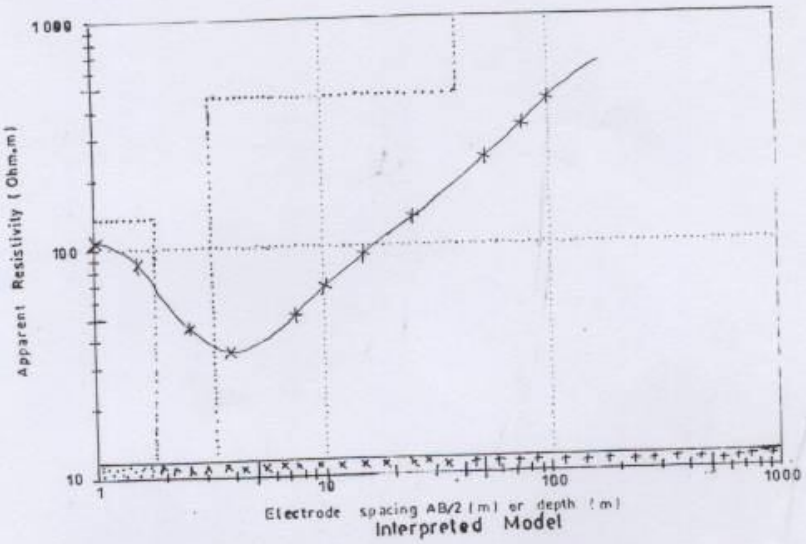
VES07

(Schlumberger Array)

NEAR EASTERN ESTATE

19 May 2000

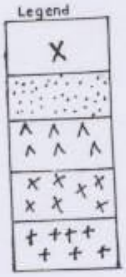
Orientation 090 K



Interpreted Model

Layer	Resistivity (ohm.m)	Thickness (m)	Depth (m)
1	137.1	1.882	1.882
2	11.72	1.47	3.352
3	451.3	39.29	42.642
4	3641.2		

Legend



Observed Apparent Resistivity Data Point

Wet Clay

Weathered Basement

Fractured Basement

Fresh Basement

Interpretation of Field Curve for VES07

VES 08

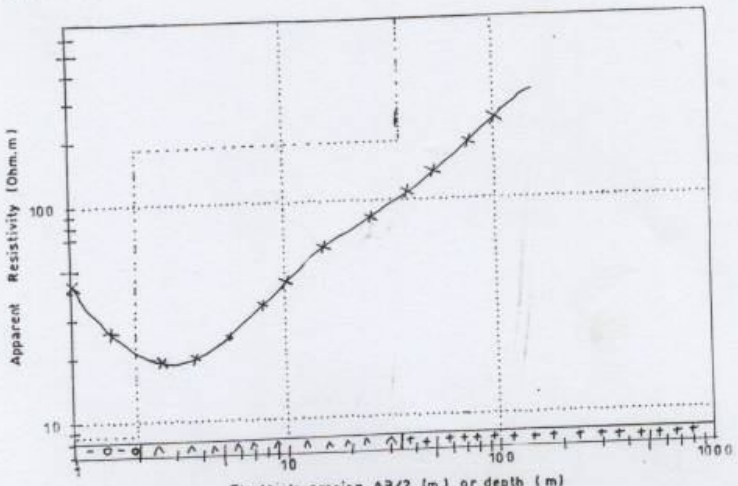
Vertical Electrical Sounding

(Schlumberger Array)

EASTERN ESTATE

19 May 2000

Orientation 001A



Interpreted Model

Layer	Resistivity (ohm m)	Thickness (m)	Depth (m)
1	43.82	0.713	0.713
2	176	1.32	2.043
3	1761	33.74	35.783
4	1324.6		

Legend

Observed Apparent Resistivi Data Point

Weathered Laterite

Weathered Basement

Fresh Basement

Interpretation of Field Curve for VES 08

Vertical Electrical Sounding

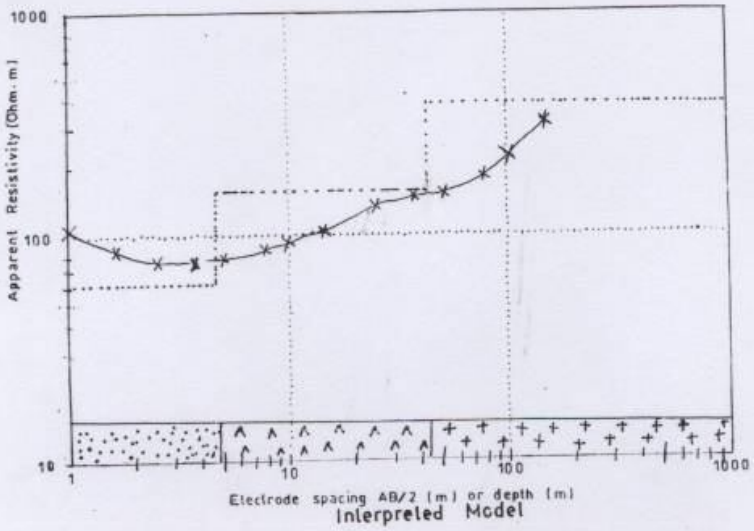
VES 09

(Schlumberger Array)

OPPOSITE CATHOLIC CHURCH SAMARU

Orientation 090M

18 June 2000



Interpreted Model

Layer	Resistivity (ohm-m)	Thickness (m)	Depth (m)
1	74	6.00	6.00
2	194	16.24	22.24
3	111	25.61	47.85
4	1430		

X Observed Apparent Resistivity Data Point

Wet Sand

Weathered Basement

Fresh Basement

Interpretation of Field Curve for VES 09

VES10

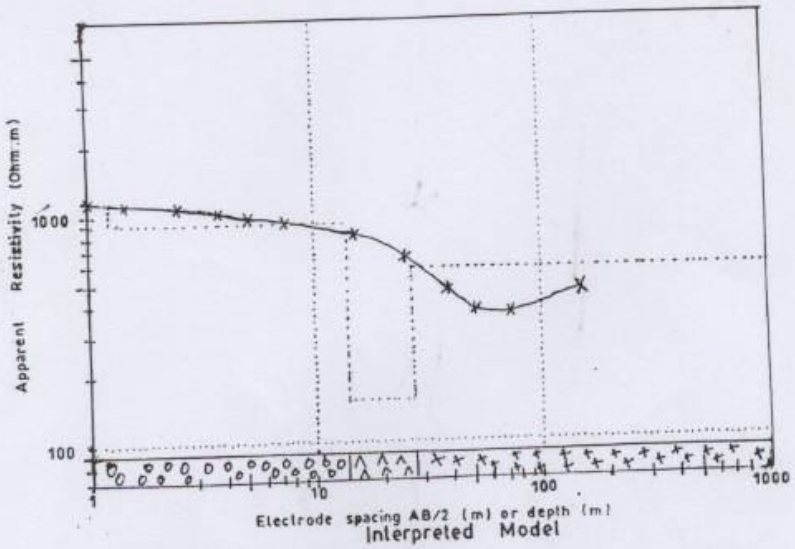
Vertical Electrical Sounding

(Schlumberger Array)

AREA G EXTREME SW

18 June 2000

Orientation 090M



Interpreted Model

Layer	Resistivity (ohm.m)	Thickness (m)	Depth (m)
1	1165.1	1.39	1.39
2	920.9	2.17	3.56
3	132.7	34.96	38.52
4	557.4		



Interpretation of Field Curve for VES10

Vertical Electrical Sounding

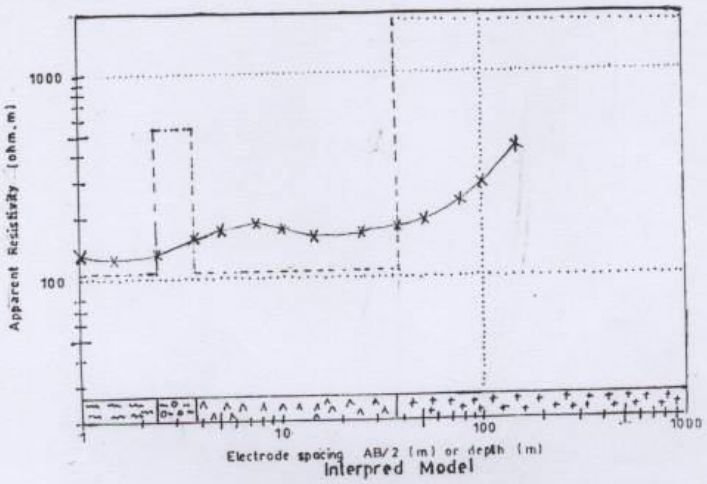
VES 11

(Schlumberger Array)

AREA G NO 24

25 May 2000

Orientation 090µ



Interpred Model

Layer	Resistivity (ohm. m)	Thickness (m)	Depth (m)
1	122.7	2.33	2.33
2	559.7	1.23	3.56
3	438.6	34.96	38.52
4	1929.2		

Legend

X Observed Apparent Resistivity Data Point

Fadama Loam

Weathered Laterite

Weathered Basement

Fresh Basement

Interpretation of Field Curve for Ves11

Vertical Electrical Sounding

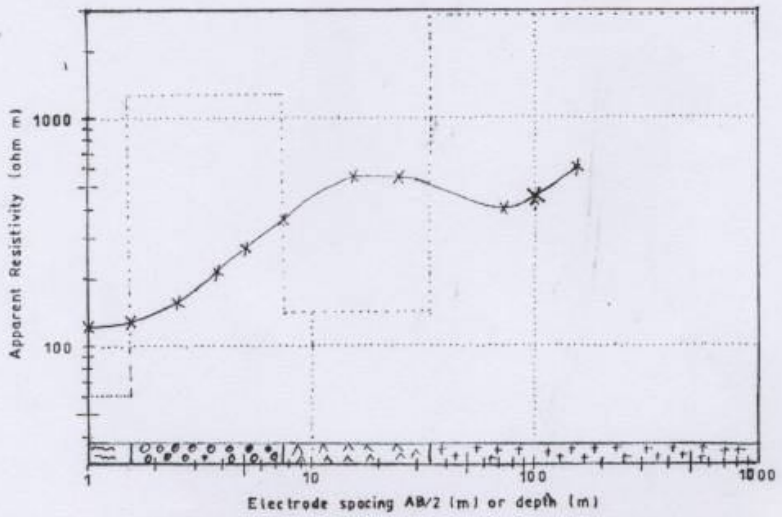
VES12

(Schlumberger Array)

CLOSE TO AREA E 47

Orientation 001μ

11 June 2000



Layer	Resistivity (ohm m)	Thickness (m)	Depth (m)
1	121	0.7	0.7
2	6814	0.8	1.5
3	49	6.0	7.5
4	1213		



Observed Apparent Resistivity Data Point

Fadama Loam

Fresh Laterite

Weathered Basement

Fresh Basement

Interpretation of Field Curve for Ves 12

X:1400
Y: -346

Vertical Electrical Sounding

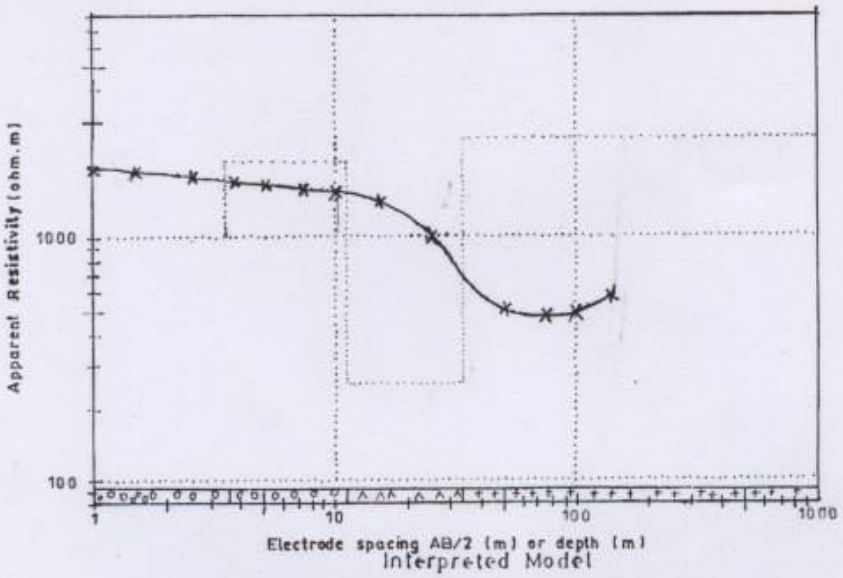
VES13

(Schlumberger Array)

EAST OF AREA E

Orientation 001M

25 May 2000



Interpreted Model

Layer	Resistivity (ohm m)	Thickness (m)	Depth (m)
1	1350	3.5	3.5
2	2005	7.7	11.2
3	250	22.8	34.0
4	2501		

Legend

X Observed Apparent Resistivity Data Point

Fresh Laterite

Weathered Basement

Fresh Basement

Interpretation of Field Curve for Ves13

Vertical Electrical Sounding

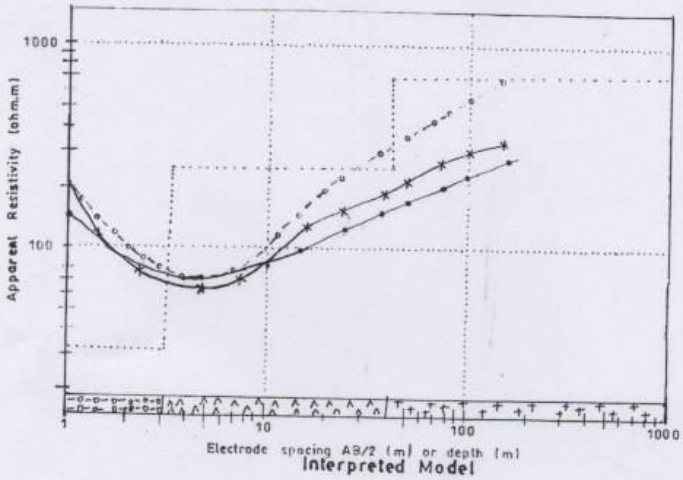
(Schlumberger Array)

VES 14

INSIDE STADIUM

Orientation 001p.

6 June 2000



Interpreted Model

Layer	Resistivity (ohm.m)	Thickness (m)	Depth (m)
1	216.3	0.841	0.841
2	32.54	2.44	3.281
3	2234	38.67	41.951
4	693.0		

Legend

X Azimuth N_S

o Azimuth SW_NE

Azimuth NW_SE



Weathered Laterite

Weathered Basement

Fractured Basement

Radial Depth Sounding Field Curve for Ves 14

VES15

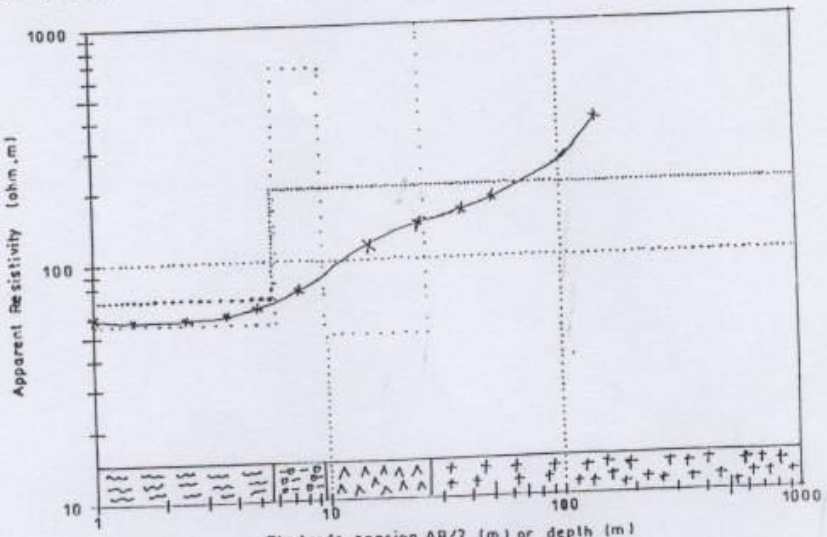
Vertical Electrical Sounding

(Schlumberger Array)

DEPT OF CROP PROTECTION

25 May 2000

Orientation 090



Interpreted Model

Layer	Resistivity (ohm.m)	Thickness (m)	Depth (m)
1	57.91	5.71	5.71
2	625.3	4.15	9.86
3	49.96	14.17	24.03
4	1302.13		

Legend

X Observed Apparent Resistivity Data Point

Fadama Loam

Weathered Laterite

Weathered Basement

Fresh Basement

Interpretation of Field Curve for Ves 15

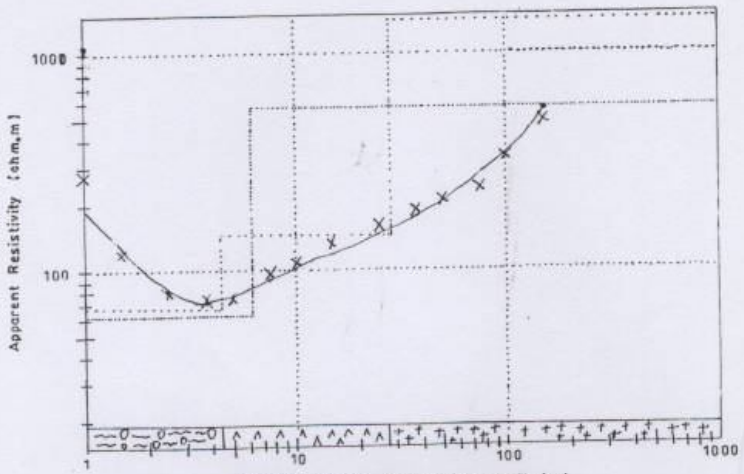
Vertical Electrical Sounding VES 16

(Schlumberger Array)

NAERLS FOOTBALL PITCH

Orientation 090°

26 May 2000



Interpreted Model

Layer	Resistivity (ohm.m)	Thickness (m)	Depth (m)
1	1262.6	0.347	0.347
2	67.10	3.87	4.217
3	357.6	23.32	27.537
4	1814.2		



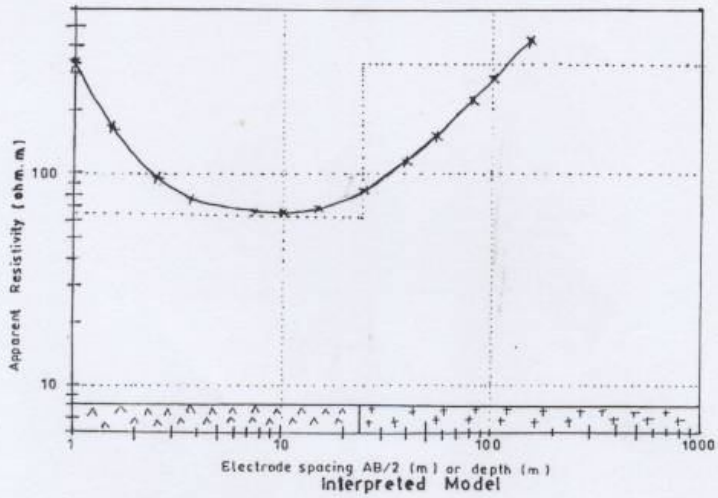
Interpretation of Field Curve for Ves 16

Vertical Electrical Sounding VES17

(Schlumberger Array)

NAERLS SOUTH EAST CORNER

Orientation 090μ 26 May 2000



Interpreted Model

Layer	Resistivity (ohm.m)	Thickness (m)	Depth (m)
1	336.8	0.613	0.613
2	66.38	23.02	23.633
3	3165.16		



Interpretation of Field Curve for Ves17

VES18

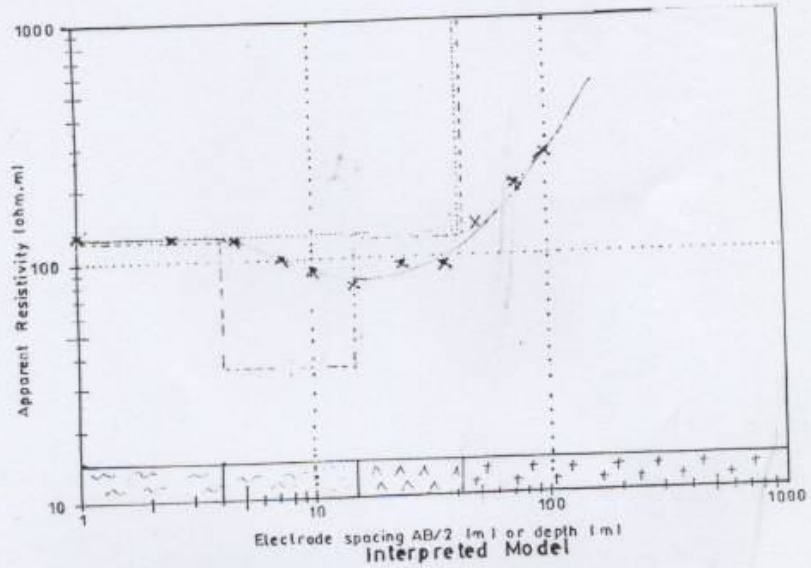
Vertical Electrical Sounding (Schlumberger Array)

X: 3400
Y: - 346

SS-E ROAD TO NAERLS

26 May 2000

Orientation 090∠



Interpreted Model

Layer	Resistivity (ohm m)	Thickness (m)	Depth (m)
1	130	4.0	4.0
2	35	9.0	13.0
3	125	29.0	42.0
4	1587		



Interpretation of Field Curve for ves18

Vertical Electrical Sounding

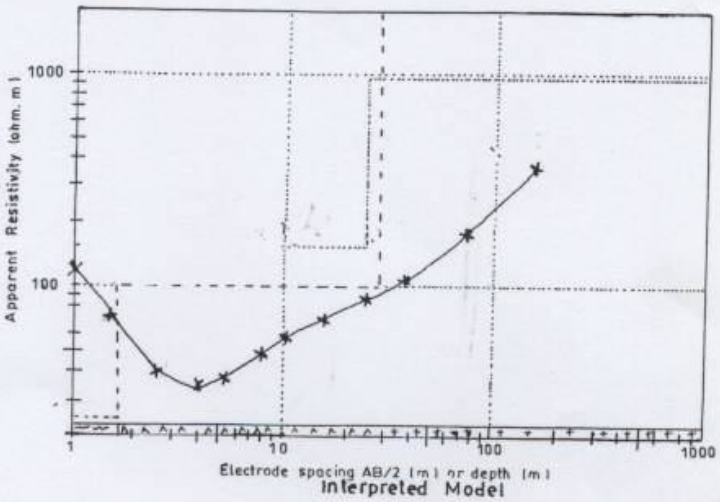
VES 19

(Schlumberger Array)

EASTERN B Z

Orientation 001μ

27 May 2000



Interpreted Model

Layer	Resistivity (ohm.m)	Thickness (m)	Depth (m)
1	119.1	0.831	0.831
2	91.2	0.855	1.686
3	100.1	27.98	29.665
4	3009.8		

Legend

X — Observed Apparent Resistivity Data Point

Fadama Loam

Weathered Basement

Fresh Basement

Interpretation of Field Curve for Ves 19

Vertical Electrical Sounding

(Schlumberger Array)

X: 4200

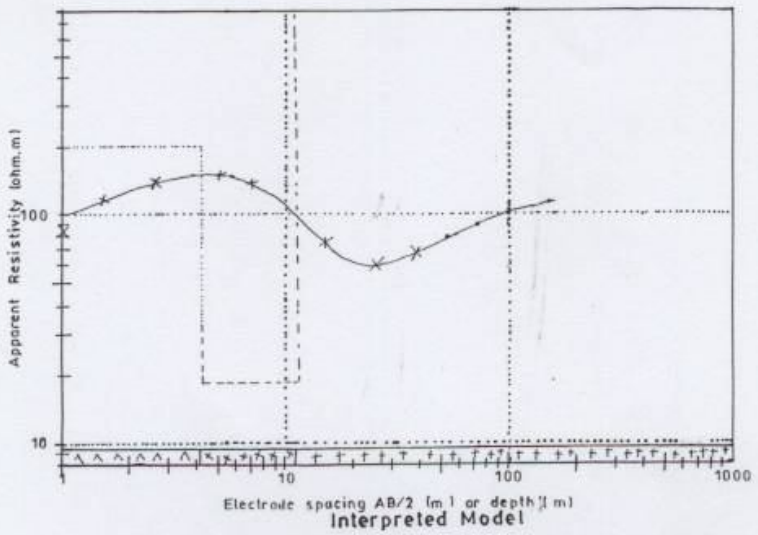
Y: -346

VES20

BEHIND PHARMACY

Orientation 045K

8 June 2000



Interpreted Model

Layer	Resistivity (ohm.m)	Thickness (m)	Depth (m)
1	84	0.61	0.61
2	194	2.97	3.58
3	17	8.12	11.60
4	3080		

Legend

X Observed Apparent Resistivity Data Point

Weathered Basement

Fractured Basement

Fresh Basement

Interpretation of Field Curve for Ves20

Vertical Electrical Sounding (Schlumberger Array)

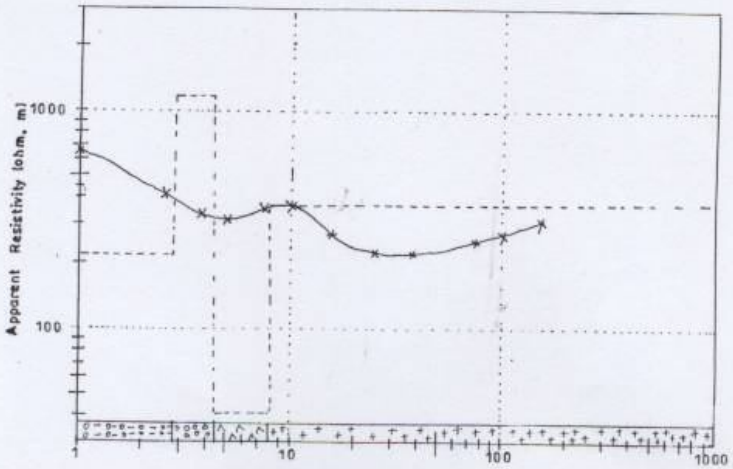
X : 1200
Y : -692

VES 21

TRIPLE JUNCTION

Orientation 045μ

24 May 2000



Interpreted Model

Layer	Resistivity (ohm m)	Thickness (m)	Depth (m)
1	698.0	0.88	0.88
2	230.0	1.95	2.83
3	113.2	1.50	4.53
4	39.61	3.6635	8.1935
5	360		

Legend

- X — Observed Apparent Resistivity Data Point
- Weathered Laterite
- Fresh Laterite
- Weathered Basement
- Fresh Basement

Interpretation of Field Curve for Ves 21

Vertical Electrical Sounding (Schlumberger Array)

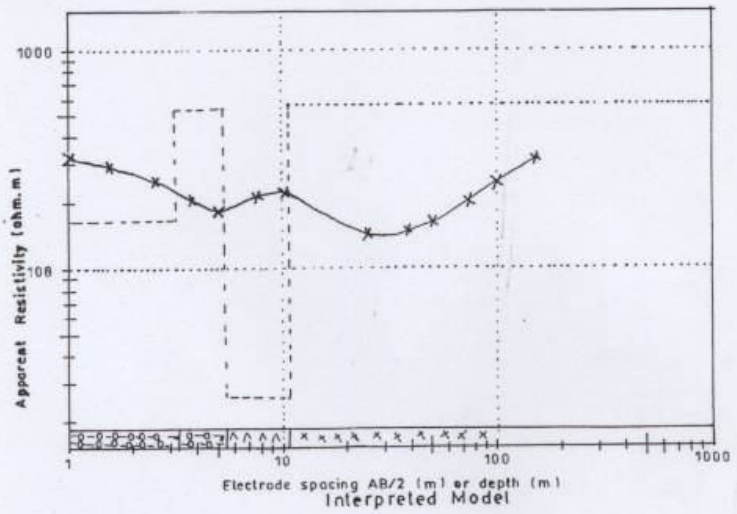
X: 1600
Y: -692

VES 22

TRIPLE FLAT JUNCTION

Orientation 090∆

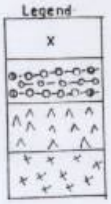
24 May 2000



Interpreted Model

Layer	Resistivity (ohm.m)	Thickness (m)	Depth (m)
1	398	0.49	0.49
2	179	2.77	3.26
3	511	2.24	5.50
4	27	5.31	10.81
5	513		

Legend



X Observed Apparent Resistivity Data Point

Weathered Laterite

Weathered Basement

Fractured Basement

Interpretation of Field Curve for Ves 22

Vertical Electrical Sounding
(Schlumberger Array)

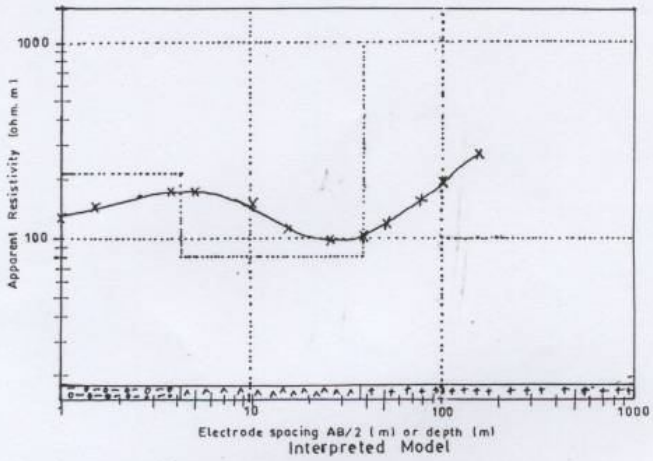
X: 2000
Y: -692

VES 23

INSIDE AREA F

Orientation 090m.

24 May 2000



Interpreted Model

Layer	Resistivity (ohm.m)	Thickness (m)	Depth (m)
1	120	0.8	0.8
2	210	44	4.2
3	81	33.8	38.0
4	1025		

Legend

- Observed Apparent Resistivity Data Point
- Weathered Laterite
- Weathered Basement
- Fresh Basement

Interpretation of Field Curve for Ves 23

VES 24

Vertical Electrical Sounding

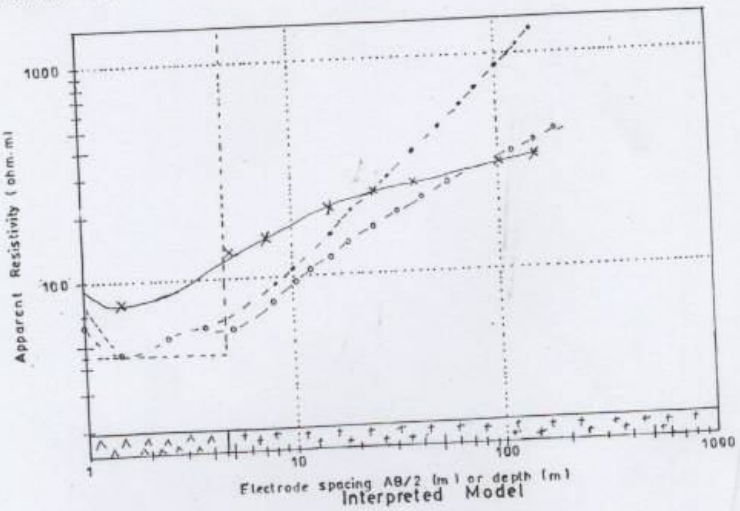
X: 2400
Y: -692

(Schlumberger Array)

EAST OF AREA F

26 May 2000

Orientation 001°



Interpreted Model

Layer	Resistivity (ohm.m)	Thickness (m)	Depth (m)
1	75	0.53	0.53
2	45	4.09	4.62
3	5015		

Legend

- X — Azimuth N E
- o — Azimuth NW–SW
- • — Azimuth E–W
- Weathered Basement
- Fresh Basement

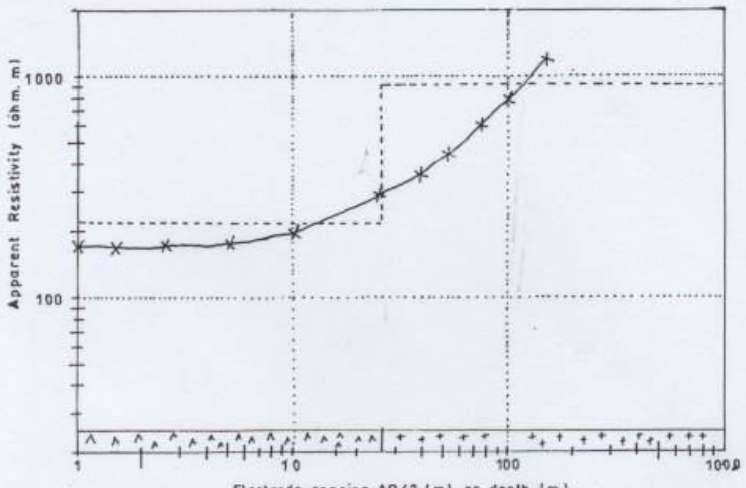
Radial Depth Sounding Curve for Ves 24

Vertical Electrical Sounding X: 2800 VES 25
Y: -692

(Schlumberger Array)

EAST OF ROAD TO AGRIC ENG

Orientation 090°. 26 May 2000



Interpreted Model

Layer	Resistivity (ohm.m)	Thickness (m)	Depth (m)
1	170	1.0	1.0
2	222	26.5	27.5
3	9241		



Legend

Observed Apparent Resistivity Data Point

Weathered Basement

Fresh Basement

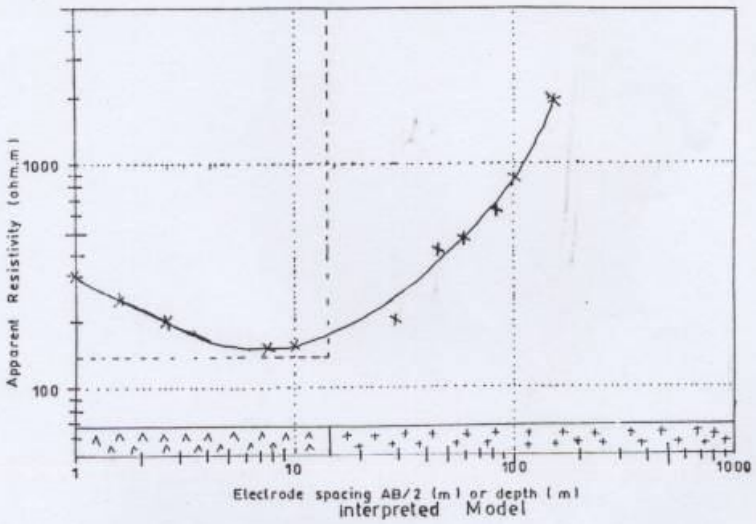
Interpretation of Field Curve for Ves 25

Vertical Electrical Sounding X: 3200 VES 26

(Schlumberger Array) Y: -692

200 M FROM STADIUM JUNCTION

Orientation 001μ 25 May 2000



Interpreted Model

Layer	Resistivity (ohm. m)	Thickness (m)	Depth (m)
1	329	0.32	0.32
2	146	14.98	15.30
3	8573		

Legend

X Observed Apparent Resistivity Data Point

Weathered Basement

Fresh Basement

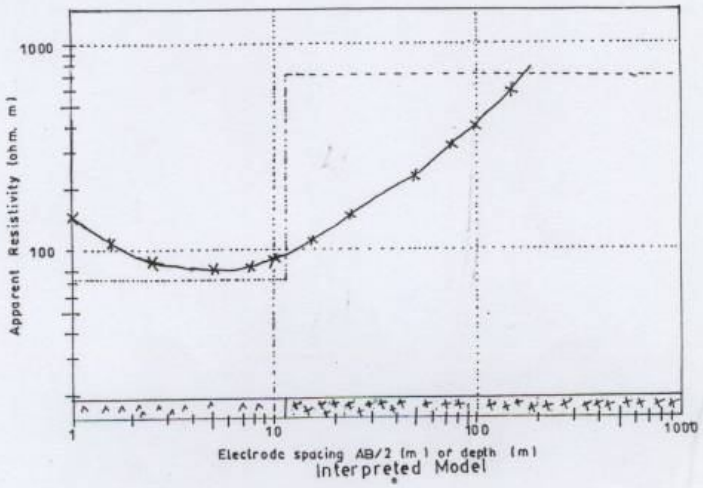
Interpretation of Field Curve for Ves 26

Vertical Electrical Sounding X: 3600 VES 27

(Schlumberger Array) Y: -692

INSIDE STADIUM

Orientation 001μ 8 June 2000



Interpreted Model

Layer	Resistivity (ohm. m)	Thickness (m)	Depth (m)
1	102	0·75	0·75
2	78	11·33	12·08
3	719		

Legend

X Observed Apparent Resistivity Data Point

Weathered Basement

Fractured Basement

Interpretation of Field Curve for Ves 27

Vertical Electrical Sounding

(Schlumberger Array)

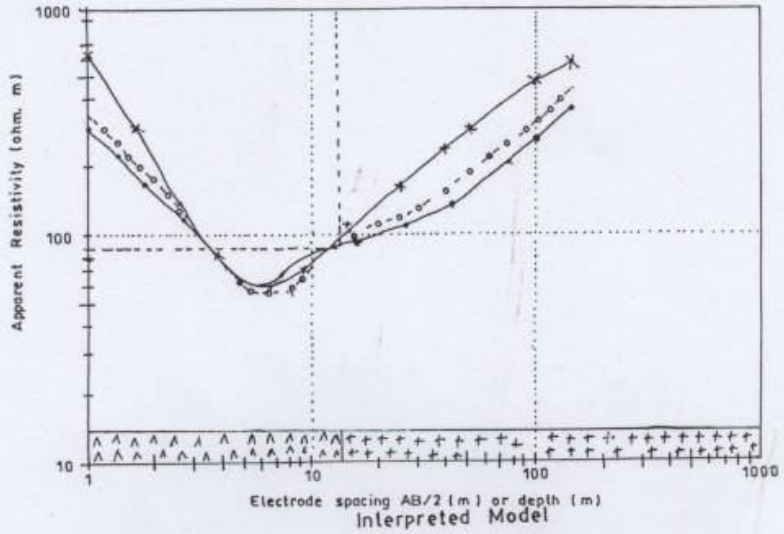
X: 4000
Y: -692

VES 28

ABU WATER WORKS

Orientation 001

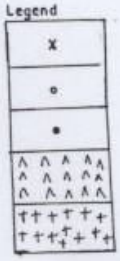
9 June 2000



Interpreted Model

Layer	Resistivity (ohm.m)	Thickness (m)	Depth (m)
1	601	0.73	0.73
2	87	13.67	14.4
3	5435		

Legend



Azimuth SE-NW

Azimuth E-N-WSW

Azimuth NNE-SSW

Weathered Basement

Fresh Basement

Radial Depth Sounding Curves for Ves 28

Vertical Electrical Sounding

(Schlumberger Array)

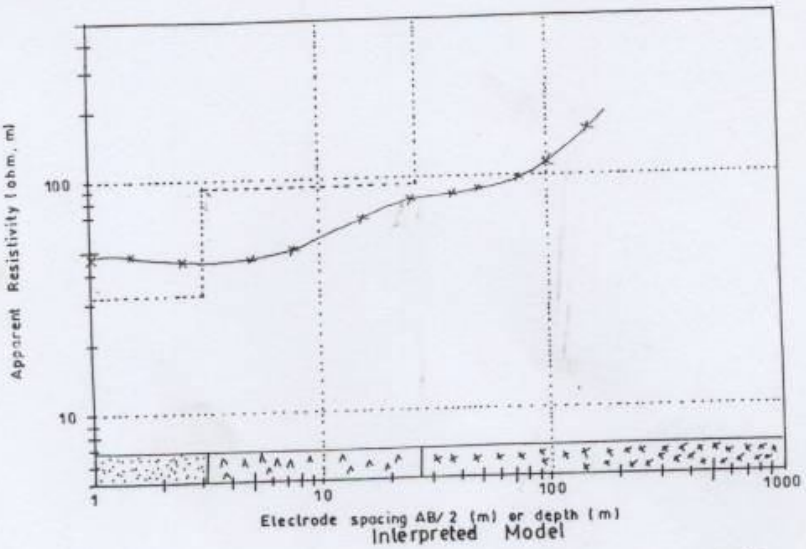
X: 4400
Y: -692

VES 29

DEPT OF WATER RESOURCES

Orientation 001μ

9 June 2000



Interpreted Model

Layer	Resistivity (ohm m)	Thickness (m)	Depth (m)
1	134	0.35	0.35
2	33	2.79	3.14
3	91.2	23.02	26.2
4	742		

Legend

X — Observed Apparent Resistivity Data Point

Sand Clay

Weathered Basement

Fractured Basement

Interpretation of Field Curve for Ves 29

Vertical Electrical Sounding (Schlumberger Array)

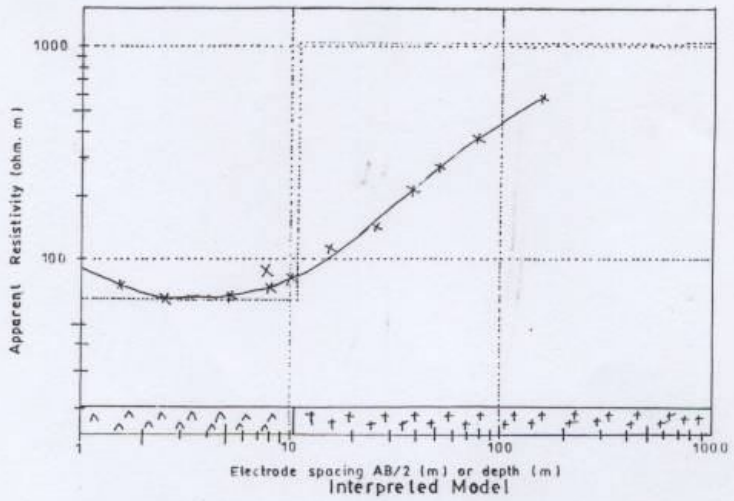
X: 1800
Y: -1039

VES30

INSIDE AREA A

Orientation 090°.

19 May 2000



Interpreted Model

Layer	Resistivity (ohm. m)	Thickness (m)	Depth (m)
1	86.4	0.53	0.53
2	72	9.94	10.47
3	104.8		

Legend

X — Observed Apparent Resistivity Data Point

Weathered Basement

Fresh Basement

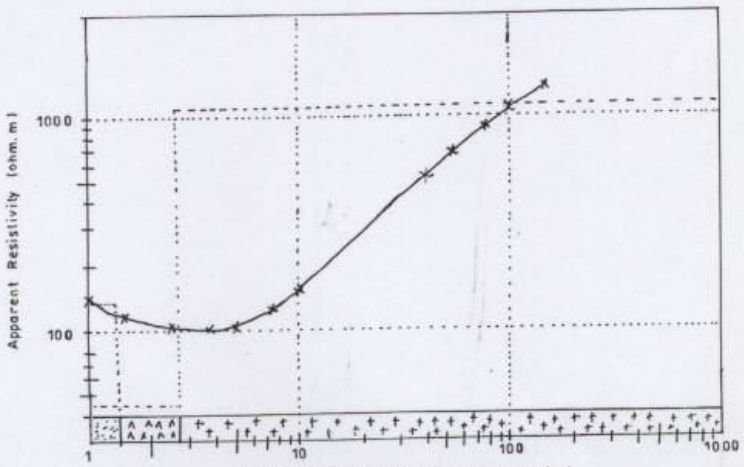
Interpretation of Field Curve for Ves 30

Vertical Electrical Sounding X: 2200 VES31

(Schlumberger Array) Y: -1039

SOUTH EAST OF AREA F

Orientation 045μ 19 May 2000



Interpreted Model

Layer	Resistivity (ohm m)	Thickness (m)	Depth (m)
1	149	1.32	1.32
2	43	1.36	2.68
3	1504		



Interpretation of Field Curve for Ves 31

Vertical Electrode Sounding (Schlumberger Array)

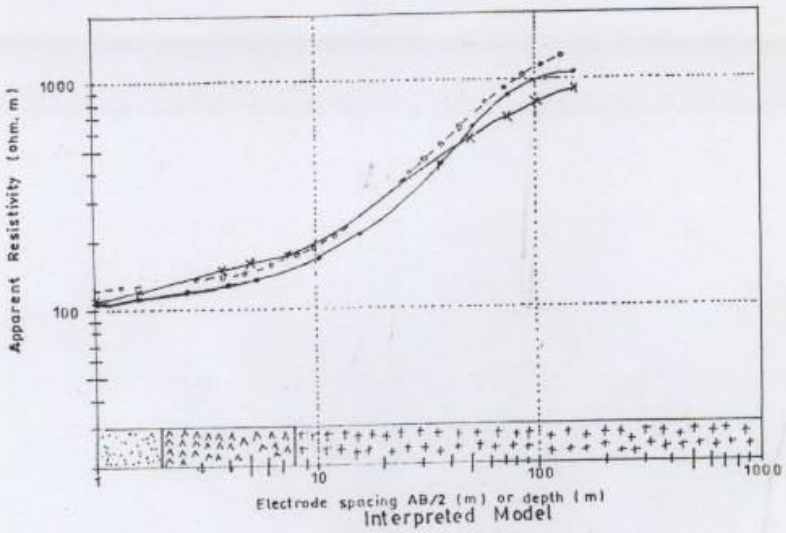
X: 2600
Y: -1039

VES32

SOUTH EAST OF AREA F

Orientation 001A

26 May 2000



Interpreted Model

Layer	Resistivity (ohm m)	Thickness (m)	Depth (m)
1	110	2	2
2	150	5.9	7.9
3	1125		

Legend

- Azimute NW SW
- Azimuth NE SW
- Azimuth E W
- Sandy Clay
- Weathered Basement
- Fresh Basement

Interpretation of Field Curve for Ves 32

Vertical Electrical Sounding (Schlumberger Array)

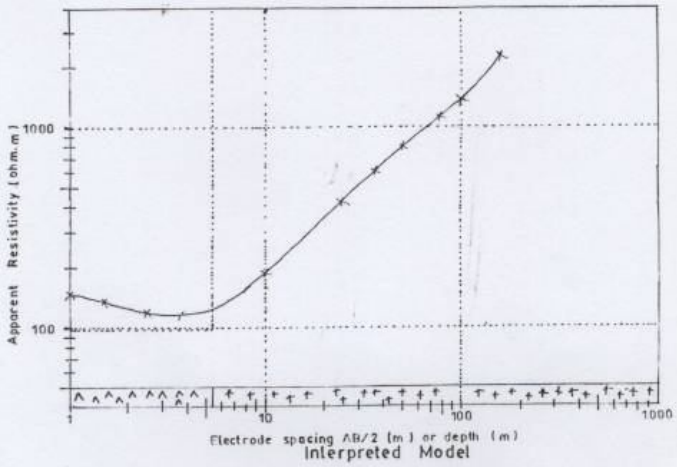
X: 3000
Y: -1039

VES 33

WEST OF BZ 5

Orientation 001°

26 May 2000



Interpreted Model

Layer	Resistivity (ohm m)	Thickness (m)	Depth (m)
1	158	0.8	0.8
2	98	4.6	5.4
3	3875		

Legend

X — Observed Apparent Resistivity Data Point

Weathered Basement

Fresh Basement

Interpretation of Field Curve for Ves 33

Vertical Electrical Sounding (Schlumberger Array)

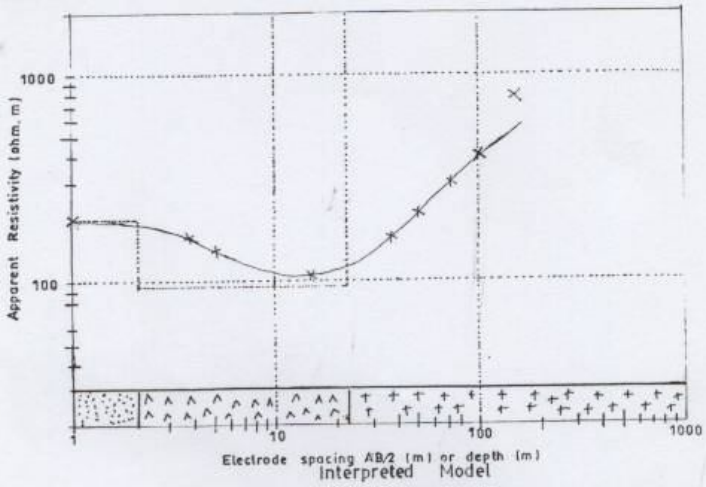
X: 3400
Y: -1039

VES 34

SARDAUNA ROAD AREA BZ

Orientation 001°

27 May 2000



Interpreted Model

Layer	Resistivity (ohm m)	Thickness (m)	Depth (m)
1	199	2.1	2.1
2	94	20.4	22.5
3	2587		



Interpretation of Field Curve for Ves 34

Vertical Electrical Sounding
(Schlumberger Array)

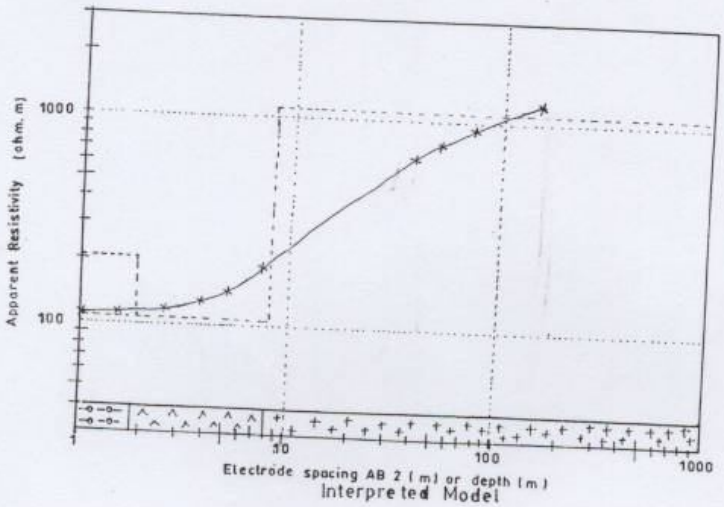
X: 3800
Y: -1039

VES35

Orientation 001/

158 BZ

27 May 2000



Interpreted Model

Layer	Resistivity (ohm.m)	Thickness (m)	Depth (m)
1	202	1.71	
2	106	6.31	1.71
3	1109		8.02

Legend

X	Observed Apparent Resistivity Data Point
	Weathered Laterite
	Weathered Basement
	Fresh Basement

Interpretation of Field Curve for Ves 35

Vertical Electrical Sounding
(Schlumberger Array)

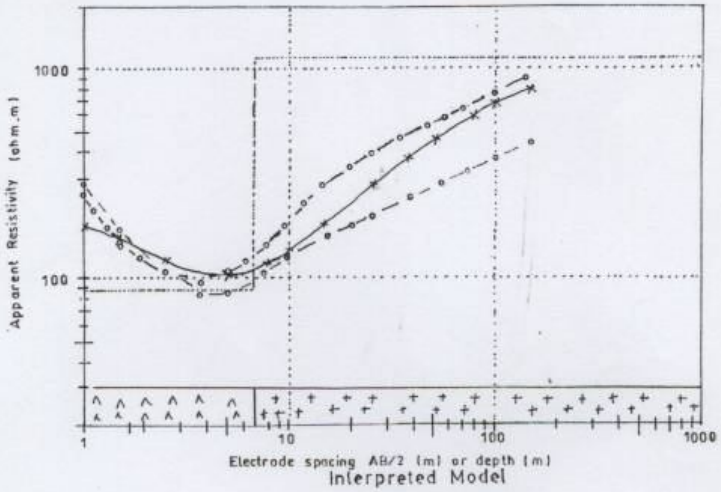
X: 4200
Y: -1039

VES 36

EASTERN BZ

Orientation 090°

8 June 2000



Interpreted Model

Layer	Resistivity (ohm m)	Thickness (m)	Depth (m)
1	201	0.8	0.8
2	88	5.0	5.8
3	1124		

Legend

- x — Azimuth NW-SE
- o — Azimuth NE-SW
- • — Azimuth E-W
- Weathered Basement
- Fresh Basement

Radial Depth Sounding Field Curves for Ves 36

VES 37

Vertical Electrical Sounding

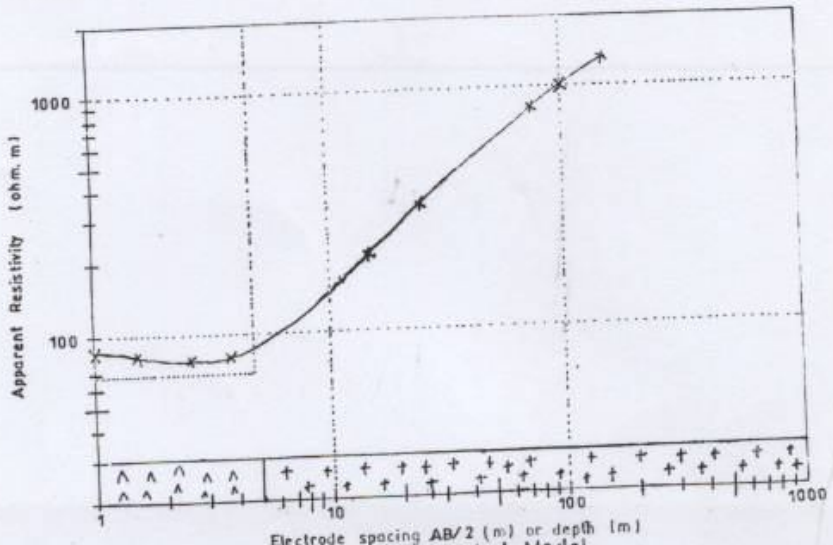
X: 3200
Y: -1386

(Schlumberger Array)

SW OF BZ

27 May 2000

Orientation 090M



Interpreted Model

Layer	Resistivity (ohm. m)	Thickness (m)	Depth (m)
1	92	0.7	0.7
2	68	4.0	4.7
3	2514		

Legend

X Observed Apparent Resistivity Data Point

Weathered Basement

Fresh Basement

Interpretation of Field Curve for Ves37

Vertical Electrical Sounding

(Schlumberger Array)

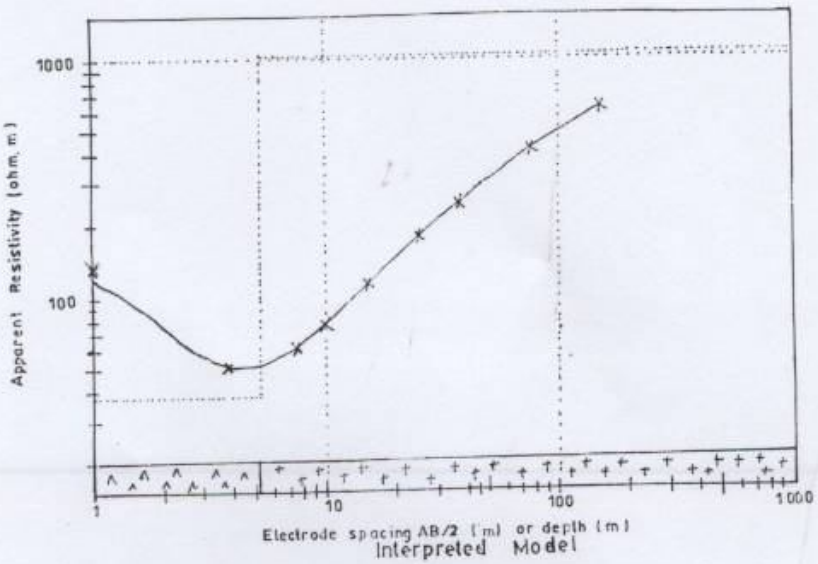
X: 3600
Y:-1386

VES38

SOUTH OF BZ

27 May 2000

Orientation 045∠



Interpreted Model

Layer	Resistivity (ohm m)	Thickness (m)	Depth (m)
1	138	0.8	0.8
2	38	4.4	5.2
3	1023		

Legend

X — Observed Apparent Resistivity Data. Point

Weathered Basement

Fresh Basement

Interpretation of Field Curve for Ves 38

VES 39

Vertical Electrical Sounding

(Schlumberger Array)

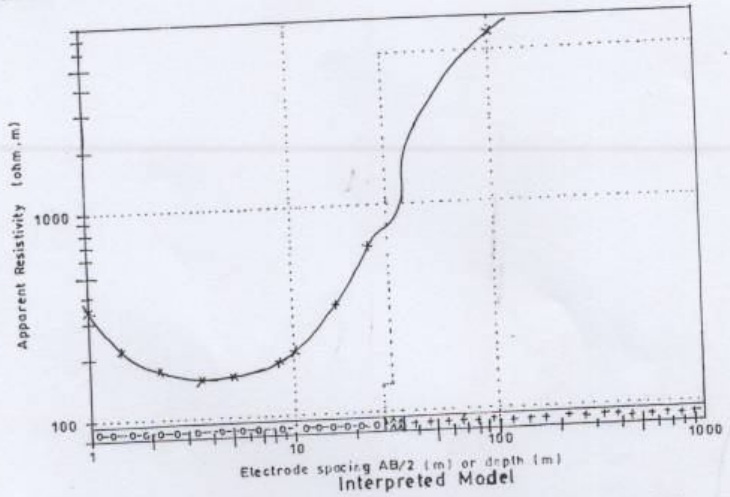
X: 4000

Y: -1386

SOUTH OF BZ

25 May 2000

Orientation 001μ



Interpreted Model

Layer	Resistivity (ohm.m)	Thickness (m)	Depth (m)
1	363	0.63	0.63
2	97	26.37	27.63
3	145	3.63	30.00
4	512.6		

Legend

X Observed Apparent Resistivity Data Point

Weathered Laterite

Weathered Basement

Fresh Basement

Interpretation of Field Curve for Ves 39

APPENDIX II

GEOELECTRIC STRATIFICATION OF THE STUDY AREA

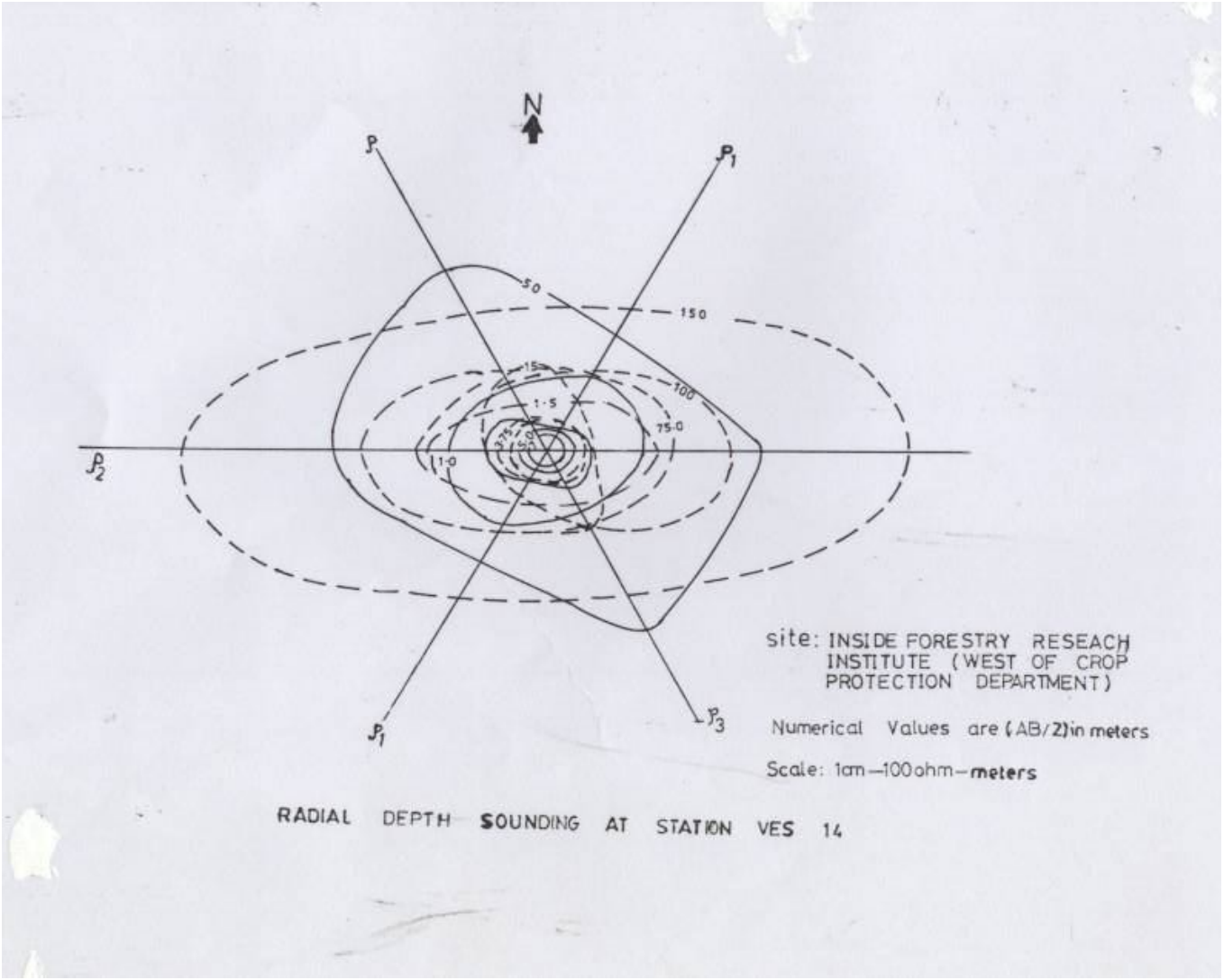
VESStation No.	Layer No.	Resistivity Values (Ωm)	Thickness layers (m)	Depth to the top of the layer (m)
VES01	1	280	1.2	0.0
	2	650	10.0	1.2
	3	175	24.8	11.2
	4	1895	∞	36.0
VES02	1	250	0.2	0.0
	2	75	1.6	1.2
	3	135	8.0	1.8
	4	55	11.2	9.8
		1522	∞	21.0
VES03	1	240.5	1.69	0.0
	2	449.5	30.18	1.69
	3	3568.8	∞	31.87
VES04	1	343.8	1.04	0.0
	2	147.1	29.70	1.04
	3	279.6	∞	30.74
VES05	1	552.7	0.6	0.0
	2	344.6	29.81	0.6
	3	160.0	22.74	30.41
	4	1063.4	∞	53.15
VES06	1	113.0	1.50	0.0
	2	124.6	7.83	1.50
	3	354.8	27.62	9.33
	4	872.0	∞	36.95
VES07	1	137.1	0.882	0.0
	2	11.72	1.47	0.713
	3	451.2	25.61	2.043
	4	3641.2	∞	35.783
VES08	1	43.82	0.713	0.0
	2	8.23	1.32	0.713
	3	176.1	33.74	2.043
	4	1324.6	∞	35.783
VES09	1	73.95	6.00	0.0
	2	193.5	16.24	6.00
	3	111.3	25.61	22.24
	4	1429.8	∞	47.85
VES10	1	1165.1	1.39	0.0
	2	920.9	13.22	2.33
	3	132.7	11.68	3.56
	4	557.4	∞	38.52
VES11	1	122.7	2.33	0.0
	2	559.7	1.23	2.33
	3	138.6	3496	3.56
	4	1929.2	∞	38.52
VES12	1	121.2	2.02	0.0
	2	6814.0	1.85	2.02
	3	48.67	6.25	3.87
	4	1213.3	∞	10.12
VES13	1	1350	3.5	0.0
	2	2005	7.7	3.5
	3	250	22.8	11.2
	4	2501	∞	34.10

VESStation No.	Layer No.	Resistivity values (Ωm)	Thickness layers (m)	Depth to the top of the layer (m)
VES14	1	218.3	0.841	0.0
	2	32.54	2.44	0.841
	3	223.1	38.67	3.28
	4	693.0	∞	41.96
VES15	1	57.91	5.71	0.0
	2	625.3	4.15	5.71
	3	49.96	14.17	9.86
	4	1302.13	∞	24.03
VES16	1	1262.6	0.347	0.0
	2	67.10	3.87	0.347
	3	157.6	23.32	4.22
	4	1814.2	∞	27.57
VES17	1	336.8	0.613	0.0
	2	66.38	23.02	0.613
	3	3165.17	∞	23.64
VES18	1	130	4.0	0.0
	2	35	9.0	4.0
	3	125	29.0	13.0
	4	1587	∞	42.0
VES19	1	119.1	0.831	0.0
	2	91.2	0.855	0.831
	3	100.0	27.98	1.68
	4	1009.8	∞	29.67
VES20	1	84	0.61	0.0
	2	194	2.97	0.61
	3	17	8.12	3.58
	4	3080	∞	11.00
VES21	1	698	0.88	0.0
	2	230	1.95	0.88
	3	113.22	1.70	2.83
	4	39.61	5.66	4.53
	5	360	∞	8.19
VES22	1	398	0.49	0.0
	2	179	2.77	0.49
	3	511	1.24	3.26
	4	27	5.31	5.50
	5	513	∞	10.81
VES23	1	120	0.8	0.0
	2	210	3.4	0.8
	3	81	33.8	4.2
	4	1025	∞	38.0
VES24	1	76	0.53	0.0
	2	45	4.09	0.53
	3	5015	∞	4.62
VES25	1	170	1.0	0.0
	2	222	26.5	1.0
	3	9241	∞	27.5
VES26	1	329	0.32	0.0
	2	146	14.98	0.32
	3	8573	∞	15.30
VES27	1	102	0.75	0.0
	2	78	11.33	0.75
	3	719	∞	12.08

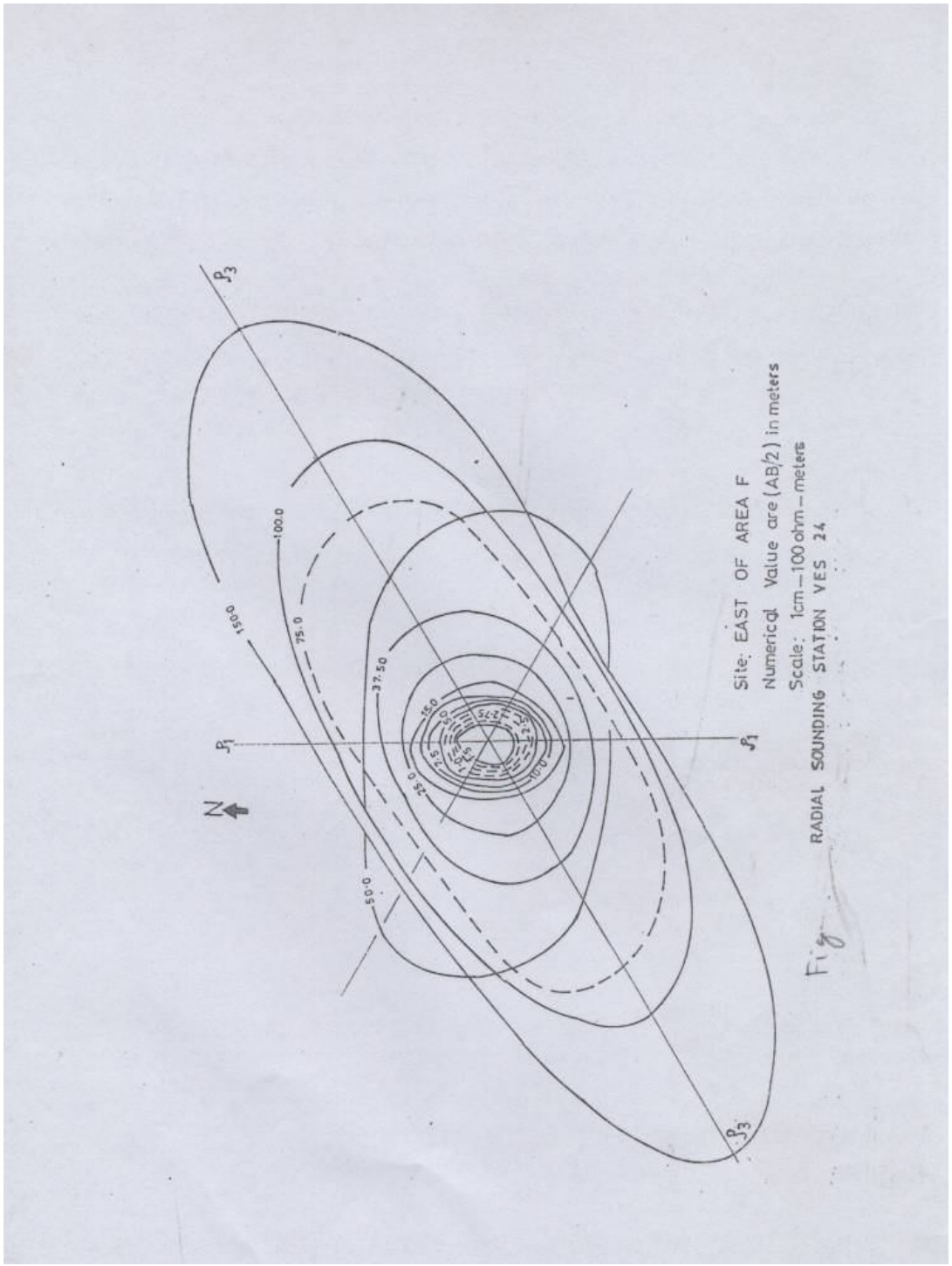
VESStation No.	Layer No.	Resistivity values (Ωm)	Thickness layer (m)	Depth to the top of the layer (m)
VES28	1 2 3	601 87 5435	0.73 13.67 ∞	0.0 0.73 14.4
VES29	1 2 3 4	134 33 91.2 742	0.35 2.79 23.06 ∞	0.0 0.353 3.14 26.2
VES30	1 2 3	86.4 72 1048	0.53 9.94 ∞	0.0 0.53 10.47
VES31	1 2 3	149 43 1504	1.32 1.36 ∞	0.0 1.32 2.68
VES32	1 2 3	110 150 1125	2 5.9 ∞	0.0 2 7.9
VES33	1 2 3	158 98 3875	0.8 4.6 ∞	0.0 0.8 3.8
VES34	1 2 3	199 94 2587	2.1 20.4 ∞	0.0 2.1 22.5
VES35	1 2 3	202 106 1109	1.71 6.31 ∞	0.0 1.71 8.02
VES36	1 2 3	201 88 1124	0.8 6.0 ∞	0.0 0.8 6.8
VES37	1 2 3	92 68 2514	0.7 4.0 ∞	0.0 0.7 4.7
VES38	1 2 3	138 38 1023	0.8 4.4 ∞	0.0 0.8 5.2
VES39	1 2 3 4	363 97 145 5126	0.63 26.37 3.63 ∞	0.0 0.63 27.10 30.73

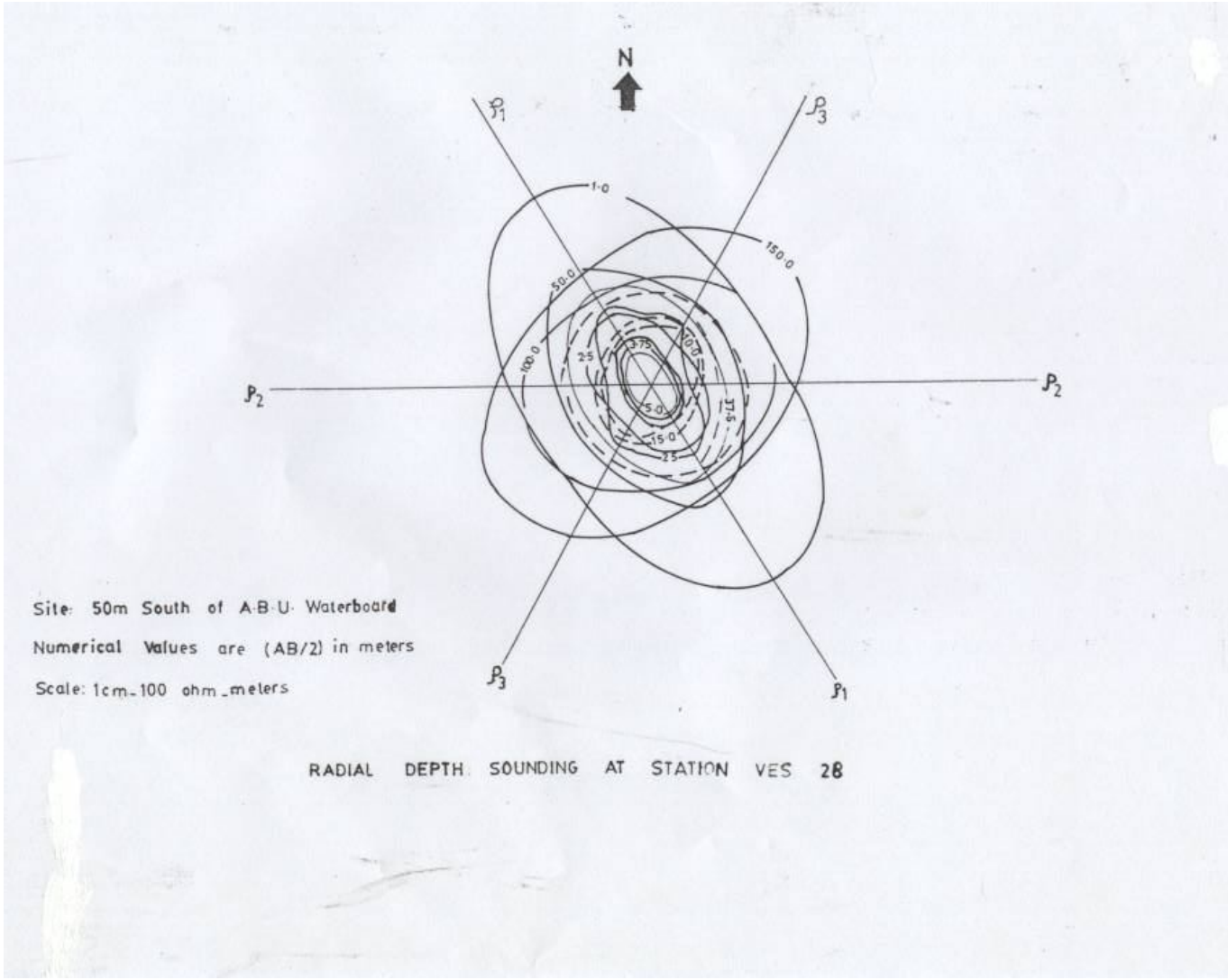
APPENDIX III

RADIAL DEPTH SOUNDING PLOTS

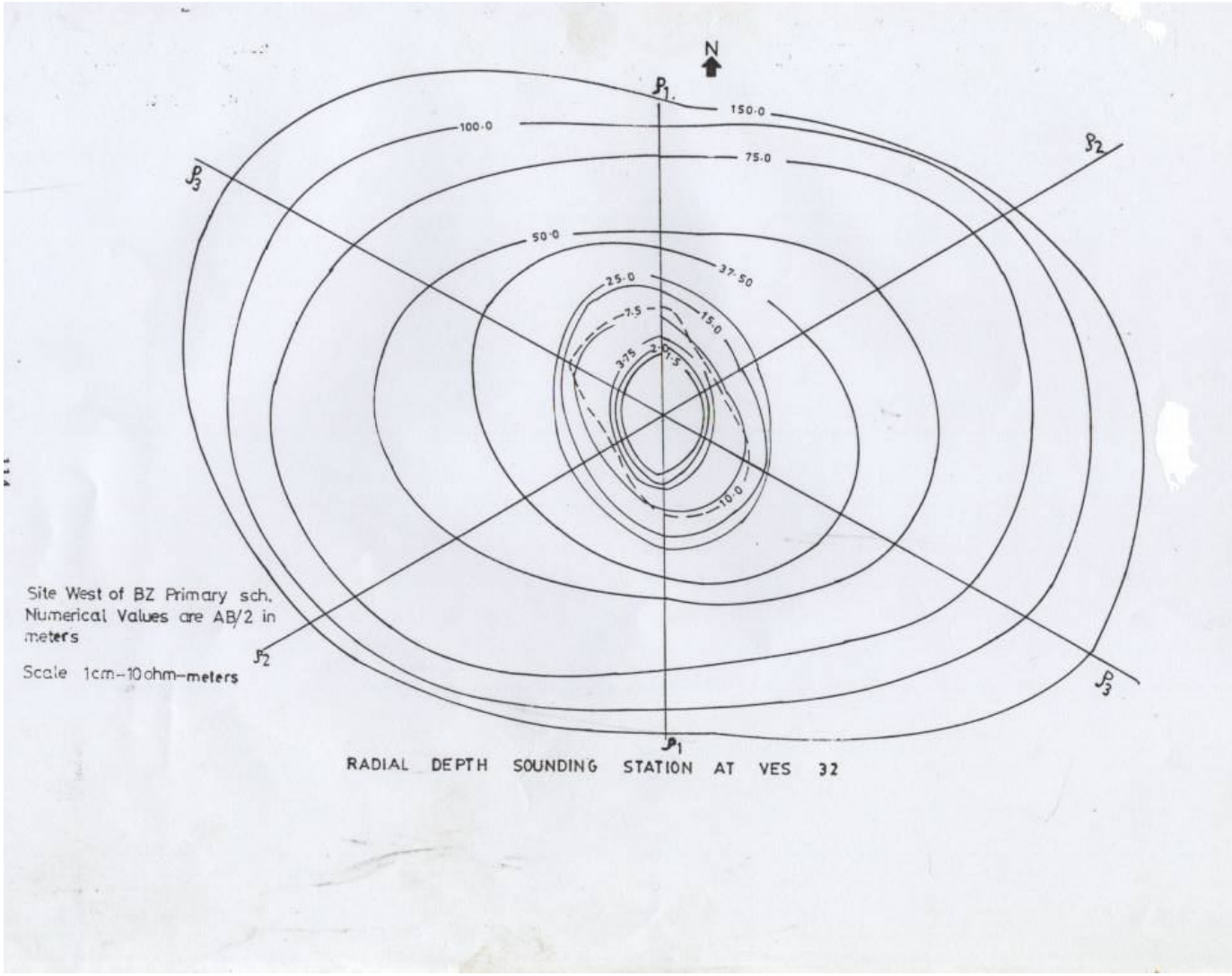


RADIAL DEPTH SOUNDING AT STATION VES 14


P3
P1
P1
P3
N
150.0
100.0
75.0
37.50
25.0
15.0
50.0
Site: EAST OF AREA F
Numerical Value are (AB/2) in meters
Scale: 1cm—100 ohm—meters
RADIAL SOUNDING STATION VES 24



RADIAL DEPTH SOUNDING AT STATION VES 28



RADIAL DEPTH SOUNDING STATION AT VES 32

N
P1
P2
P3
150.0
100.0
50.0
25
75
10.0
SITE EAST OF BZ INSIDE DANFODIYO RIVER
Scale 1cm 100 ohm.meters
Numerical Values refer to (AB/2) in meters
RADIAL DEPTH SOUNDING AT STATION VES 36